2008-01-01

Structure property relationships in electron donating systems for potential photovoltaic applications.

Jonathan Moghal
Technological University Dublin

Structure Property Relationships in Electron Donating Systems for Potential Photovoltaic Applications

By

Jonathan Moghal

A thesis submitted to the Dublin Institute of Technology, for the award of PhD

FOCAS INSTITUTE / SCHOOL OF PHYSICS,
DUBLIN INSTITUTE OF TECHNOLOGY,
KEVIN STREET, DUBLIN 8

Supervisors:

DR. G. CHAMBERS
DR. H.J. BYRNE

September 2008

Declaration

I certify that this thesis which I now submit for examination for the award of Ph.D. is entirely my own work and has not been taken from the work of others save and to the extent that such work has been cited and acknowledged within the text of my work.

This thesis was prepared according to the regulations for postgraduate study by research of the Dublin Institute of Technology and has not been submitted in whole or in part for an award in any other Institute or University.

The work reported on in this thesis conforms to the principles and requirements of the Institute's guidelines for ethics in research. The Institute has permission to keep, to lend or to copy this thesis in whole or in part, on condition that any such use of the material of the thesis be duly acknowledged.

Signature 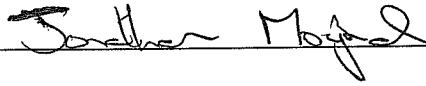 Date 25/09/08

Acknowledgements

I wish to sincerely thank the following people without whom the completion of this thesis would not have been possible.

Firstly I would sincerely like to thank Dr. Gordon Chambers for allowing me to undertake this course of study and for all his help and guidance in the preparation and correction of this document. I would also like to thank my co-supervisor, Dr. Hugh Byrne for his valuable experimental and theoretical input into the project over the last number of years. What else can I say about this project, many ups and downs, maybe more of the latter but it was worth it in the end; I was seriously beginning to think the project was jinxed.

I would like to thank Dr. Michael Seery, for proof reading this document. Without the polymers, I would not have been able to complete this project so thanks must go to Paddy. Many thanks to Dr. Fran Pedreschi for all his help over the past three years, I have lost count of the number of times you came over to the EA lab but I will always remember the time the lockin amplifier was sizzling. Special thanks to Dr. Garrett Farrell for all his help over the course of the project and I am eternally grateful for all the trips he made back up to Dublin and for all the phone calls when things did not go according to plan with the EA.

Thanks to all in FOCAS for all the good times and mayhem and especially those in the ground floor office. Over the course of my time in Kevin Street, I have been lucky

enough to have found some very good friends, thanks to John and Kevin and the other boys for the constant entertainment, support and discouragement during our time in college together and over the last three years.

Finally on a personal not I would like to thank to Ann, Jack, Alan, Denise, Ben, Theresa, Philip and kids, I have been very lucky to have such special people in my life who have stuck by me through the thick and the thin. Special thanks to my mother who never seem to give up on me. Thanks to Ailbhe for her constant support and encouragement throughout my many PhD crises.

"In Europe there is a boy daring to think high. He was ambitious, wanting to be informed, courageous in his entry into a world dominated by people united by links and conservative principles. It was domineering like an iceberg in which the mass of what we see at the surface makes us think there is nothing below. The kid arrived, said he wanted to win and won. He said he was one of the best and he proved it. He said he did not want to be an integral part of the plan and remained independent. He said the sharks around him did not frighten him and swan between them... The moral of the story is not to listen to those who tell you not to play the violin but stick to the tambourine."

José Mourinho

Abstract

Conjugated polymers are considered to be one-dimensional semiconductors. In conjugated polymers single and double bonds alternatively bind the carbon atoms along the polymer chain. The loosely bound π electrons determine the electronic properties of conjugated polymers. In order to utilise the properties of conjugated polymers in terms of a photovoltaic (PV) device application an acceptor material must be added. The acceptor material used in this study is used is buckminsterfullerene (C_{60}). C_{60} was selected for this purpose due to its size and the fact that it can accept up six additional electrons. Ultrafast charge transfers from a conducting polymer onto C_{60} were first reported in 1992 by Sariciftci *et al.* in a blend of MEH-PPV (poly (2-methoxy-5-(2'-ethylhexyloxy)-1,4-phenylenevinylene) and since then its properties as an electron acceptor have been widely investigated. The debate of the exact mechanism of the charge transfer in polymer/fullerene blends is still on going today. The investigation of these systems is predominately done using time resolved spectroscopy (photoinduced absorption, PIA), which is still considered to be the most effective way of investigating charge transfer between polymer/fullerene composites. However time resolved spectroscopy is expensive and is not readily available for use.

The aim of this study is to explore charge transfer signatures in polymer/fullerene composites without using PIA spectroscopy. This study proposes to use steady state spectroscopic techniques coupled with electrochemical and conductivity measurements to characterise charge transfer signatures in polymer fullerene composites. The much studied MEH-PPV/C_{60} model system was initially employed in a systematic approach to try and elucidate charge transfer indicators between the polymers and C_{60} Fluorescence

spectroscopy, cyclic voltammetry, spectroelectrochemical and conductivity measurements provided evidence of charge transfer signatures in the model composite and were seen to be potentially viable techniques for assessing novel systems.

The study was then extended to a homologous series of polymers which have continuously varying electronic and optical properties. The polymer series was synthesised in house and characterised for the first time in the solid state as part of this work. Electronic spectroscopy of the polymer series revealed that aggregation was occurring in the solid-state form of the polymers. The electronic properties of the molecular and solid-state forms are different and the structure property relationships previously determined for the molecular forms could not be applied to the solid-state. It was observed that emission spectra of the polymers were all seen to be red shifted compared to those of their isolated molecular form. The fluorescence yield was also low, which also confirmed that there are aggregates within the polymers in their solid-state form. Cyclic voltammetry measurements allowed calculation of the exact positioning of the HOMO-LUMO levels of each polymer. The precise levels of the HOMO-LUMO levels are important when matching the energy levels of the polymer to the energy levels of C_{60}. Electrochemical bandgaps were in close accordance to the optical bandgaps. In-situ spectroelectrochemical measurements allowed observations of the bipolaron energy states of each polymer. Electroabsorption studies showed that each polymer was dominated by the quadratic Stark effect. The electroabsorption spectrum of each polymer closely resembled a first derivative lineshape of its absorption spectrum indicating a dominance of intramolecular transitions within each of the polymers.

Using two of the new polymers a systematic probe of the charge transfer mechanism was obtained. Charge transfer markers were evident in the new composites using fluorescence spectroscopy, cyclic voltammetry, spectroelectrochemical measurements

and conductivity measurements. For the results it was seen that the interaction of the two polymers with the C_{60} varied. From this systematic approach it was possible to observe which of the polymers showed the most potential for a device application by matching of the appropriate energy levels to achieve a more efficient charge transfer.

In general it can be said that using a approach it was possible to match up the energy levels of a polymer/fullerene composite in order to achieve a more efficient interaction, which can measured without the need for time resolved spectroscopy.

List of Figures

List of Tables

List of Abbreviations

Btu	British thermal unit (1Btu=1000 Joules)
MEH-PPV	Poly (2-methoxy-5- (2'-ethylhexyloxy)-1,4-phenylenevinylene
LED's	Light Emitting Diodes
PV Cell	Photovoltaic Cell
HOMO	Highest Occupied Molecular Orbital
LUMO	Lowest Unoccupied Molecular Orbital
PIA	Photoinduced Absorption
ITO	Indium Tin Oxide
POPV	Poly (para-2,5-bis-(n-octyloxy)- phenylenevinylene
POPV-ONV	Poly(2,5-bis(n-octyloxy)-1,4-phenylene vinylene-1,5 bis(octyloxy)- 2,6-naphthylene vinylene)
PONV	Poly(2,6-bis-(n-octyloxy)-1,5-NaphthyleneVinylene)

POPV-OAV	Poly(2,5-bis(n-octyloxy)-1,4-phenylene vinylene-co-1,5-bis(n-octyloxy)-2,6-anthracene vinylene)
PONV-OAV	Poly(2,5-bis(n-octyloxy)-1,5-naphthylenevinylene-co-1,5-bis(n-octyloxy)-2,6-anthracene vinylene), (5)
IC	Internal Conversion
ISC	Inter System Crossing
IP	Ionisation Potential
EA	Electron Affinity
CT	Charge Transfer
PEDOT	Poly (styrenesulfonate)/poly (2,3-dihydrothieno(3,4-b)-1,4-dioxin
Δp	Change in Polarisability
fcc	Face Centred Cubic

Table of Contents

Chapter 1: Introduction and Thesis Outline

Chapter 2: Introduction to Conjugated Polymers

Chapter 3: Experimental Methodology

Chapter 4: Characterisation of Reference Materials

Chapter 7: Electroabsorption Spectroscopy

Chapter 8: General Discussion and Conclusions

Chapter 1: Introduction and Thesis Outline

1.1 Introduction

Over the past two decades society has become more aware of the damage caused by the use of fossil fuels to the environment. The damage caused to the ozone layer (caused by use of fossil fuels) and the melting of the polar ice caps has forced scientists to search for new sources of energy. In this 'eco-era', the sustainability and renewability of any potential energy sources has become increasingly important. New regulations are being enforced across the European Community to ensure that individual countries reduce their fossil fuel consumption and failure to do so will result in face heavy fines for offenders (Irish Statute Book, 2008). As a result of this 'energy economics' a considerable amount of investment in renewable energy research has materialised over the last number of years and is set to increase significantly within the coming decade. Indeed Science Foundation Ireland (SFI), the Irish government's science funding agency, has recently had its remit amended to reflect this growing trend and now specifically includes sustainable energy and energy efficient technology research as a priority area (Science Foundation Ireland, 2008). Photovoltaic research for harnessing solar energy fits into this niche promising clear benefits with respect to sustainability and renewability. This thesis explores the use of organic based solar cell devices as an alternative to the more expensive, currently employed silicon based devices. It investigates the intricacies of the intermolecular interaction and charge transfers associated with organic photovoltaics. It looks specifically at the fundamental characterisation of the donor and acceptor materials used as well as the influence of the donor structure on the efficiency of the charge transfer process and thus the potential of

such composite systems in photovoltaic devices. The background of the importance of renewable energy sources and the growing need to reduce global dependency on fossil fuels is presented in this chapter as the underlying context of the work described in this thesis.

1.2 Fossil fuels

Fossil fuels are non-renewable energy sources; such as coal, oil and natural gases. These energy sources have been used for centuries at a local level. However the emergence and evolution of the industrial age led to global dependence on mass produced energy from these materials. The burning of fossil fuels by humans is the major source of emissions of carbon dioxide, which is one of the greenhouse gases that is known to contribute to global warming (Intergovernmental Panel on Climate Change (IPCC), 2008). Currently over 85 % of our energy demands are met by the combustion of these non renewable fossil fuels, with additional pressure coming form the rapidly growing Chinese, Indian and South American economies. In addition to the potentially catastrophic emission of greenhouse gases from these fuel sources, it should be noted that these fuels are not renewable and the earth can only supply a finite amount. In fact most experts now believe that in less than 20 years reserves of oil and natural gas will start to decrease significantly (National Geographic, 2008). It is these considerations that have led to interest in renewable energy. Figure 1.1 shows the percentage breakdown of the total energy provided by fossil fuels and renewable sources (Renewable Energy Annual Web site, 2008).

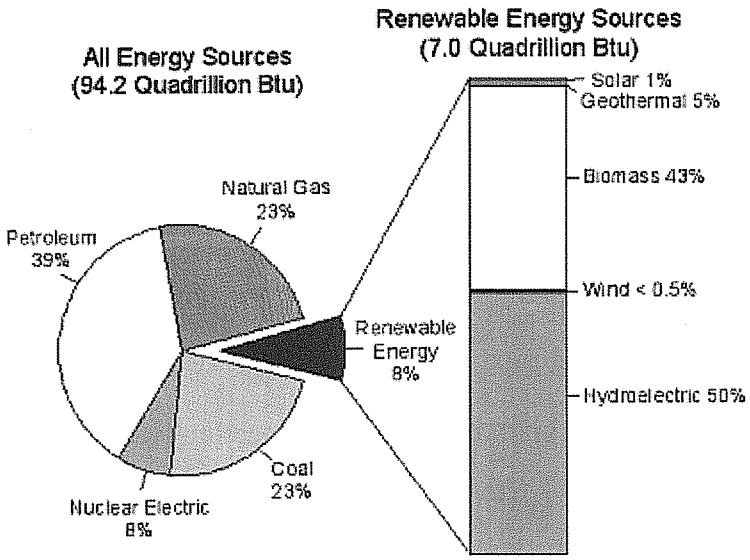

Figure 1.1: Percentage breakdown of total energy provided from fossil fuels and renewable energy sources (taken from Renewable Energy Annual Web site).

1.3 Renewable energy

Renewable energy utilises natural resources such as sunshine, wind, flowing water, biological processes and geothermal heat flows. Unlike fossil fuels the harnessing of these resources poses no known threat to the welfare of the planet and significantly they are also sustainable. The downside is that current renewable energy systems often struggle to mass produce energy in an uninterrupted manner in comparison to conventional fossil fuel power plants which can. In fact it is accepted that for large-scale implementation of renewable energy power plants, it will be necessary to develop systems that can compete on an economic level with fossil fuel facilities, either by decreasing cost, increasing efficiency, or a combination of both. There are several potential avenues available for the development of renewable energy sources. The most viable route is solar energy. The harnessing of solar energy has become increasingly

popular since the energy crisis in the early 1970's. However solar power played only a very minor role in alleviating the crippling fuel costs during this period. Nevertheless its potential was noted for future crises. Today solar technology can be found in homes across the globe, where the energy provided by the sun is used in solar collector systems to provide households with hot water or by direct conversion into electrical energy in photovoltaic devices. Although solar energy is still seen as a developing technology it will undoubtedly play a significant role in the coming years of uncertainty in the international energy and fuel market. Most commercially available PV cells are based on silicon technology and as a result can be expensive. This thesis explores the potential use of alternatives to silicon, namely organic conjugated polymers and how best the properties of these materials can be adapted and controlled for applications in devices such as PV cells.

1.4 Organic photovoltaics and conjugated polymers

Photovoltaic (PV) cells are an attractive way of converting direct sunlight into electrical energy. The sun supplies a peak intensity of about 1 kW/m^2 (Renewable Energy Annual Web site, 2008) on the surface of the earth. This intensity is reduced when the sun is not at its peak due to location or time of day. This energy can be harvested and converted into a usable electrical signal through photovoltaic technology. Most PV cells today are silicon based. Silicon is an extrinsic semiconductor; it must be p-doped or n-doped with impurities to modify the number and type of free charge carriers present. Therefore most inorganic (silicon) photovoltaic cells are based on p-n junctions.

The main problem with the current technology is the high cost of production of silicon. The most efficient solar cells available today consist of crystalline silicon, which is

extremely expensive to produce. Therefore in practice silicon cells are only used extensively in extreme cases such as in deserts where there are no other available power sources. With the high costs of production the PV cells are no competition for fossil fuels. Only about 1 % of the planet's renewable energy (Figure1.1) consumption is solar power (Sustainable Energy Ireland, 2007). To make solar cell systems more competitive with fossil fuel power plants, a significant reduction in cost must be achieved.

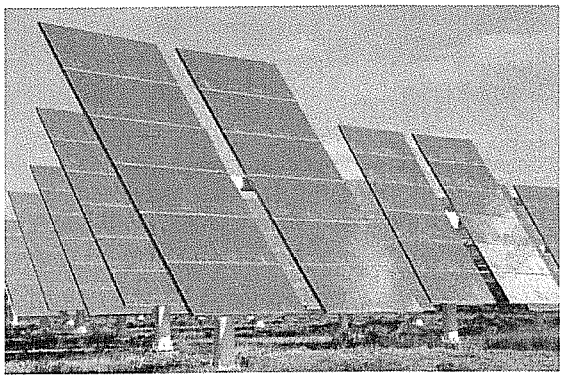

Figure 1.2: Solar power plant in Tabernas desert, Andalusia, Spain (Britannia Encyclopaedia, 2008).

A promising approach towards new low cost PV cells is fabrication of a device based on organic materials (Granstrom, 1998, Shaheen, 2001). Figure 1.3 shows a flexible organic photovoltaic cell. In the case that is most relevant to this study the silicon is replaced by a semiconducting polymer in combination with an acceptor material as the active layer. These materials are usually soluble in common organic solvents. This solubility makes device production relatively easy and low cost. Thin films are spin cast (Granstrom, 1998) from solution. The advantage of organic materials is that they can also be applied to flexible plastic substrates making the whole device flexible and allowing for cheap roll-to-roll production methods and hence cheaper costs of production (Gelinck, 2000). Another advantage of polymer materials is that the optical

and electrical properties can be changed relatively easily by altering the molecular structure of the monomers. It is therefore possible to tune the optical and electronic properties of the polymer to maximize the efficiency of any device.

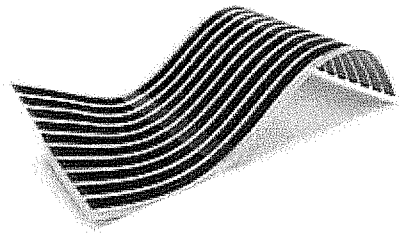

Figure 1.3: Flexible organic photovoltaic cell (Gizmag, 2008).

The main challenge with organic PV devices is to achieve efficient charge separation of electrons and holes that are created by the absorption of a photon, giving rise to the photovoltaic effect (Becquerel, 1839). A conjugated polymer with the addition of an acceptor material results in an efficient charge separation (Sariciftci, 1992). One of the most commonly used acceptor materials is buckminsterfullerene (C_{60}). Charge separation in polymer/fullerene systems is achieved by ultrafast transfer of photoexcited electrons from the polymer to the C_{60} fullerene (Sariciftci, 1992). This ultrafast charge transfer from a conducting polymer (donor) onto C_{60} (acceptor) was first reported by Sariciftci *et al.* in a blend with MEH-PPV (poly (2-methoxy-5- (2'-ethylhexyloxy)-1,4-phenylenevinylene) using time resolved photoinduced absorption spectroscopy (PIA). Charge transfer from the polymer to the fullerene leads to a spatial separation of electrons and holes that is needed for efficient photovoltaic devices (Sariciftci, 1992). An upper limit for the electron transfer time was found to be 300 femtoseconds (fs) in this system versus a photoluminescence lifetime of 550 picoseconds (ps) in the pristine

polymer, implying that the charge transfer process should dominate over competing energy relaxation mechanisms.

Early studies showed how important it was for the polymer and C_{60} to be in close proximity to each other for the efficiency of the PV devices. Several studies determined the charge transfer range to be within 5 to 10 nm (Kraabel, 1994, Halls, 1996, Vacar, 1997). Therefore the C_{60} molecule has to be within ~10 nm of the location of the photoexcitation for the charge transfer to occur (Vacar, 1997). Since the electron transfer time is 3 orders of magnitude faster than the competing process of photoluminescence, the probability of charge transfer is close to unity if the C_{60} is within transfer range.

Devices produced in a bilayer structure with a single interface between electron donor and electron acceptor (Haugeneder, 1999) had low efficiencies because the volume of the active layer, where efficient charge separation occurred, was limited to a small fraction at the interface. This problem was overcome by Yu *et al.* who prepared devices from a solution containing a blend of MEH-PPV and the methanofullerene (phenyl-[6,6]-C61)-butyric acid methyl ester (PCBM) (Yu, 1995). The derivatization of C_{60} leads to better solubility of the fullerene in organic solvents and to better miscibility of polymer and fullerene. The donor-acceptor junction was thus distributed throughout the bulk of the material rather than being confined to an interface.

With this device structure, the efficiency was improved by nearly two orders of magnitude. In a similar approach, in which the active layer was cast from a blend solution of polymer and fullerene, the total power conversion efficiency under simulated sunlight conditions was improved to 2.5 % (Yu, 1995, Shaheen, 2001). This is to be compared to 10-25 % power conversion efficiencies in commercial silicon solar cells.

To further enhance the efficiency of devices, a slightly more complicated structure is suggested where the interface between electron donor and acceptor is diffuse, but at the electrodes only the donor material has contact to the anode and only the acceptor material has contact to the cathode (Chen, 2000). This structure should enhance the transport of electrons and holes through the acceptor and donor material respectively in a preferred direction to the extracting electrodes. In addition, this structure is believed to enhance rectification of the photovoltaic devices by preventing direct pathways for the charge carriers from the cathode to the anode through either of the materials. Better rectification will improve the fill factor (Chen, 2000) and with that the efficiency of the PV cells. Despite steady improvements over the past decade, the exact charge transfer mechanisms between polymer/fullerene composites is still not fully understood. One of the underlying themes in this thesis is to try to elucidate the exact interactions of polymer/fullerene composites which enable will enable a clearer understanding of the charge transfer mechanism, thus leading to improved systems.

Original explorations on polymer/fullerene composites utilised time resolved femtosecond photoinduced absorption spectroscopy. This type of spectroscopy is expensive and considered to be a specialist technique and is therefore not readily available. There is a need for a more routine screening of these composites and their charge transfer process. This study proposes to use steady state spectroscopy coupled with cyclic voltammetry and conductivity measurements to try and find charge transfer signatures between polymer/fullerene composites. Further to this the thesis will explore the effect of charge transfer in relation to variation of polymer bandgap, electron affinity and ionisation potential.

1.5 Overview of project and thesis outline

The aim of this study is to explore charge transfer signatures in polymer/fullerene composites without using time resolved photoinduced absorption (PIA) spectroscopy. This study proposes to use steady state spectroscopic techniques coupled with electrochemical and conductivity measurements to characterise charge transfer signatures in polymer fullerene composites. The much studied MEH-PPV/C_{60} model system will initially be employed in a systematic approach to try and understand the exact charge transfer between the polymers and the C_{60} and the characteristic signatures which identify and quantify the efficiency of the process.

Once the steady state experimental signatures of the charge transfer process in the model system have been established, the study will be extended onto a homologous series of polymers which have continuously varying electronic and optical properties. Thus a systematic probe of the charge transfer mechanism can be obtained. A systematic probe of polymer/fullerene composites may fill in some of the gap regarding the understanding of the exact charge transfer mechanism, which to date are not fully understood.

In chapter two the background theory of conjugated polymers will be explained. The chapter then goes on to focus on the charge transfer mechanisms of photovoltaic cells, highlighting the differences between inorganic and organic. Finally the chapter gives a review of the previous research reported on organic PV cells and how this study intends to contribute to and extend this previous work. The polymers and acceptor materials used throughout this study are also mentioned in this chapter. As a result this chapter essentially sets up the arguments for doing the research.

Chapter 3 explains the methodology used throughout the study. A full explanation is given of the sample preparation that was used for each different technique. The spectroscopic techniques and instruments used in this study are also discussed; UV/VIS, fluorescence and electro-absorption spectrometers were all used. The other techniques such as cyclic voltammetry, conductivity and in-situ cyclic voltammetry measurements are also discussed. The chapter also gives some of the background which is relevant to the study.

Chapter 4 begins the experimental exploration of the acceptor material C_{60}. The chapter characterises and shows the difference between C_{60} in its molecular and solid-state form. The first part of the chapter deals with spectroscopic characterisation. This deals with the optical and electronic properties of the C_{60}. The charge transfer mechanism of C_{60} is then explored via electroabsorption and cyclic voltammetry techniques. The charge transfer technique provides an explanation of why the C_{60} is seen as an ideal acceptor material for organic PV cells. The second part of chapter 4 deals with the polymeric standard used in this study, MEH-PPV (poly (2-methoxy-5- (2'-ethylhexyloxy)-1,4-phenylenevinylene). A full characterisation of MEH-PPV is provided using the same techniques as above.

The final part of the chapter starts the investigation of charge transfer signatures using steady state spectroscopy measurements, cyclic voltammetry and conductivity measurements. Fluorescence, electroabsorption, cyclic voltammetry and conductivity measurements provided evidence of charge transfer between MEH-PPV and C_{60}.

Chapter 5 begins the characterisation of the polymer series. The electronic properties of each of the individual polymers are explored. The different bandgaps and emission energies obtained are examined and compared to the structural variation. The chapter explains the rationale for choosing the respective polymers that were used in the

composites. Investigation of the new polymer/C_{60} composites is conducted using electronic spectroscopy.

Chapter 6 examines the cyclic voltammetry of the polymers and polymer composites. Cyclic voltammetry measurements can provide information on the redox behaviour of the polymers and also when combined with in-situ spectroelectrochemical results enabled an illustration of the bandgaps and excited state levels within the polymer series. Electrochemical measurements may provide a new and novel way of indicating charge transfer between polymer/fullerene composites. The last part of the chapter includes conductivity measurements on the composite which may be used to reaffirm the cyclic voltammetry measurements.

Chapter 7 deals with the electroabsorption spectroscopy. Electroabsorption spectroscopy provided information on the excited electronic states in the polymers. Using the equation proposed by Sebastian *et al.* the change in polarisability value was obtained for each polymer and this value was plotted against the bandgap. The second part of the chapter concludes the exploration of the composite materials; electroabsorption helps to tie together the previous results and observations.

The final chapter of the thesis provides a summary of work conducted and a general discussion of the work presented. Finally the closing remarks of the thesis indicate some future directions that might be taken with the polymer/fullerene composites used throughout the study

References:

Becquerel A.E., Compt. Rend. Acad. Sci. 9, p. 145. (1839)

Becquerel A.E., Compt. Rend. Acad. Sci. 9, p. 561. (1839)

Britannica Encyclopaedia, http://www.britannica.com, 01/07/08,(2008)

Chen L, Godovsky D, Inganäs O, Hummelen J.C., Janssens R.A.J., Svensson M, Andersson M.R., *"Polymer photovoltaic devices from stratified multilayers of donor acceptor blends"*, Advanced Materials, 12,1367, (2000).

Gelinck G.H., Geuns T.C.T., de Leeuw D.M., *"High-performance all-polymer integrated circuits"*, Appl. Phys. Lett. 77, 1487, (2000).

Gizmag, http://www.gizmag.com/, 28/06/08, (2008).

Granstrom M, Petritsch K, Arias A.C., Lux A, Andersson M.R., Friend R.H., *"Laminated fabrication of polymeric photovoltaic diodes"*, Nature, 395, 257 (1998).

Halls J.J.M., Pichler K, Friend R.H., Moratti S.C, Holmes A.B., *"Exciton diffusion and dissociation in a poly(p-phenylenevinylene)/C_{60} heterojunction photovoltaic cell"*, Appl. Phys. Lett. 68 (22), 3120, (1996).

Haugeneder A, Neges M, Kallinger C, Spirkl W, Lemmer U, Feldmann J, Scherf U, Harth E, Gügel A, Müllen K, *"Exciton diffusion and dissociation in conjugated polymer/fullerene blends and heterostructures"*, Phys. Rev. B 59, 15346, (1999).

Irish Statute Book, http://www.irishstatutebook.ie, 29/06/08, (2008).

Kraabel B, McBranch D, Sariciftci N.S., Moses D, Heeger A.J., *"Ultrafast spectroscopic studies of induced electron transfer from semiconducting polymers to C_{60}"*, Phys. Rev. B 50, 18543, (1994).

Renewable Energy Annual, www.eia.doe.gov/fuelrenewable, 11/12/07, (2007).

Sariciftci N.S, Smilowitz L, Heeger A.J, Wudl F, *"Photoinduced electron transfer from a conducting polymer to buckminsterfullerene"*, *Science* 258, 1474-1476 (1992).

Science Foundation Ireland, http://www.entemp.ie, 04/05/08, (2008).

SEI - Sustainable Energy Ireland, www.irish-energy.ie, 03/12/07, (2007).

Shaheen S.E., Brabec C.J., Sariciftci N.S., Padinger F, Fromherz T, Hummelen J.C., *"2.5 % Efficient Organic Solar Cells"*, Appl. Phys. Lett. 78, 841, (2001).

The National Geographic, http://ngm.nationalgeographic.com, 22/06/08, (2008).

Vacar D, Maniloff E.S., McBranch D.W, Heeger A.J., *"Charge-transfer range for photoexcitations in conjugated polymer/fullerene bilayers and blends"*, Phys. Rev. B 56(8), 4573 (1997).

Yu G, Gao J, Hummelen J.C, Wudl F, Heeger A.J., *"Polymer photovoltaic cells: enhanced efficiencies via a network of internal donor-acceptor heterojunctions"*, Science, 270, 1789, (1995).

Chapter 2: Introduction to Conjugated Polymers

2.1 Introduction

Interest in conjugated polymers stems back to the early 1960's (Pope, 1963). However the potential of conducting polymers as novel electronic materials was not realised until it was shown that polyacetylene could be doped by charge-transfer reactions with an oxidizing or reducing agent (Shirakawa, 1977). The discovery showed that the doped polymer exhibited a dramatic increase in conductivity with values of 30 $\Omega^{-1}cm^{-1}$ which are in the metallic regime (Shirakawa, 1977). This crucial discovery coupled with an observation of electroluminescence and charge storage in poly (*p*-phenylenevinylene) (PPV) (Burroughes, 1990) led to extensive research into the electronic properties of conjugated polymers. In particular PPV and its derivatives have received a significant amount of attention due to their potential application as emissive layers in light-emitting diodes (LED's) (Friend 1999 and Shim 2002), and as donor materials in organic photovoltaic devices (Sariciftci, 1992). The materials chosen for this thesis are PPV derivatives and so the techniques and approaches explored in this body of work may potentially be used to examine other PPV based materials and systems. This chapter explores the background theory to conjugated polymer research, highlighting key studies from literature and identifies how this work will further contribute to the body of knowledge in the field.

2.2 Semiconductor background theory

Structure and bonding play an important role in the electronic and optical properties of a molecule. However it is the conjugated nature of polymers that give rise to the semiconductor behaviour that has made these materials interesting in terms of organic LED's and photovoltaic cells (Burroughes, 1990, Friend, 1999, Shim, 2002, Sariciftci, 2002).

In general a semiconductor material can be described as having an electrical conductivity that is intermediate between that of an insulator and a conductor. In order to understand how semiconductors work it is important to look at their band structure. The band structure of a semiconductor consists of a valence band and a conduction band as illustrated in Figure 2.1.

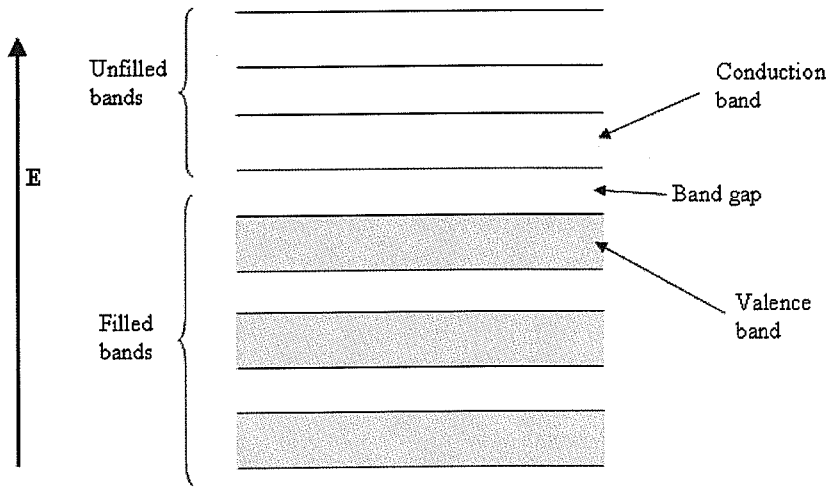

Figure 2.1: Band structure of semiconductor showing a full valence band and an empty conduction band. The Fermi level lies within the band gap (Turton, 2000).

At 0 K the valence band is completely filled with electrons and is separated by only a small forbidden energy gap from the conduction band (~ 1 eV or less). In this situation there is no electrical conduction because the electrons are unable to change their state in small electric fields. However at higher temperatures there is sufficient thermal energy for some of the electrons to be excited from the lower band (valence band) to the upper band (conduction band). An external electric field can be used to influence the electronic states in both bands and a current can flow (Christman, 1988, Turton, 2000). The higher the temperature, the more electrons will be excited into the conduction band. Therefore as temperature increases conductivity increases whereas in a metal the conductivity tends to decrease with temperature because of electron-phonon scattering. The ease with which electrons in a semiconductor can be excited from the valence band to the conduction band depends on the bandgap. Different semiconductors have different bandgaps, e.g. silicon has a band gap of 1.11 eV at 300 K and gallium arsenide has a band gap of 1.43 eV at 300 K (Turton, 2000). In general the bandgap in semiconductors is less than 5 eV. There are two well-known types of semiconductor, intrinsic and extrinsic semiconductors (Christman, 1988, Turton, 2000).

2.2.1 Intrinsic and extrinsic semiconductors

Intrinsic Semiconductors:

Intrinsic semiconductors are known as pure semiconductors or undoped semiconductors. The number of charge carriers is therefore determined by the properties of the material itself instead of the amount of impurities and therefore impurities do not affect the electric behaviour of intrinsic semiconductors. Intrinsic semiconductors have

an equal number of electrons and holes (n = p) meaning that there is neither an excess of positive nor negative charge in the system as shown in Figure 2.2. The charge carriers in this type of semiconductor are created by either thermally or optically exciting electrons from a full valence band to the empty conduction band (Christman, 1988, Turton, 2000).

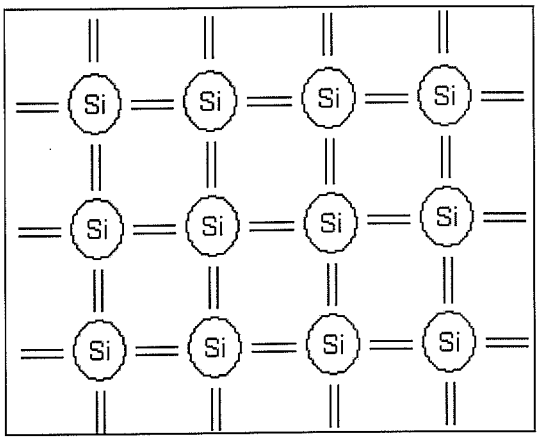

Figure 2.2: Intrinsic silicon semiconductor.

Electrons and holes flow in opposite directions in an applied electric field, though they contribute to current in the same direction since they are oppositely charged. Electron current and hole current are not necessarily equal in an intrinsic semiconductor, because electrons and holes have different effective masses (crystalline analogues to free inertial masses). The concentration of carriers in an intrinsic semiconductor is strongly temperature dependant. At lower temperatures the valence band is completely full and hence the material behaves like an insulator. An increase in temperatures leads to an increase in carriers and hence conductivity increases.

Extrinsic semiconductors:

An extrinsic semiconductor is one which has been doped with impurities to modify the number and type of free charge carriers present. There are many methods that can accomplish controlled doping in crystals. Depending on what impurity the semiconductor is doped with, the electronic properties can become dominated by electron or hole conduction, or at least the balance of carriers is adjusted. Doping is classified into two types n-type doping and p-type doping.

2.2.2 Doping

n-Type doping:

Semiconductors that are doped with a predominant number of donor impurities are known as n-type materials. A donor impurity is an atom that has one more valence electron than the atom it replaces. An example of this is a phosphorus atom in silicon. Phosphorus has five valence electrons and silicon has four. Considering a silicon crystal, each atom uses four valence electrons to form a covalent bonds with four neighbouring atoms. If a phosphorus atom is substituted for one of the silicon atoms, the phosphorus atom forms bonds with the four neighbouring silicon atoms thus leaving one electron over as shown in Figure 2.3 (Turton, 2000).

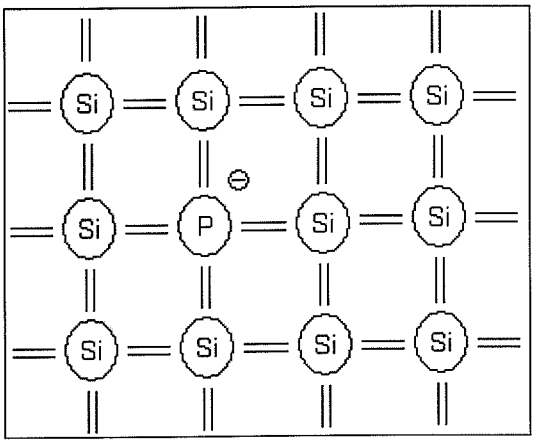

Figure 2.3: Silicon atoms doped with phosphorus.

p-Type doping:

p-Type doping is the opposite of n-type doping. n-Type doping involves introducing donor impurities into a crystal, whereas in p-type doping an excess amount of acceptor impurities or atoms are introduced. An acceptor atom has one fewer valence electrons than the atom it replaces. Electrons from the host are shared with the guest acceptor and so the valence band is partially depleted. The introduction of the holes in the valence band renders the other electrons more mobile, as there are additional energy states into which they can move. Figure 2.4 illustrates the difference between n-type and p-type doping. An example of p-type doping is when an aluminium atom is introduced to a silicon lattice. Aluminium has just three valence electrons. The presence of an incomplete band means that there is a hole in the valence band. This statement is not quite true as the hole is bound to the acceptor impurity, just as in the previous case where the extra electron is bound to the donor impurity. In order to create a hole, which can move through the valence band, a valence electron needs to be excited into this incomplete bond so as to ionise the acceptor impurity. The acceptor state is just above

the valence band as shown in Figure 2.4. It is assumed that all acceptors are ionised at room temperature (Christman, 1988, Turton, 2000).

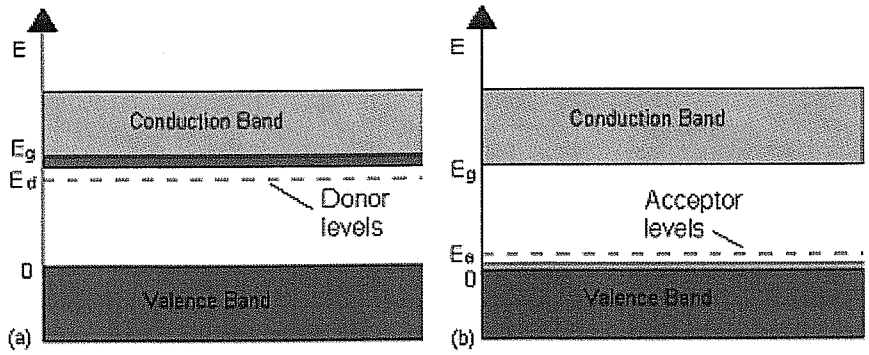

Figure 2.4: (a) n-Type doped material and (b) p-Type doped material.

2.3 p-n Junctions

As discussed previously, silicon can be doped with phosphorus or aluminium to produce an n-type or p-type semiconducting material. It is possible to place an n-type and a p-type material together. This is known as a p-n junction. The n-type region is electron rich and the p-type is electron deficient. In contact the electrons diffuse from the n-type region into the p-type region. The diffusion is limited by the lattice ions from where the electrons originate and an equilibrium distribution is established. This distribution can give rise to preferential directionality of current flow in, for example a p-n junction diode (diodes and their characteristics are discussed in greater detail in Chapter 3). p-n Junctions are the basis for most semiconductor devices ranging from bipolar transistors to optoelectronic devices (e.g. LED's and photovoltaic cells). The device most relevant to this work is a photovoltaic cell (PV cell). It should be noted that one could not simply make a p-n junction by placing n-type and p-type material into contact as lattice

matching is essential. A p-n junction is fabricated by taking a single crystal and introducing donor impurities into one region and acceptor into another. This is usually done by ion implantation into the pristine material.

2.4 Photovoltaic devices

The discovery of the photovoltaic (PV) effect is commonly ascribed to Becquerel who discovered a photocurrent when platinum electrodes, covered with silver bromide or silver chloride, were illuminated in aqueous solution (strictly speaking this is a photoelectrochemical effect) (Becquerel, 1839). A modern day photovoltaic cell is a semiconductor device consisting of a large area p-n junction diode, which in the presence of sunlight is capable of generating usable electrical energy. In the early 1950's, Bell Laboratories began a search for a dependable way to power remote communication systems. Bell scientists discovered that silicon, the second most abundant element on earth, was sensitive to light and, when treated with certain impurities, generated a substantial voltage. By 1954, Bell Labs developed a silicon-based photovoltaic cell that achieved six percent efficiency. In the 1980's the first polymers (including poly (sulfur nitride) and polyacetylene) were investigated in PV cells (Skotheim, 1986). A major breakthrough came in 1986 when Tang discovered that bringing a donor and an acceptor together in one cell could dramatically increase the power conversion efficiency to 1 % (Tang, 1986). Since then scientists have been looking at more novel ways of producing PV cells with greater quantum efficiency and longer life times. However most PV cells these days are still made up of silicon as it has a higher efficiency than most organic materials.

2.5 Inorganic photovoltaic cells

Inorganic PV cells are currently the mostly widely used cells. The power conversion efficiency of a Silicon PV cell is around 25 % (EuroAsia Semiconductor, 2008). Figure 2.5 shows the schematic of an inorganic PV cell. When a photon of light is absorbed by the silicon cell (this will happen if the photon energy is greater than the bandgap energy of silicon) its energy is given to an electron in the crystal lattice. Usually this electron is in the valence band, and is tightly bound by covalent bonds between neighbouring atoms, and hence unable to move. The energy given to it by the photon excites it into the conduction band, where it is free to move around within the semiconductor. The covalent bond that the electron was previously a part of now has one less electron thus creating a hole.

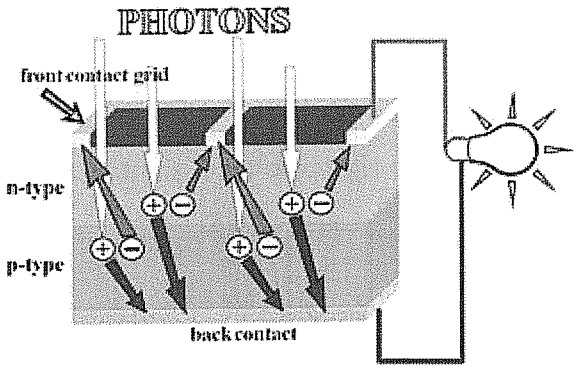

Figure 2.5: The absorption of photons creates electron-hole pairs, which diffuse to the electrical contacts and can be extracted to power electrical devices (picture taken from Solar Navigator web site, 2008).

The presence of a missing covalent bond allows the bonded electrons of neighbouring atoms to move into the hole, leaving another hole behind and in this way a hole can move through the lattice (Myers, 2001). Thus, it can be said that photons absorbed in

the semiconductor create mobile electron-hole pairs. A photon only needs to have energy greater than the band gap energy to excite an electron from the valence band into the conduction band. Although the electron and hole are still bound by electrostatic interaction, they can be separated in the presence of an electric field giving rise to an electrical potential or photovoltaic response. In p-n junctions, the field is internally generated by the charge distribution generated by the dopant ions. The main problem however with this current technology is the high cost of production associated with silicon, which has forced researchers to look towards cheaper materials such as conjugated polymers as alternative systems.

2.6 Electronic structure in conjugated polymers

The structure and bonding of conjugated polymers plays a pivotal role in determining their optical and electronic properties. A carbon atom has six electrons, which occupy $1s^2$, $2s^2$, and $2p^2$ atomic orbitals. The $1s^2$ orbital contains two strongly bound electrons and are known as the core electrons. Four electrons occupy the $2s^22p^2$ orbitals, and these weakly bound electrons are valence electrons. Chemical bonding can be described in terms of atomic orbital hybridisation. In carbon based molecules and the polymers that are relevant to this study, atomic orbital hybridisation involves the mixing of the four valence orbitals, 2s, $2p_x$, $2p_y$ and $2p_z$. This type of hybridisation is known as sp^n hybridisation and can occur in three forms (Barford, 2005).

The first type of bonding known as sp hybridisation involves linear molecules such as acetylene (H-C≡C-H). There are two sp hybrids per carbon atom, formed from mixing of the 2s and 2p orbitals to form sigma (σ) bonds. σ bonds are strong and are responsible for the molecular or crystalline structure. Figure 2.6 shows a schematic

representation of this in which it can be seen that the two σ orbitals are orientated at 180° to each other giving rise to the linear symmetry of such molecules. The remaining $2p_x$ and $2p_z$ are not hybridised and are known as pi (π) orbitals as they overlap with one another across the carbon-carbon bond. π bonds are weaker bonds and as the electrons are weakly bound they contribute significantly to the electronic and optical properties of the polymer.

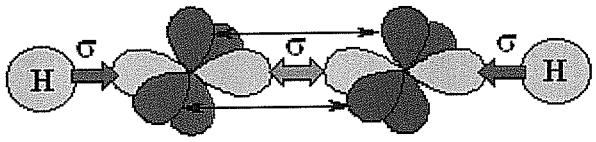

Figure 2.6: Bonding orbitals in acetylene. The carbon sp hybrid orbitals are shown in light blue, with the unhybridised p_y and p_z orbitals shown in dark blue and red. The red arrows indicate the σ bonding between the carbon and the hydrogen atoms. The green arrows shows the overlap of the sp hybrid orbitals of the carbon atoms to form a σ bond between them and the black arrows show the overlap of the unhybridised 2p orbitals to create two π bonds (Carey and Atkins, 2002).

In the second type of orbital hybridization there are three sp hybrids created per carbon atom, utilising the 2s, $2p_x$ and $2p_y$ orbitals. The orbitals form the basis for double bond carbon molecules such as ethene (H_2-C=C-H_2) as shown in Figure 2.7. The first σ hybrid orbital is constructed from the 2s and 2p orbitals. The remaining two hybrid orbitals are created from a mixing of all three orbitals. The first σ orbital lies along the x-axis of the molecule and the two remaining orbitals lie on a plane at an angle of ±120° with respect to each other. The unhybridised $2p_z$ orbital is arranged perpendicular to the plane of the molecule and with the σ orbitals form the double bond between the two carbon atoms.

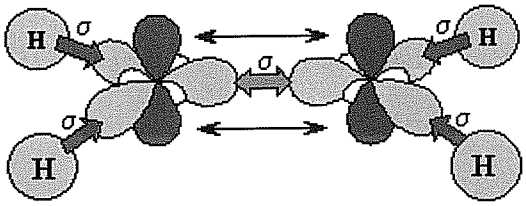

Figure 2.7: The electron orbital structure of ethene. The light blue carbon orbitals are those created by the hybridization of the 2s, $2p_x$ and $2p_y$ orbitals. The dark blue orbitals are the $2p_z$ orbitals. The red arrows indicate σ bonding between the carbon and hydrogen atoms. The green arrow shows the overlap of the first σ orbitals to form a σ bond and the black arrows show the overlap of the $2p_z$ orbitals to create a π bond between the carbon atoms. (Carey and Atkins, 2002).

The third type of hybridization involves all of the valence orbitals, resulting in a four sp^3 orbitals per carbon atom forcing the bonds into a tetrahedral arrangement. sp^3 Hybridisation is found in saturated molecules where the bonding is dominated by single carbon-carbon bonds. As this type of orbital hybridization does not leave any unhybridised orbitals, it is incapable of forming π bonds and does not allow for conduction and therefore is not of relevance in the study of conjugated polymers.

2.7 Organic conjugated polymers

The property that gives rise to conductance or charge transfer in a polymer is its alternating single and double bonds between the carbon atoms on the polymer backbone *i.e.* its conjugation, as shown if Figure 2.8. If two π bonds interact and increase delocalisation, the polymer can be said to be conjugated. In larger molecules with extended conjugation, the molecular levels can be grouped into bands and in the limit of

very long conjugation length, the band structure models associated with inorganic semiconductors can be applied. This is the case with organic conjugated polymers (Yu, 1995) which can be referred to as quasi-one-dimensional semiconductors.

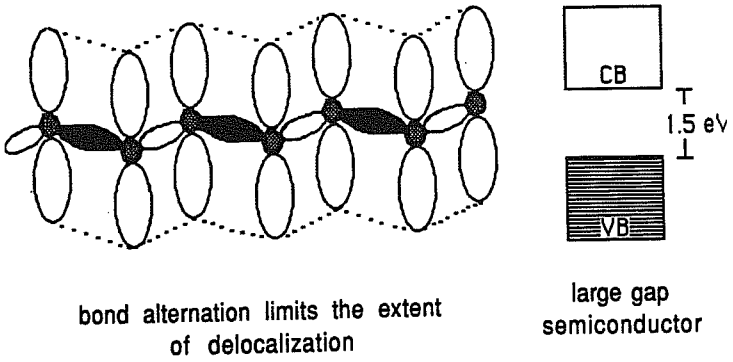

Figure 2.8: Alternation of bond lengths along a conjugated polymer results in a material with the properties of a large gap semiconductor (Dalton, 1999).

2.7.1 Photoexcitation in organic materials

The band structure picture associated with inorganic semiconductors (Section 2.2) can be applied to organic semiconductors. The band edge of the valence band is referred to as the "Highest Occupied Molecular Orbital" (HOMO) and the edge of the conduction band is called the "Lowest Unoccupied Molecular Orbital" (LUMO). The HOMO is a π orbital and the LUMO is a π^* orbital. The energy gap between the HOMO and the LUMO level in conjugated polymers is usually within the range of visible photons (3.55 eV $\rightarrow$1.78 eV). When an incoming photon is absorbed, one of the electrons is promoted into the LUMO level, thus leaving behind a hole in the HOMO. There are two types of excited species that result from this absorption, singlet excitons and polarons (or bipolarons) (Pope, 1995).

An exciton can be considered as a bound electron-hole pair within a solid and may be classified as a Frenkel exciton if the electron-hole pair is located on one lattice site or as a Mott-Wannier exciton if it extends over many. The intermediate case, where the exciton extends over a few adjacent sites is termed a charge transfer exciton (Pope and Swenberg, 1995). In molecular crystals the site is considered a molecular unit and in polymers a monomer unit. Excitons are quasi particles whose properties are determined by the coulomb interaction between the electron in the conduction band and the hole in the valence band.

A polaron is a quasi particle consisting of a charge and the polarisation field that it creates by moving through a medium (Kittel, 2005). Polarons are the result of electron phonon coupling in a crystal. In conjugated polymers, a polaron can be considered as the bound states of the electronic excitation and the nuclear distortion within the backbone. The result of the electron-lattice coupling is the formation of bonding and antibonding polaron levels in the π-π^* energy gap. A bipolaron is the bound state of two polarons. Quasi particles such as solitions, polarons and bipolarons are discussed in greater detail in Chapter 6.

The excited state in a material can thus be energetically influenced by coulomb and/or electron – vibrational interactions in the solid state. In general coulomb interactions are manifest within the Franck – Condon transition lifetime and thus all absorption transitions can be considered excitonic in nature. Electron-vibrational coupling occurs on a longer time scale according to the Born-Oppenheimer approximation and thus polaronic states evolve after the optical transition. Thus in this thesis, an excitonic picture of the excited states is utilised for optical absorption and electroabsorption spectroscopy whereas a polaronic model is used for excited state, doping and charge transfer processes.

2.8 Charge transfer and hetrojunction interface

Whether the excited states in a polymer are better defined as excitons or (bi) polarons the excited electron is bound to the positively charged vacancy, the quasi-particles are neutral and as such do not contribute to electron transport. An essential process for all solar cells after photoexcitation is charge separation. One of the problems with organic materials is that excitations do not dissociate readily and relaxation to the ground state occurs rapidly. In order to overcome this, a heterojunction (donor acceptor interface) is used. The idea behind this is to mimic p-n junctions in organic semiconductors by using two materials with different electron affinities and ionisation potentials. This will increase the probability of exciton dissociation. The main condition for the exciton dissociation to occur is that the electron affinity of the polymer (acceptor) is larger than the ionisation potential of the donor material. As a result, the donor is left with a positive charge that can drift through the film to the anode while the electron in the acceptor material and can be transported to the cathode. Organic polymers have been shown to be effectively intrinsic p-type semiconductors and therefore act as ideal donors in such hybrid systems, the most commonly used p-type conjugated polymer being (2-methoxy-5-(2'-ethylhexyloxy)-1,4 phenylenevinylene) hereafter referred to as MEH-PPV.

An acceptor material which is often used and the one used here is buckminsterfullerene (C_{60}). C_{60} can accept up to six electrons at any given time as will be discussed in greater detail in Chapter 4. Although a molecular insulator, C_{60} has shown metallic and even superconductivity when doped (Hebard, 1991, Haddon, 1991) and an optically pumped insulator to metal transition can also occur (Byrne, 1992, Chambers, 1999). In 1992, Sariciftci *et al.* demonstrated ultra fast charge transfer from conjugated polymers to C_{60}

(Sariciftci, 1992), and since then its properties as an electron acceptor have been widely investigated. Figure 2.9 shows a schematic representation and explanation given by Sariciftci *et al.* of the charge transfer between a polymer fullerene composite using time resolved photoinduced absorption (PIA) spectroscopy (Sariciftci, 1995). Firstly the polymer is excited by a photon of light using an argon ion laser at 50 mW/cm^2. Sariciftci explained the charge transfer process in terms of five steps. The donor (D) and acceptor (A) units are either covalently bound (intramolecular), or spatially close but not covalently bonded (intermolecular); step 1 and step 3 denote the singlet or triplet excited states, respectively (Sariciftci, 1995).

Step 1: $D+A \rightarrow {}^{1,3}D^{*}+A$, (excitation on D);
Step 2: ${}^{1,3}D^{*}+A \rightarrow {}^{1,3}(D\text{-}A)^{*}$, (excitation delocalised on the D-A complex);
Step 3: ${}^{1,3}(D\text{-}A)^{*} \rightarrow {}^{1,3}(D^{\delta+}\text{-}A^{\delta-})^{*}$, (charge transfer initiated);
Step 4: ${}^{1,3}(D^{\delta+}\text{-}A^{\delta-})^{*} \rightarrow {}^{1,3}(D^{+\bullet}\text{-}A^{-\bullet})$, (ion radical pair formed);
Step 5: ${}^{1,3}(D^{+\bullet}\text{-}A^{-\bullet}) \rightarrow D^{+\bullet}+A^{-\bullet}$, (charge separation);

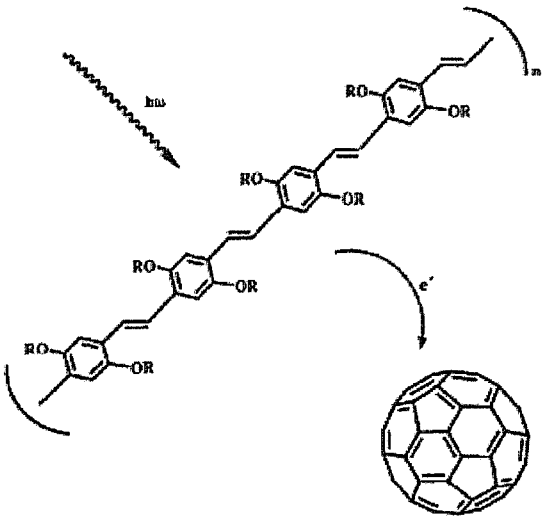

Figure 2.9: Schematic illustration of the photoinduced electron transfer from semiconducting polymers onto C_{60} (Sariciftci, 1995).

The partial charge transfer at Step 3 is strongly dependent on the nature of the surrounding medium, such as the polarity of the solvent *etc.* resulting in a continuous range for the transfer ratio $0 < \delta < 1$. At step 4, a whole electron is transferred, i.e. $\delta = 1$ (Sariciftci, 1995). At each step, the D-A system can relax back to the ground state either by releasing energy to the 'lattice' (in the form of heat) or through light emission (provided the radiative transition is allowed). The electron transfer (Step 4) describes the formation of an ion radical pair; this does not occur unless $I_D^* - A_A - U_C < 0$, where I_D^* is the ionisation potential of the excited state (D*) of the donor, A_A is the electron affinity of the acceptor and U_C is the Coulomb energy of the separated radicals (including polarisation effects) (Sariciftci, 1995). Stabilisation of the charge separation (step 5) can be affected by carrier delocalisation on the D+ (and/or A-) species and by structural relaxation. A highly polar environment can also stabilize charge separation by screening the separated charges (Sariciftci, 1995).

The photoinduced absorption spectrum of pristine MEH-PPV is characterised by subgap electronic absorptions in the infrared region (a lower energy feature superposed with two peaks at 0.25 eV and 0.4 eV and a higher energy feature with onset at 1.1 eV) together with infrared active vibrational (IRAV) modes below the lower energy electronic absorption feature (Sariciftci, 1992, Lee, 1995). The 0.4 eV and 1.1 eV features are assigned to the lower and upper energy bipolaron transitions, another energy peak at 0.25 eV, which is absent in the photoinduced absorption of PPV, is assigned to a lower polaron transition. The interchain transport is inhibited by large interchain separation leading to the suppression of bipolaron formation; the early time recombination is enhanced, resulting in a weak spectral response (Sariciftci, 1992, Lee, 1995). The photoinduced absorption spectrum of the MEH-PPV/C_{60} composite changes the infrared spectrum dramatically. First the overall strength of the PIA spectrum (both

electronic subgap and the associated IRAV modes) is increased by two orders of magnitude. Secondly new peaks were observed at 1.15 eV and 1.25 eV together with a bleaching at around 1 eV. The increase in oscillator strength of the IRAV modes and the subgap electronic excitations in polymer/C_{60} result from photoinduced electron transfer, which improves the quantum efficiency for charge carrier generation and suppresses recombination (Sariciftci, 1992, Lee, 1995). As a result more charged excitations live for longer times, thereby leading to an increase in strength of the PIA signals by two orders of magnitude upon adding C_{60} to the polymer and hence the appearance of the bands at 1.15 eV and 1.25 eV which are associated with C_{60}^{-}(Sariciftci, 1992, Lee, 1995). To distinguish the spin multiplicity photoinduced absorption magnetic resonance experiments were performed. The PIA band at 1.35 eV in pristine MEH-PPV shows a strong response at the (forbidden) half field resonance of spin = 1, indicating triplet character for this PIA band and dominance of the neutral photoexcitations in MEH-PPV (Sariciftci, 1992). There is a small spin, residual spin = ½ response even with the pure MEH-PPV. Upon adding of the C_{60}, the triplet signal for the 1.35 eV PIA band is completely quenched. Instead a strong spin = ½ signal dominates, indicating charged polarons as photoexcitations on the polymer donor. This confirms that the photoinduced electron transfer occurs on a time scale sufficiently fast to quench the intersystem crossing to the triplet state (Sariciftci, 1992).

The charge transfer typically occurs within the femtosecond (fs) time regime. An upper time limit of 300 fs was established (Kraabel, 1994), which is three orders of magnitude faster than any electron-hole recombination process within the polymer. As said previously the charge transfer range is about 10 nm. Therefore it is essential the C_{60} be close to the polymer for a charge transfer to occur.

However there has been some controversy over the mechanism leading to the charge transfer from the polymer to the fullerene. Halls *et al.* (Halls, 1996) suggested that the singlet excitons diffuse from the location of photoexcitation to the polymer-fullerene interface and are dissociated at the interface. They studied the PV response in devices prepared from poly (phenylenevinylene) (PPV) and C_{60} and modelled the photocurrent spectra under the assumption that all absorbed photons create singlet excitons and all singlet excitons within the diffusion range of the interface are dissociated and contribute to the photocurrent. From the quantitative agreement of the modelled current spectra and the experimental spectra they deduced a diffusion range of 6-8 nm and it was concluded by Halls *et al.* (Halls, 1996) that the agreement was strong evidence for the diffusion model. Vacar *et al* (Vacar, 1997) however disputed this model. From transient photo-induced absorption experiments on MEH-PPV/C_{60} bilayer films, they found that the ultra fast charge transfer occurs on a picosecond time scale. Using this time scale and a diffusion range of 10 nm, the necessary diffusion constants and mobilities in the polymer would have to be much higher (at least 2 orders of magnitude) than they are known to be. Instead, they suggest that the wave functions of the primary excitations on the polymer must be spatially extended over 10 nm to explain the rapid charge transfer. Further analysis of their data leads to a charge transfer range of approximately 8 nm in the MEH-PPV/C_{60} system. Although this argument remains unresolved, the charge transfer range was determined to be the same in both models. This thesis does not resolve this above issue, as it is not essential to the work. The transfer range, which is of importance, was assumed to be in the range of 8-10 nm. Therefore it is assumed that if the acceptor material (C_{60}) was within 10 nm of the photoexcitation, the probability of charge transfer was close to unity because it is 3 orders of magnitude faster than the

competing recombination processes. Back transfer onto the polymer does not occur, which makes the charge separated state metastable (Sariciftci, 1992).

In general there are two ways in which to create a heterojunction interface organic device. The first is to bring two films together. The films are contacted at the surface, which creates a heterojunction. In this case, only a fraction of the bulk of the materials within 10 nm of the interface builds a donor acceptor interface. The second way is to mix the two materials to form a single mixed layer. With a mixed single layer the whole bulk of the device has a donor-acceptor interface. These devices are known as bulk heterojunction devices. There are various methods to achieve this. Blending the materials in a solution and then spin coat the solution onto an electrode (which is the process used throughout this study), interdiffusion of the two materials or evaporation of both materials are alternative methods (Yu, 1995).

2.9 Organic photovoltaic cells

Organic photovoltaic cells are comprised of electron donor and electron acceptor materials rather than semiconductor p-n junctions. Compared to silicon-based devices, polymer solar cells are lightweight, disposable, inexpensive to fabricate, flexible, customisable on the molecular level, and have lower potential for negative environmental impact. Organic photovoltaic cells usually consist of a hetrojunction. As aforementioned a hetrojunction is basically a device with two materials in conjunction with each other. In the case of organic PV cells, one material is the semiconducting polymer and the second is an acceptor material (C_{60}). In general it is analogous to p-doping a material as explained in Section 2.2. Figure 2.10 shows an organic PV cell consisting of MEH-PPV and C_{60}.

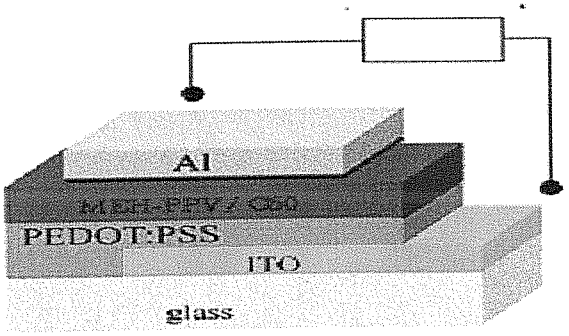

Figure 2.10: Organic photovoltaic cell consisting of MEH-PPV and C_{60}.

As well as having the MEH-PPV/C_{60} layer the cell also consists of a layer of poly (styrenesulfonate)/poly (2,3-dihydrothieno(3,4-b)-1,4-dioxin) (PEDOT, Chapter 3). The PEDOT has a higher workfuction than the indium tin oxide (ITO) and provides a better alignment of the workfuction with the HOMO level and thus acts like a charge injecting layer within the device.

Figure 2.11 shows the energy level diagram for an MEH-PPV/C_{60} heterojunction device (note HOMO-LUMO levels are not to scale, *i.e.* approximation). The ITO and aluminium have well known workfunctions of 4.8 eV and 4.2 eV respectively. The HOMO-LUMO levels of MEH-PPV are well know from literature, however for the purpose of this project they will be calculated in Chapter 4 using cyclic voltammetry. Once these values are obtained in Chapter 4 they will then be compared to the literature values. At this moment of the study it is not possible to determine the device properties without the exact HOMO-LUMO levels. For example does the position of the HOMO level provide good hole blocking properties to the device. In order for a device to contain good hole blocking properties it is desirable that the HOMO level of the polymer be greater than that of the ITO.

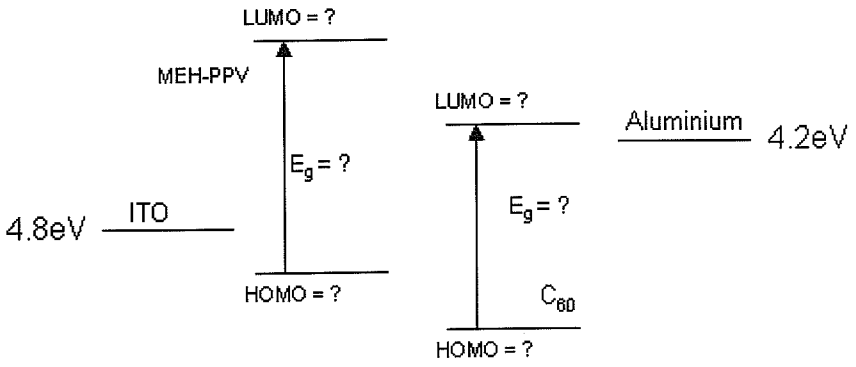

Figure 2.11: Energy level diagram of MEH-PPV and C_{60} device.

Upon electron doping hole carriers are created along the polymer backbone. The higher the HOMO level the harder it is to generate a hole-carrier. Reductions of the population of hole carriers improves charge separation as the electron carriers have fewer holes to recombine with. The bandgap relationship of donor acceptor composites is still not fully understood. The exact HOMO-LUMO levels of each material are also required in order to investigate the charge transfer mechanisms.

2.10 Structural relationships and polymer series

Over the past fifteen years a number of polymers have been shown to be capable of charge transfer with C_{60} (Sariciftci, 1992, Kraabel, 1994, Frankevich, 1996, Hoppe, 2004, Cheyns, 2007). The choice of polymer has been somewhat random however and few structure property relationships have been established to contribute to the further understanding and optimisation of charge transfer mechanisms with respect to the different polymers. This study proposes to explore the charge transfer between a set of conjugated polymers that have been systematically synthesised and C_{60}. Such investigations should help in understanding the role of structure property relationships

in the final application of a material. The polymer series to be used will be initially characterised to investigate their inherent properties, *i.e.* the optical and electronic solid properties and correlations to their structure will be made. This characterisation will be performed in both solution and solid phases. The information gathered will assist in the investigation and identification of any charge transfer mechanisms when composites are formed with C_{60}. Detailed analysis of the composites and pristine polymer will thus allow the development of a systematic approach to device design beginning with the fundamental design of the materials.

The conjugated polymers used in this study are a relatively newly synthesised set of PPV derivatives The polymer systems investigated were (poly (para-2,5-bis-(n-octyloxy)- phenylenevinylene), POPV (1), Poly(2,5-bis(n-octyloxy)-1,4-phenylene vinylene-1,5-bis(octyloxy)- 2,6-naphthylene vinylene), POPV-ONV (2); Poly(2,6-bis-(n-octyloxy)-1,5-NaphthyleneVinylene), PONV (3); Poly(2,5-bis(n-octyloxy)-1,4-phenylene vinylene-co-1,5-bis(n-octyloxy)-2,6-anthracene vinylene), POPV-OAV (4) and Poly(2,5-bis(n-octyloxy)-1,5-naphthylenevinylene-co-1,5-bis(n-octyloxy)-2,6-anthracene vinylene), PONV-OAV (5). Synthesis of the novel polymers 1-5 have been published elsewhere (Lynch, 2006). Figure 2.12 shows the molecular structures of the polymers. The octyloxy substituted PPV derivative POPV (1) was first synthesised. The structure of the polymer was then varied. The introduction of naphthyl units begins first by replacing alternate phenyl units with naphthyl units in POPV-ONV (2) and finally all phenyl units are replaced to produce a fully conjugated naphthalene polymer, PONV (3). All side chains were maintained in equivalent positions in the polymer studied. Anthryl units were then introduced into the polymer. This was done in the same manner as the naphthalene structures, first with alternating phenyl units (4) and then with alternating naphthyl units (5) (Lynch, 2006). The polymers have been previously

characterised in their molecular form (O'Neill, 2007) and it was seen that their bandgaps and photophysical properties can be related to the systematic structural changes.

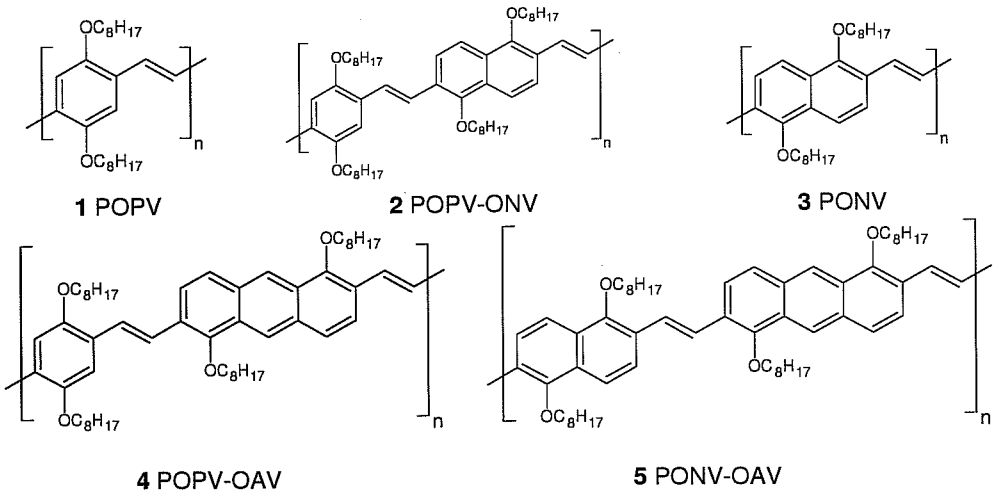

Figure 2.12: Molecular structure of conjugated polymers.

Table 2.1 provides a summary of the results of electronic spectroscopic investigations of the solution form of the polymer series. The absence of any reported solvato-chromic behaviour indicates that the solvated polymers are a good approximation to isolated molecules. The sequential replacement of the phenyl units by naphthyl units resulted in an increasing hypsochromatic shift of both the absorption and emission spectra, indicating a disruption of the conjugation by the larger naphthyl units. The replacement of the naphthyl units by anthryl in the POPV-OAV polymer reverses this trend. In order to understand this behaviour, empirical relationships were found to accurately predict the bandgap of the polymer series based on a extension of the Donor-Acceptor model of dual effects proposed by Meier *et al.* (Meier , 2005) in which the competing effects of donating or accepting substituents in a conjugation chain were calculated. In the

polymer series in Figure 2.9, although the acene units of increasing length are intrinsically more conjugated, they can be electron withdrawing or donating with respect to the vinyl bond and a balance between the increased conjugation and the contribution to the extended backbone conjugation determines the electronic properties of the polymers.

Table 2.1: Electronic properties of polymer series in solution form.

	Optical Bandgap	Emission Energy	
Polymer	**Solution / eV**	**Solution / eV**	**Stokes Shift / eV**
POPV	2.41	2.27	0.14
POPV-ONV	2.58	2.43	0.15
POPV-OAV	2.48	2.38	0.10
PONV	2.81	2.69	0.12
PONV-OAV	2.63	2.53	0.10

An electron affinity (EA) parameter, a sum of the electron affinities of the constituent components was calculated for each of the polymers. A plot of bandgap of each polymer against the calculated EA value resulted in a linear relationship and hence the formulation of the electronic structure-property relationship for complex polymers akin to the much vaunted inverse conjugation length relationship found in short chain oligomers. The observed correlation of the Stokes shift to the EA parameters is an indication that changes to the electronic structure as a result of structural progression are mirrored in the vibrational structure (Lynch, 2006, O'Neill, 2007) and this can be extended to the vibrational spectroscopy. The controlled variation of the polymer properties could provide an ideal situation for probing mechanisms of charge transfer in the polymer/C_{60} composites. Changes in bandgaps, electron affinities and ionisation

potentials due to the structural variations may result in a more efficient interaction with C_{60}.

2.11 Transient vs Steady state spectroscopy

Time resolved spectroscopy is still considered to be the most effective way of investigating charge transfer between polymer/fullerene composites. However time resolved spectroscopy is expensive and is not readily available. This study proposes to use steady state spectroscopic techniques coupled with electrochemical and conductivity measurements to characterise charge transfer signatures in polymer fullerene composites. Some steady state techniques such as fluorescence and Electroabsorption spectroscopy have already be utilised to show charge transfer between fullerene polymer composites.

Fluorescence quenching in conjugated polymer systems upon addition of C_{60} has been shown to be consistent with efficient photoinduced electron charge transfer (Morita, 1992, Sariciftci, 1992). Also Liess *et al.* has shown the formation of bound pairs of MEH-PPV and C_{60}^{-} during electroabsorption measurements (Liess, 1997). These bound pairs of MEH-PPV/C_{60} coexist with a broadening of the first excitonic electroabsorption band due to the energy distribution. These methods will be explored in a model system and charge transfer signatures will be examined and the techniques will be applied to the novel system of polymers to observe if there are similar charge transfer markers in the new polymer/C_{60} composites.

2.12 Summary

Conjugated polymers have been shown to be effectively intrinsic p-type semiconductors and can therefore act as ideal donors in photovoltaic hybrid devices. In order to achieve efficient charge separation in polymer devices, an acceptor material must be included. C_{60} is the ideal acceptor material as it can accept up to six electrons. The discovery of charge transfer between MEH-PPV and C_{60} in 1992 led to intense research involving conjugated polymers and their interaction with C_{60}. Firstly this study proposes to replace time resolved photoinduced absorption spectroscopy with steady state spectroscopic techniques, electrochemical and conductivity measurements. These steady state techniques will be used to characterise charge transfer signatures between MEH-PPV/C_{60}. Identification of charge transfer indicators using these techniques may eliminate the need for time resolved spectroscopy which is expensive (and not readily available). Over the past twenty years a number of different types of organic polymers have been shown to charge transfer with C_{60}. The choice of polymer has been somewhat random and few structure property relationships have been established to further understand and the charge transfer mechanisms with respect to the different polymers. Here a more systematic approach will be taken to investigate the charge transfer interaction between conjugated polymers and C_{60}. The next chapter gives a detailed explanation and description of the experimental techniques used throughout this study.

References:

Barford W, *"Electronic and Optical Properties of Conjugated Polymers"*, Oxford University Press, (2005).

Becquerel A.E., Compt. Rend. Acad. Sci. 9, p. 145. (1839).

Becquerel A.E., Compt. Rend. Acad. Sci. 9, p. 561. (1839).

Burroughes J.H., Bradley D, Brown A.R., Marks R.N., Mackay K, Friend R.H., Burn P.L., Holmes A.B., *"Light-emitting diodes based on conjugated polymers"*, Nature, 539, 347 (1990).

Byrne H.J., Maser W.W., Rühle, Mittelbach A, Roth S, *"Nonlinear Luminescence Phenomena in Fullerene Crystallites"*, Appl. Phys. A, 56, 235 (1992).

Carey F, Atkins R, *"Organic Chemistry: A Brief History 3rd Edition"*, McGraw-Hill, Inc, (2002).

Chambers G, Byrne H.J., *"Raman spectroscopic study of excited states and photo-polymerisation of C_{60} from solution"*, Chem Phys Lett. 302, 307, (1999).

Cheyns D, Gommans H, Odijka M, Poortmans J, Heremans P, *"Stacked organic solar cells based on pentacene and C_{60}"*, Solar Energy Materials & Solar Cells, 91, 399, (2007).

Christman J.R., *"Fundamentals of Solid-State Physics"*, John Wiley & Sons Australia, Limited Publication, (1988).

Dalton A.B., *"Morphological Influences on the Excited State Dynamics of Conjugated Polymers"*, PhD Dissertation, Trinity College, Dublin, (1999).

EuroAisa Semiconductor, Vol 30, 3, (2008).

Frankevich E.L., Zakhidov A, Yoshino K, *"Photoconductivity of poly (2,5-diheptyloxy-p-phenylenevinylene) in the air atmosphere: Magnetic field effect and mechanism of generation and recombination of charge carriers"*, Phys. Rev. B 53, 4498, (1996).

Friend R.H., Gymer R.W., Holmes A.B., Burroughes J.H., Marks R.N., Tiliani C, Bradley D, Santos D.A., Bredas J.L., Logdlund M, Salaneck W, *"Electroluminescence in conjugated polymers"* Nature, 121, 397, (1999).

Haddon R.C., Hebard A.F., Rosseinsky M.J., Murphy D.W., Duclos S.J., *"Conducting films of C_{60} and C_{70} by alkali-metal doping"*, Nature, 350, 320, (1991).

Halls J.J.M., Pichler K, Friend R.H., Moratti S.C., Holmes A.B., *"Exciton diffusion and dissociation in a poly(p-phenylenevinylene)/C_{60} heterojunction photovoltaic cell"*, Appl. Phys. Lett. 68 (22), 3120, (1996).

Hebard A.F., Rosseinsky M.J., Haddon R.C., Murphy D.W., Glarum S.H., Palstra T.T.M., Ramirez A.P., Kortan A.R., *"Superconductivity at 18K in potassium-doped C_{60}"*, Nature, 350, 600, (1991).

Hoppe H, Egbe D.A.M., Muhlbacher D , Sariciftci N.S., *"Photovoltaic action of conjugated polymer/fullerene bulk heterojunction solar cells using novel PPE-PPV copolymers"*, Journal of Material Chemistry, 14, 3462, (2004).

Kittel C, *"Introduction to Solid-State Physics"*, John Wiley & Sons Australia, (2005).

Kraabel B, McBranch D, Sariciftci N.S., Moses D, Heeger A.J., *"Ultrafast spectroscopic studies of induced electron transfer from semiconducting polymers to C_{60}"*, Phys. Rev. B 50, 18543, (1994).

Lee K, Sariciftci N.S., Heeger A.J., *"Infrared photoexcitation in soluble derivatives of poly (p-phenylenevinylene) and composites with C_{60}"*, Synthetic Metals, 69, 445, (1995).

Liess M, Jeglinski S, Vardeny Z.V., *"Electroabsorption spectroscopy of luminescent and nonluminescent π-conjugated polymers"*, Phys. Rev. Lett, Vol 56, 2415, (1997).

Lynch P, O'Neill, L McNamara M, Byrne H. J., *"A Systematic Study of the Effects of Naphthalene and Anthracene Substitution on the Properties of PPV Derivative Conjugated Systems"*, Macromolecules, 40, 7895, (2007).

Meier H, *"Conjugated Oligomers with Terminal Donor-Acceptor Substitution"*, Chem. Int. Ed., 44, 2482, (2005).

Morita S, Zakhidov A.A., Yoshino K, *"Doping effect of buckminsterfullerene in conducting polymer: Change of absorption spectrum and quenching of luminescence"*, Sol. State Commun, 82, 249, (1992).

Myers H.M., *"Introductory Solid State Physics, Second Edition"*, Oxford University Press, (2001).

O'Neill L, Lynch P, McNamara M, Byrne H.J., *"Spectroscopic Characterisation of Novel Polycyclic Aromatic Polymers"*, J. Phys.Chem A, 111 (2), 299-305, (2007).

Pope M, Kallmann H.P., Magnante P, *"Electroluminescence in organic crystals"*, J Chem. Phys, 38, 2042, (1963).

Pope M and Swenberg C.E., *"Electronic Processes in Organic Crystals"*, Oxford University Press, (1995).

Sariciftci N.S., Smilowitz L, Heeger A.J., Wudl F, *"Photoinduced electron transfer from a conducting polymer to buckminsterfullerene"*, Science 258, 1474-1476 (1992).

Sariciftci N.S., *"Role of Buckminsterfullerene, C_{60} in Organic Photoelectric Devices"*, Prog. Quant. Electr, 19, 131, (1995).

Shim H.K., Jin J.I., *"Light-Emitting Characteristics of Conjugated Polymers"*, Adv. Polym. Sci, 158, 194 (2002).

Shirakawa H, Louis E.J., MacDiarmid A.G.; Chiang C. K; Heeger A.J., *"Synthesis of electrically conducting organic polymers: halogen derivatives of polyacetylene,$(CH)_x$"*, J. Chem. Soc., Chem. Commun, 578, (1977).

Skotheim T.A., *"Handbook of Conducting Polymers"*, Vol. 1 and 2, Marcel Dekker, New York, (1986).

Solar Navigator, http://www.solarnavigator.net/images, 03/07/08, (2008).

Tang C.W., *"Two layer organic photovoltaic"* Appl. Phys. Lett. 48, 183, (1986).

Turton R, *"The Physics of Solids"*, Oxford University Press, (2000).

Vacar D, Maniloff E.S., McBranch D.W., Heeger A.J., *"Charge-transfer range for photoexcitations in conjugated polymer/fullerene bilayers and blends"*, Phys. Rev. B 56(8), 4573 (1997).

Yu G, Gao J, Hummelen J.C., Wudl F, Heeger A.J., *"Polymer photovoltaic cells: enhanced efficiencies via a network of internal donor-acceptor heterojunctions"*, Science, 270, 1789, (1995).

Chapter 3: Experimental Methodology

3.1 Introduction

In this chapter a general description of the various materials, instruments and techniques used throughout this study is given. A broad range of instruments and procedures have been used and adapted throughout the course of this study and where necessary further details about specific experimental set-ups will be described in the relevant chapters. Firstly the materials used throughout this study are described, followed by the experimental techniques. These techniques include electronic spectroscopy and electroabsorption spectroscopy, cyclic voltammetry, in-situ spectroelectrochemistry, conductivity measurements and simple crude device fabrication.

3.2 Materials

Poly(2-methoxy-5-(2'-ethylhexyloxy)-1,4 phenylenevinylene), (MEH-PPV)

The semiconducting polymer poly (2-methoxy-5-(2'-ethylhexyloxy)-1,4 phenylenevinylene), has been intensely studied over the last decade for application in organic light emitting devices (Braun, 1991, Parker, 1994, Scott, 1996) as well as organic photovoltaic devices (Sariciftci, 1993, Harrison, 1997, Dittmer, 1999). Figure 3.1 shows the structure of MEH-PPV. It is a soluble derivative of the insoluble poly (phenylene vinylene) (PPV). The MEH-PPV used in this study is a copolymer purchased from Sigma Aldrich (product number 541435). The material was used as purchased with no further purification.

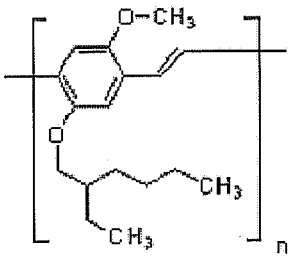

Figure 3.1: Structure of MEH-PPV.

Acceptor material: Buckminsterfullerene (C_{60})

Discovered in 1985 (Kroto, 1985) fullerenes have become more readily available over the past 20 years due to improving synthetic techniques. Fullerenes can be synthesized by virtually any high temperature process that produces carbon atoms in the gas phase and provides annealing for clusters of the carbon atoms into linear carbon chains and monocyclic rings of C_2 to C_{18}. These can then assemble themselves into fullerene molecules Cn, where n = 60, 70, 84 *etc.* A C_{60} molecule or "buckyball" is about 7 Å in diameter and is the most common fullerene, and thus the most-researched. Figure 3.2 shows the structure of C_{60}, highlighting the soccer ball or truncated icosahedral shape. It is the shape and size of the C_{60} molecule coupled with its electronic properties that makes the molecule attractive as an acceptor material in organic PV systems. The C_{60} fullerenes used in this study were purchased form Sigma Aldrich (product number 572500) and have a purity of 99 %.

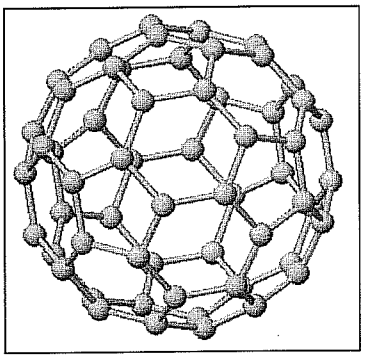

Figure 3.2: The proposed truncated icosahedron shape of C_{60}, with 20 hexagons and 12 pentagons (Kroto, 1985).

3.3 Introduction to spectroscopy

Spectroscopy is the utilisation of the absorption, emission, and scattering of electromagnetic radiation by matter, for the identification and elucidation of material properties. The interaction of electromagnetic radiation with matter causes energy to be absorbed emitted or scattered in discrete amounts or quanta. Spectroscopic investigation can allow a range of information to be deduced such as the electronic and vibrational character of a material and the perturbation, if any of these properties due to a change in the local environment. Spectroscopic characterisation of the materials used in this research involved using two well-established techniques. The first technique used was electronic spectroscopy. The second spectroscopic technique used in this study was electroabsorption spectroscopy which is described in the latter parts of the chapter.

3.4 Electronic spectroscopy: Absorption and Emission

Absorption and fluorescence spectroscopy examine the electronic transitions within a molecule or solid and hence provide information about the electronic structure of a material and its local environment. The absorption and emission of light by an organic molecule can be depicted by the Jablonski diagram in Figure 3.3. The act of absorption involves the interaction of electromagnetic radiation with the chromophores of a molecule. The energy separation of the ground state (highest occupied molecular orbital or HOMO) and the lowest lying excited state (lowest unoccupied molecular orbital or LUMO) in conjugated materials is determined by conjugation length and any effects of electron donating or retracting substituents (Pope and Swenberg 1999). Since in organic materials the bonds are formed by the binding of two singly occupied, spin paired electronic states, the HOMO is normally a singlet state, S_0. The initial absorption step takes the molecule to an excited electronic state. A photon has zero spin and therefore the transition is to a state of the same spin multiplicity, the lowest lying of which is the first excited singlet state, S_1. Since electronic transitions take place on a much faster time scale than nuclear motion, most electronic transitions are completed before the nuclei can alter their spatial relationships to the new electronic configuration. Such a transition is denoted as a Franck-Condon transition and is indicated in Figure 3.3 by the solid lines. The Franck-Condon principle states that an electronic transition occurs so rapidly in comparison with vibration frequencies that no change occurs in inter-nuclear separation during the course of the transition (Wayne, 1970). After excitation of the molecule to an upper vibronic state, the nuclear coordinates are not in their equilibrium configuration for the new electronic state and hence non-radiative relaxation between the vibrational states occurs.

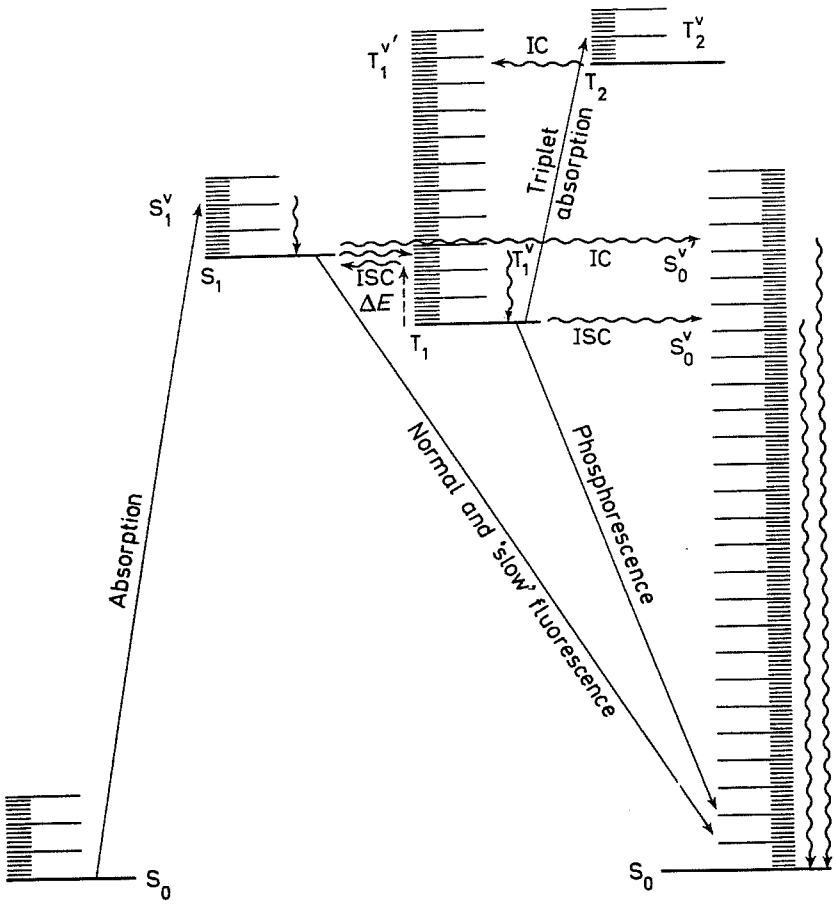

Figure 3.3: Jablonski diagram showing the sequence of steps leading to radiative decay (Wayne, 1970). After initial absorption the upper excited vibrational states undergo non radiative decay by giving up energy to the surroundings. A radiative transition then occurs from the lowest vibrational level of the excited electronic state (Wayne, 1970). S_0 is the singlet ground electronic state and S_1 is the singlet excited electronic state; with T_1 representing the triplet state. ISC and IC represent intersystem crossing of an electron from the S_1 to T_1 excited states or vice versa and internal conversion where the electron orients itself so that it may return from T_1 to S_0 respectively.

Generally, after relaxing to the lowest vibrational state, the electron can return to the ground state by emitting the excess energy as a photon or by radiationless channels of decay. The emitted photon is characteristically of longer wavelength than that of the exciting light, the difference being the Stokes shift. The wavy horizontal lines in Figure

3.3 represent radiationless energy conversion. The vertical wavy lines within a particular electronic state indicate degradation of vibrational excitation, while the horizontal wavy lines indicate changes of state. The term "internal conversion" is applied to radiationless transitions between states of the same spin multiplicity, while "intersystem crossing" refers to transitions between states belonging to different spin systems (Wayne, 1970). Deactivation through emission of radiation can happen in one of two ways. These two processes were originally distinguished in terms of whether or not there was an observable afterglow. In 1935, Jablonski interpreted phosphorescence as being emission from some long lived metastable electronic state lying lower in energy than the state populated by the absorption of radiation (Wayne, 1970). This was in fact a triplet state of a species. The long lifetime of the emission is a direct consequence of the forbidden nature of a transition from an excited triplet to the ground state singlet. Hence, phosphorescence can be described as a radiative transition between states of different multiplicity. Fluorescence is then understood to be a radiative transition between states of the same multiplicity (Wayne, 1970).

3.4 1: Perkin Elmer Lambda 900 UV/VIS/NIR spectrometer

UV/ Visible (UV/ Vis) absorption measurements were taken using a Perkin Elmer Lambda 900 UV/VIS/NIR spectrometer. Figure 3.4 shows the schematic set-up of the spectrometer. It is a double-beam, double monochromator ratio recording system with pre-aligned tungsten-halogen and deuterium lamps as sources. The wavelength range is from 175 nm to 3300 nm with an accuracy of 0.08 nm in the UV-visible region and 0.3 nm in the near IR region. Accessories available included a 60 mm Spectralon coated integrating sphere with a range from 200nm to 2500 nm for measurement of samples of

high optical density. Solution spectra were taken in a 1 cm quartz cell with the solvent system as reference whereas solid samples were mounted in the cell compartment and run against a blank substrate as reference.

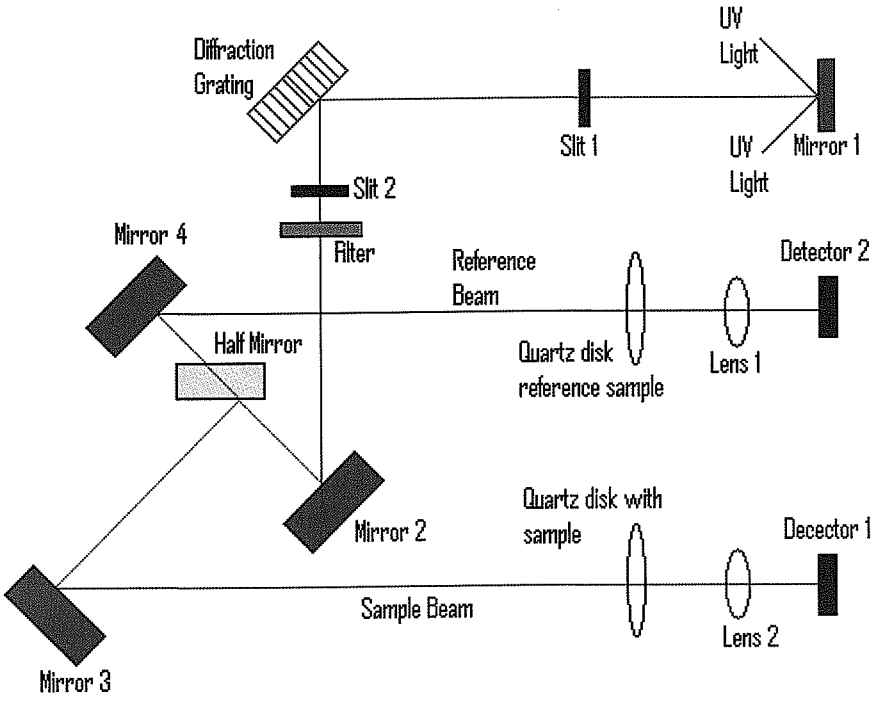

Figure 3.4: Schematic set-up of Perkin Elmer Lambda 900 UV/VIS/NIR spectrometer.

3.4 2: Perkin Elmer LS55 Luminescence spectrometer

The Perkin Elmer LS55 luminescence spectrometer used throughout this research was computer controlled. Excitation is provided by a pulsed Xenon discharge lamp with a pulse width at half peak height of < 10 μs and pulse power 20 kW. The source is monochromated using a Monk-Gillieson type monochromator and can be scanned over

the range of 200-800 nm. The luminescence is passed through a similar monochromator, which can be scanned over the range of 200-900 nm.

3.5 Introduction to electrochemistry

Cyclic voltammetry is a dynamic electrochemical method in which the potential applied to an electrochemical cell is scanned and any resulting changes in cell current are monitored to yield a cyclic voltammogram of the redox (reduction and oxidation) properties of the material under study. Conjugated polymers are capable of being electrochemically oxidized or reduced by the withdrawal or injection of electrons. When in an oxidized state, electrolyte anions are doped into the polymer to keep electroneutrality (p-doping); on the other hand when the polymer is in the reduced state, cations are doped (n-doping) (Kosuke, 2002). The doped and undoped polymers have completely different properties. The most important factor is that the doped polymer has a high conductivity (polyacetylene, which has an intrinsic conductivity much lower than 10^{-5} S m^{-1}, could be made highly conducting by doping (10^{3} S m^{-1}), which can be comparable to that of metal (copper has a conductivity of $6x10^{5}$ S m^{-1}) (Kosuke, 2002), while the undoped polymer is practically an insulator. Cyclic voltammetry has been recognised as an important technique for measuring bandgaps, electron affinities and work functions of various conjugated polymers (Helbig, 1993). The oxidation peak corresponds to the removal of electrons from the highest occupied molecular orbital (HOMO) and the energy can be related to the ionisation potential, whereas the reduction peak corresponds to the electron addition to the lowest occupied molecular orbital LUMO and can be related to the electron affinity (EA). The difference between the two can be used to work out the electrochemical bandgap of the polymers (Cervini, 1997).

Another point to mention is that the processes probed by cyclic voltammetry are similar to those involved in charge injection and transport processes in LED devices. Therefore the cyclic voltammetry measurements can provide addition information on the charge transport properties of the polymers *e.g.* potential hole blocking properties as described in Chapter 2.

3.5 1 Cyclic voltammetry

Cyclic Voltammetry (CV) is the most widely used technique for performing qualitative analysis about electrochemical reactions. CV can rapidly provide considerable information on the thermodynamics of redox process, kinetics of heterogeneous electron reactions, and on coupled chemical reactions or absorption process (Wang, 1994). In particular, it offers a quick location of redox potentials of the electroactive species, and convenient evaluation of the effect of media upon the redox process. CV entails linearly scanning the potential of a stationary working electrode using a triangular potential waveform as shown in Figure 3.5.

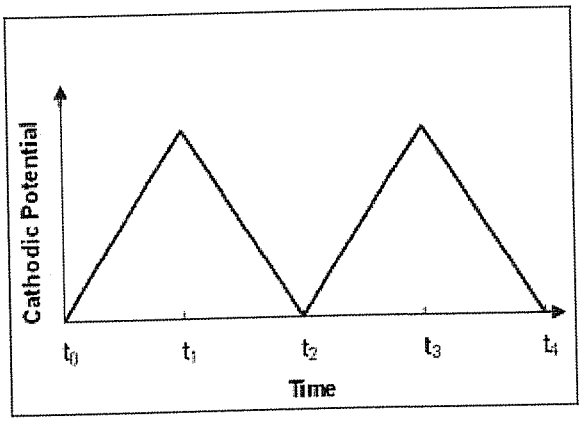

Figure 3.5: Cyclic voltammetry potential ($t_0 - t_1$ is one scan cycle) waveform (Bard, 1980).

Depending on the information sought, single or multiple scans can be obtained. During the potential sweep, a potentiostat measures the current resulting from an applied potential. The result can then be plotted, giving a plot of current versus potential. The resulting plot is termed a cyclic voltammogram.

Figure 3.6 shows a cyclic voltammogram of potassium ferricyanide on a glassy carbon working electrode with a scan rate of 0.1 V/s. The scan was obtained using a PGSTAT12 Autolab potentiostat which has been used for all CV scans obtained in this thesis. It can be seen from Figure 3.6 that the potential was initially scanned in the negative direction giving rise to the anodic peak or reduction peak E_{pa}, the system is cycled as indicated in the direction giving the cathodic peak or oxidation peak E_{pc} completing the reversible couple. Half-wave potential ($E_{½}$) is a potential at which the wave current is equal to one half of diffusion current (i_d) (Bard, 1980).

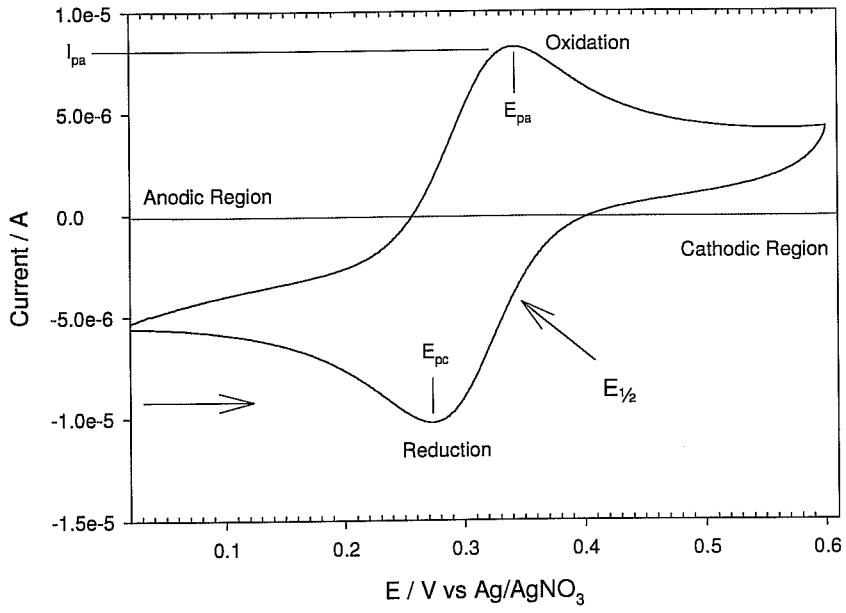

Figure 3.6: Cyclic voltammogram of potassium ferricyanide@0.1 V/s.

The characteristic peaks in the cyclic voltammogram are caused by the formation and recombination of ionic species at specific voltages near the electrode surfaces (i.e. the reduction and re-oxidation of the starting species (or vice versa)). The current peaks thus reflect the continuous change in the concentration of the ionic species with potential.

The peak current (i_p) in a cyclic voltammogram, for a reversible system under ambient conditions, can be characterised by several important parameters given by the Randles-Sevcik equation (Wang, 1994),

$$i_p(V/s) = (2.69x10^5)n^{\frac{3}{2}}ACD^{\frac{1}{2}}v^{\frac{1}{2}} \qquad \text{(Eq 3.1)}$$

where υ is the scan rate, set on the potentiostat, D is the diffusion coefficient, C is the concentration of the analyte, A is the electrode area and n the number of electrons involved. Thus it can be seen that the current is directly proportional to the concentration and increases with the square root of the scan rate.

The position of the current peaks on the potential axis can be related to the formal potential of the redox process E^o as follows (Wang, 1994).

$$E^o = \frac{E_{pa} + E_{pc}}{2} Volts \qquad \text{(Eq 3.2)}$$

where E_{pa} is the peak position of the reduced species (anodic) and E_{pc} the position of the oxidised species (cathodic) (as shown in Figure 3.6). Information about the ionisation potential and the electron affinity of a system may also be derived through electrochemical techniques. Systems with low electron affinity can be readily reduced at

low negative voltages and similarly a system with a low ionisation potential can be easily oxidised at low positive voltages. Hence the ionisation potential and electron affinity of a system will ultimately dictate the formal potential of that system. The separation of the reduced and oxidised peak potentials (for a reversible couple) is given by (Bard, 1980):

$$\Delta E_p = E_{pa} - E_{pc} = \frac{0.059}{n} Volts \qquad \text{(Eq3.3)}$$

where n is the number of electron transferred. Thus the peak separation can be used to determine the number of electrons transferred, and it can be seen that a reversible single electron process should exhibit an ΔE_p value of about 59 mV. In Figure 3.6 the ΔE_p was found to be 60 mV. For irreversible or quasi-reversible processes the above treatment becomes more complex will be discussed in later chapters as appropriate.

3.5.2 PGSTAT12 Autolab potentiostat

The PGSTAT12 Autolab potentiostat as aforementioned was used to carry out the cyclic voltammetry studies in this thesis. A potentiostat is basically a number of amplifiers used to control a voltage between two electrodes, a working electrode and a reference electrode, to a constant value. It is designed to work with a three-electrode cell in a way which ensures that all current will flow between the counter and working electrodes, while controlling the potential of the working electrode with respect to the reference electrode. Hence the potentiostat has two tasks (Bard, 1980):

1. To measure the potential difference between working electrode and reference electrode
2. Force a current through the counter electrode towards the working electrode.

Figure 3.7 is a schematic of the electrochemical cell used throughout this study. A three-electrode system was used: a working electrode (glassy carbon or gold), a counter electrode (platinum wire) and a non-aqueous reference electrode (contained electrolyte and 10 mM of silver nitrate). The reference electrode may be replaced by adding ferrocene to the acetonitrile. The ferrocene acts as an internal standard. A ferrocene couple (Fc/ Fc^{+}) is a well defined reversible system. For the cyclic voltammetry an electrolyte and a supporting electrolyte must be used. The support electrolyte is used for the sole purpose to increase the solution conductivity, as the electrolyte does not take part in any reactions. The electrolyte that was used was acetonitrile and the supporting electrolyte was 0.1 M of tetrabutylammonium hexafluorophosphate.

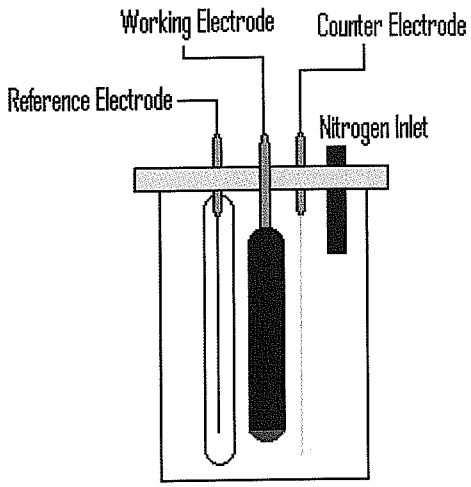

Figure 3.7: Cyclic voltammetry cell set-up.

3.5.3 In situ measurements: Spectroelectrochemistry

The coupling of optical and electrochemical methods, *i.e.* spectroelectrochemistry has been employed for over two decades to investigate a wide range of inorganic, organic, and biological redox systems (Heineman, 1986). The optical properties of conjugated polymers, when subject to electrochemical doping can provide vital information on the excited properties of the polymers. A variety of informative optical methods have been coupled with electrochemical techniques. The approach used in this study was absorption spectroelectrochemistry. In this case the ideal working electrode substrate is mirror smooth and highly reflective *i.e.* glassy carbon electrode. A fibre optics probe is used to deliver and collect the incident and reflected beams, which means that spectroelectrochemistry measurements can be carried out using a similar set-up to the cyclic voltammetry set-up. UV-VIS reflectance spectroelectrochemistry was performed on the conjugated polymers mentioned in Section 2.11 using an Ocean Optics S2000 spectrometer with a fibre optic probe attachment. The fibre optic probe was a bifurcated bundle one end of which was connected to a light source and the other was connected to the spectrometer. The arrangement allowed spectra to be collected using a 180^0 backscattering geometry. Figure 3.8 shows a schematic of the spectroelectrochemical set-up.

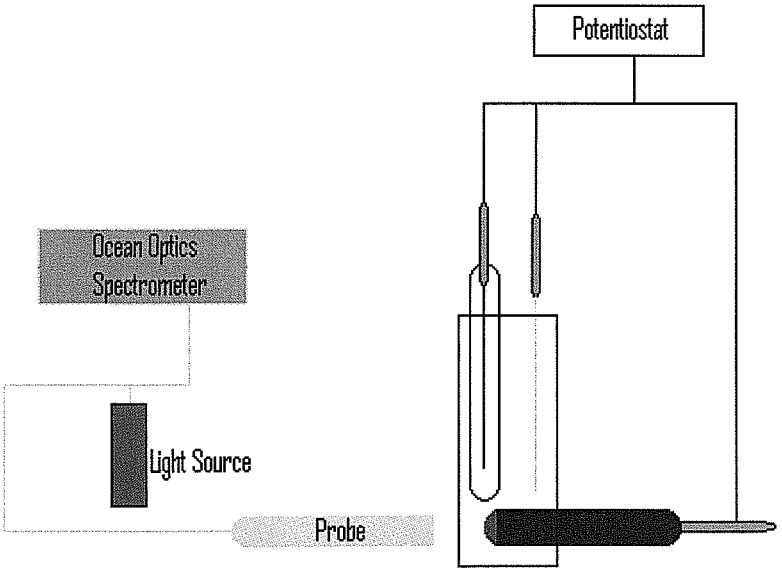

Figure 3.8: Spectroelectrochemical set-up.

3.6 Electroabsorption measurements

Electroabsorption spectroscopy is a very useful technique for probing of electronic structure in molecular crystals (Elschner, 1985, Weiser, 1998) and conjugated polymers (Liess, 1997). It is the study of the effect of an electric field of the absorption spectrum of the material. When a perturbing electric field is applied to a sample, it causes small changes in the electronic wavefunction, resulting in small shifts in the associated energy levels which are subsequently measured as a change in the absorption coefficient. This change is measured in terms of the differential transmission of light through a sample, which can then be used to calculate the change in the absorption coefficient by means of the following expression,

$$-\Delta T/T = \Delta\alpha d \qquad \text{(Eqn 3.4)}$$

where α is the absorption coefficient and d is the thickness of the sample (Sebastian and Weiser, 1981). Electroabsorption in polymers occurs via two processes, the Stark effect, which allows the probing of exciton energy levels, and the Franz-Keldysh effect, which is used to describe the mixing of continuum states associated with inter-band transitions.

3.6.1 Stark effect

The Stark effect comes in two varieties, the linear effect and the quadratic Stark effect (Cardona, 1969). For the majority of conjugated polymer systems, the quadratic Stark effect is the dominant process, with the linear effect occurring in cases of highly ordered systems.

3.6.2 Linear Stark effect

The linear Stark effect describes the change in energy of a dipole moment in the presence of an electric field, such that

$$\Delta E = \pm m.F, \qquad \text{(Eqn 3.5)}$$

where m is the permanent dipole moment and F is the electric field strength. Upon application of first order perturbation theory (Takase, 1989) and using the above relationship (Eqn 3.5), it is possible to obtain an expression for the change in the absorption coefficient as a function of energy (Sebastian and Weiser, 1981),

$$\Delta\alpha = \left\langle \frac{d\alpha}{dE}\Delta E \right\rangle + \left\langle \frac{1}{2}\frac{d^2\alpha}{dE^2}(\Delta E)^2 \right\rangle \qquad \text{(Eqn 3.6)}$$

The linear section of the above equation is negligible for polymeric systems as it relies on the presence of a permanent dipole moment in an ordered alignment. For polymer materials any dipoles present will have an isotropic distribution, so that when summed together, the net dipole moment is zero. The second order term in the above equation can have a non-zero value when averaged over all orientations. Therefore it can be concluded that the electroabsorption spectrum is proportional to the second derivative of the absorption with respect to the energy $d^2\alpha/dE^2$ and the square of the electric field strength, since $(\Delta E)^2 \propto F^2$.

Dipole moments can also be induced in materials without permanent dipole moments as a result of disorder potentials in the polymer chains. Disorder in polymer chains can lead to an asymmetric electron distribution along segments of the chain. This creates a difference in the potential on either side of the chain segment which can then induce a dipole moment (Horvath, 1995, Weiser, 1998). The contribution of the $d^2\alpha/dE^2$ term to the electroabsorption spectrum increases with increased levels of disorder; therefore the strength of this contribution to the spectrum can be used to indicate the degree of disorder in the sample (Horváth, 1995 Weiser, 1998, Bublitz and Boxer, 1997).

3.6.3 Quadratic Stark effect

The quadratic Stark effect describes the coupling of energy levels as a result of the applied electric field using second order perturbation theory (Weiser, 2004). The electric field couples an excited state in the polymer $|i\rangle$ to all the other states, $|j\rangle$ which

have a non vanishing dipole moment such that $\mu_{ij} = er_{ij}$. Applying second order perturbation theory, an expression for the shift in energy can be obtained (Weiser, 2004),

$$\Delta E_i = \sum_{j \neq 1} \frac{\left|\langle j|erF|i\rangle\right|^2}{E_i - E_j} = \sum_j \frac{\left|\mu_{ji} F\right|^2}{E_i - E_j} \qquad \text{(Eqn 3.7)}$$

The states closest in energy to one another will result in the greatest shift in energy levels.

Experimentally the energy shift is given by the expression, $\Delta E = \frac{|\Delta\alpha|}{d\alpha / dE}$. Thus the resulting expression for the change in the absorption coefficient is given by,

$$\Delta\alpha = \sum_i \frac{\left|\mu_{ji} F\right|^2}{E_i - E_j}\left(\frac{d\alpha}{dE}\right) \qquad \text{(Eqn 3.8)}$$

Therefore using the above equation it can be concluded that the electroabsorption spectrum is proportional to the square of the electric field strength, F^2 and the first derivative of absorption spectrum with respect to energy, $d\alpha/dE$ (Weiser, 2004).

3.6.4 Theoretical interpretation of electroabsorption spectra

In organic molecular crystals, the molecules interact with each other by weak van der Waals forces. Therefore, unlike inorganic crystals, the charge mobility in organic molecular crystals is rather low even in single crystals and the optical spectra of polycrystalline thin films are to some extent similar to those of their solution. Excitonic

and polaronic effects are correspondingly strong in organic solids (Bredas, 1985). The absorption spectrum of organic molecular crystals is dominated by the intramolecular excited states (called also Frenkel exciton). Early theory about electroabsorption (Houston, 1940, Aspnes, 1967, Cardona, 1969) spectroscopy based on the semiconductor band structure is of little value for organic molecular crystals. However the large interest in charge-transfer transitions in organic molecular crystals and conjugated polymers led to experimental and theoretical investigations on electroabsorption spectroscopy of organic materials. Over the past 20 years, interpretation of the electroabsorption spectrum of organic molecular crystals has made significant progress. Theoretical calculations of the electroabsorption spectra can be divided into two main branches; the first one was developed by the Weiser group in Germany (Sebastian and Weiser, 1981, Sebastian and Weiser, 1983, Weiser, 1993, Weiser and Horvàth, 1998). The second was developed by the Petelenz group in Poland (Petelenz, 1993, Petelenz, 1996). The semi-empirical approach described by Sebastian and Weiser (Sebastian and Weiser, 1981, Sebastian and Weiser, 1983) is the most relevant to this study.

3.6.5 Semi-empirical approach

As described by Sebastian, Weiser *et al.* (Sebastian and Weiser, 1981, Sebastian and Weiser, 1981, Sebastian and Weiser, 1983), the electric-field-induced change in the absorption spectrum for the excited state of a Frenkel exciton in organic molecular crystals can be given by

$$\Delta\alpha = -\frac{1}{2}\Delta p \cdot F^2 \cdot \frac{\partial \alpha}{\partial E} \qquad \text{(Eqn 3.9)}$$

where Δp is an average change in molecular polarisability of all molecules, F is the strength of the applied electric field, and $\frac{\partial \alpha}{\partial E}$ is the first order derivative of the zero-field absorption coefficient on the optical excitation energy. This treatment is only valid for a completely random system of transition dipoles. Equation 3.9 shows that the electric-field-induced change in the absorption spectrum is proportional to the square of the electric field and depends on the first derivative of the absorption spectrum. The change of the absorption coefficient is linear with the average change in molecular polarisability. For a pure charge transfer (CT) exciton, the change in absorption coefficient is given by

$$\Delta\alpha = \frac{1}{6}(\mu F \cos\theta)^2 \cdot \frac{\partial^2 \alpha}{\partial E^2} \qquad \text{(Eqn 3.10)}$$

where μ is the magnitude of the dipole moment of the CT states and θ is the angle between F and μ. Equation. 3.10 shows that the change of the absorption coefficient due to the CT exciton states is also proportional to the square of the applied electric field. The electric-field-induced change of absorption coefficient is quadratic with the static dipole moment of the CT states. Unlike for Frenkel exciton states, the change in absorption spectrum depends on the second derivative of the absorption coefficient with respect to the optical excitation energy. By electroabsorption measurements, the change of the optical absorption coefficient can be obtained. If the zero-field optical absorption spectrum is known, the relative magnitudes of the (ΔE) and $(\Delta E)^2$ of individual eigenstates can be calculated by fitting EA spectra using Equation 3.11.

$$\Delta\alpha = \frac{\partial\alpha}{\partial E}\Delta E + \frac{1}{2}\frac{\partial^2\alpha}{\partial^2 E}\Delta^2 E \qquad \text{(Eqn 3.11)}$$

This further allows for the estimation of the exciton binding energy, change of the static dipole moment (for CT excited states) and change of polarisabilities (for Frenkel excited states). From the considerations above, it should therefore be possible to distinguish between Frenkel exciton states and states which have significant CT character in a molecular system from the electroabsorption spectrum. For tightly bound (exciton binding energy ~1 eV) Frenkel excitons the change of absorption coefficient follows the first derivative of the absorption with respect to photo excitation energy (Sebastian and Weiser, 1981). For CT excitons with large transition dipoles (binding energy < 500 meV), the change of the absorption coefficient is proportional to the second derivative of the absorption spectrum (Sebastian and Weiser, 1981, Sebastian and Weiser, 1983).

It is also important to note that that the EA signal of the CT states does not need to follow the second derivative of the absorption spectrum (Petelenz, 1993). The first-derivative shape is equally probable, with a possibility of more complex behaviour. It has been shown that the second derivative spectrum can be composed of two individual first derivative absorption features from two adjacent individual eigenstates with comparable separation to the absorption bandwidths (Petelenz, 1993).

3.6.6 Electroabsorption spectrometer

Figure 3.9 shows the electroabsorption spectrometer used in this study. The instrument was built in house (Farrell, 2008) using a light source, which is dispersed through a monochromator. A Xenon light source was used, as the light source must be of sufficient intensity that the signal is not buried in the background noise, and sufficiently

stable that it does not contribute to the noise itself. It is also advantageous if the lamp has a small spot size, to enable examination of small samples. The radiant energy is then polarised, and focused through the sample. The transmitted light is then detected using a photomultiplier tube.

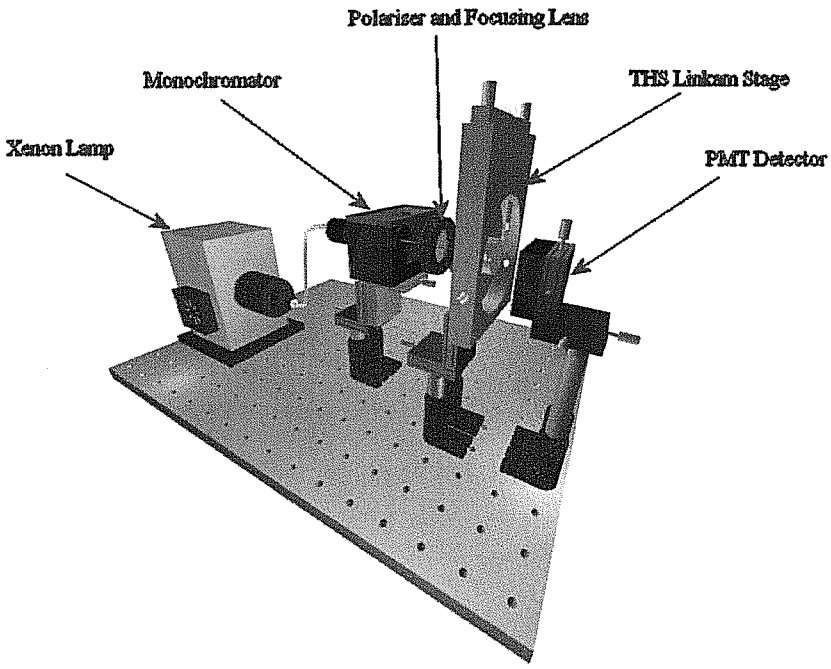

Figure 3.9: Schematic of electroabsorption spectrometer (Farrell, 2008).

3.7 Conductivity measurements and thin film fabrication

Electroluminescence (EL) in conjugated polymers was first reported in 1990 by Burroughes *et al.*(Burroughes, 1990). By investigating the dielectric properties of a thin film of poly-*p*-(phenylene vinylene) (PPV) sandwiched between two electrodes in the configuration $Al/Al_2O_3/PPV/Al$, yellow–green light was detected above a threshold field of $3x10^6$ V/cm. Although the initial internal quantum efficiency was below 0.01 %, and, consequently, the brightness of the devices was relatively low, this discovery

triggered a lot of research on polymeric electroluminescence (Braun, 1991, Bradley, 1993).

Device structures with sandwich geometry can be said to behave like diodes. A diode is an example of a p-n junction (Chapter 2). In a p-n diode, conventional current can flow from the p-type side to the n-type side, but not in the opposite direction. A semiconductor diode's current-voltage, or I-V, characteristic curve is ascribed to the behaviour of the so-called depletion layer or depletion zone which exists at the p-n junction between the differing semiconductors (Turton, 2000). When a p-n junction is first created, conduction band (mobile) electrons from the n-doped region diffuse into the p-doped region where there is a large population of holes with which the electrons recombine. When a mobile electron recombines with a hole, the hole vanishes and the electron is no longer mobile. Thus, two charge carriers have vanished. The region around the p-n junction becomes depleted of charge carriers and thus behaves as an insulator. However, the depletion width cannot grow without limit. For each electron-hole pair that recombines, a positively-charged dopant ion is left behind in the n-doped region, and a negatively charged dopant ion is left behind in the p-doped region. As recombination proceeds and more ions are created, an increasing electric field develops through the depletion zone which acts to slow and then finally stop recombination. At this point, there is a contact potential across the depletion zone. If an external voltage is placed across the diode with the same polarity as the contact potential, the depletion zone continues to act as an insulator preventing a significant electric current. However, if the polarity of the external voltage opposes the contact potential, recombination can once again proceed resulting in substantial electric current through the p-n junction. For silicon diodes, the contact potential is approximately 0.6 V (Turton, 2000). Thus, if an

external current is passed through the diode, about 0.6 V will be developed across the diode such that the p-doped region is positive with respect to the n-doped region.

Figure 3.10 shows the current voltage curve for a p-n junction diode. A p-n junction diode's I-V characteristic can be approximated by two regions of operation (Turton, 2000). Below a certain difference in potential between the two leads, the depletion layer has significant width, and the diode can be thought of as an open (non-conductive) circuit. As the potential difference is increased, at some stage the diode will become conductive and allow charges to flow, at which point it can be thought of as a connection with zero (or at least very low) resistance. In the reverse bias region for a normal p-n junction diode, the current through the device is very low (in the μA range) for all reverse voltages up to a point called the peak-inverse-voltage (PIV). Beyond this point a process called reverse breakdown occurs which causes the device to be damaged along with a large increase in current.

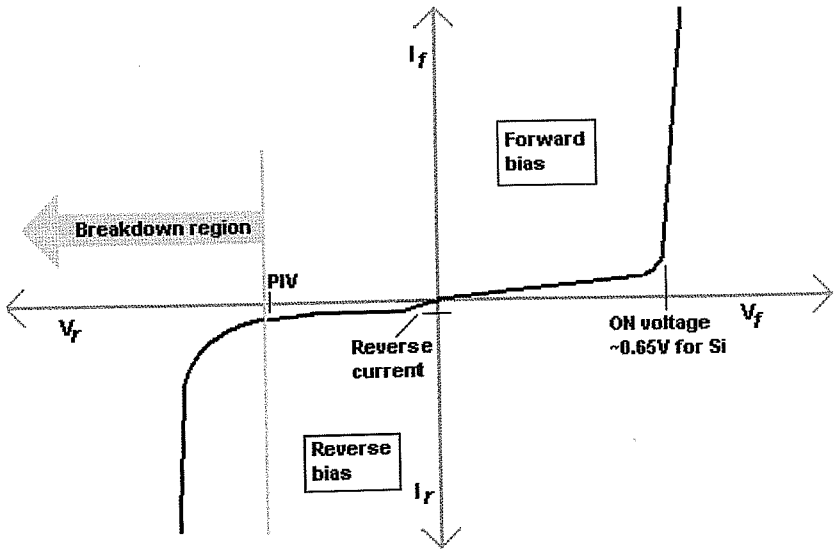

Figure 3.10: I-V characteristics of a p-n junction diode (Turton, 2000).

3.7.1 Thin film fabrication

For the electroabsorption and conductivity measurements, sandwich device like structures were constructed. The sandwich structures shown in Figure 3.11 were chosen over in plane geometries as the films are polycrystalline with crystalline sizes of ~ 0.5 μm. Planar geometry inter electrode spacings are typically of 1 μm or more, and so transport is limited by crystallite domain boundaries. In the sandwich type geometry inter electrode spacings are governed by the film thickness which is ~200 nm – 400 nm.

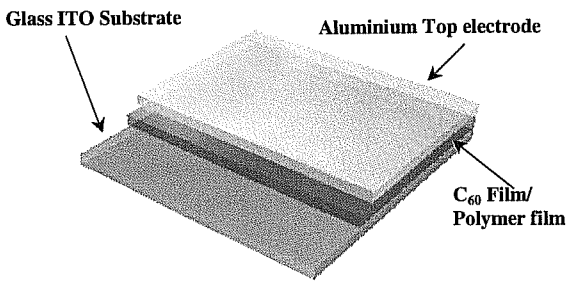

Figure 3.11: Sandwich structure device of polymer or C_{60} thin film on glass ITO substrate with aluminium top electrode (Farrell, 2008).

3.7.2 Fullerene films

C_{60} films were prepared by vacuum sublimation onto (ITO) substrates used as the bottom electrode of a sandwich type geometry with aluminium as the top electrode. This involved evaporating C_{60} through sublimation of C_{60} powder by resistively heating a molybdenum boat containing C_{60} powder in an Edwards Auto-305 evaporator, which was pumped down to a pressure of 10^{-6} mbar. An indium tin oxide (ITO) glass substrate

was also placed in the Edwards Auto-305 evaporator. The experimental set-up of the Edwards Auto-305 evaporator is shown in Figure 3.12. The Edwards consists of two heating electrodes across which the molybdenum boat containing the C_{60} is placed. The ITO glass substrates are placed above the boat with a shutter in between, which can open and close to expose or protect the substrate from evaporated material. The molybdenum boat is heated gently by passing a current through it, which is controlled by a built in power supply. The shutter is kept closed while the boat is heating and initially when C_{60} starts to sublime, allowing impurities to evaporate off first. The shutter is then opened for approximately 5 to 10 minutes to give a film thickness ranging between 200-400 nm. The system was allowed to cool under vacuum before the electrodes where removed and stored in the dark and at room temperature. The film thickness was measured using the Veeco Dektak V350 Stylus Profiler System. This system can be used for measuring step-height repeatability, surface planarity and roughness.

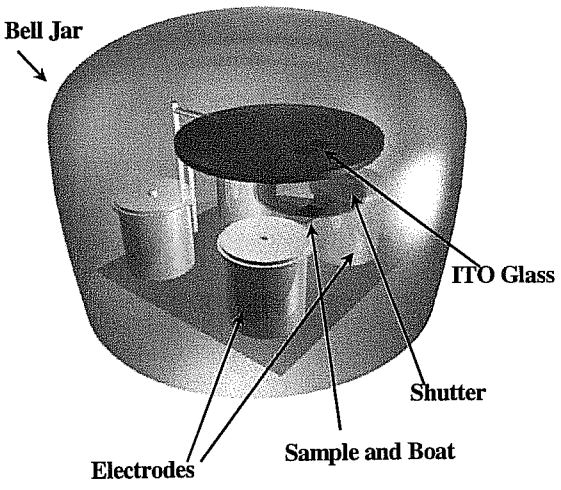

Figure 3.12: Experimental set-up for sublimation of C_{60} onto ITO glass substrates.

3.7.3 Polymer films

Polymer films were produced via a spin coating method. The films were spin coated onto an indium tin oxide (ITO) glass substrate (12 mm^2). To obtain a film thickness of about 200 nm a concentration of 1 % wt/vol (1 % wt/vol is 1 g of solute per 100 ml of solvent) was prepared and an average speed of 2000 rpm at 20 seconds was used on the spin coater. For thicker films the speed was reduced accordingly to produce the desired thickness. Once the polymer film was deposited aluminium was evaporated on as a top electrode.

For the conductivity measurements a buffer layer was added onto the ITO. The buffer layer used in this study was poly (styrenesulfonate)/poly (2,3-dihydrothieno(3,4-b)-1,4-dioxin) (PEDOT). The buffer layer has two functions, firstly it smoothens the ITO surface, which helps to prevent shorts between the positive and the negative electrode, especially if the active layer is very thin. In addition, the PEDOT has a higher workfunction (5.20 eV) than ITO which gives a better alignment of the workfunction with the HOMO level of the active layer for the polymers (Brown, 1999). PEDOT was purchased from Sigma Aldrich (product number 560596) in an aqueous solution (H_2O). Before spin coating the PEDOT was filtered through a 5 mm syringe filter. Films were prepared by spin coating, PEDOT on top of the ITO. The film thickness was typically 50nm. This usually requires a spin speed of 4000 rpm for 20 seconds. The film was then placed into an oven for five minutes at 120 degrees (Yang, 2005) After the PEDOT film has dried it is not easily removed so that spin-coating an additional layer (polymer dispersed in solvent) will not wash off the PEDOT. The PEDOT was not used for electro-absorption measurements because the injection of the extra electrons will result

in dielectric breakdown across the film, thus leading to a false reading. The conductivity experimental set-up will be described and discussed in the relevant chapter.

3.8 Summary

A broad range of experimental techniques has been utilised throughout this project to study the optical and electronic characteristics and charge transfer properties of conjugated polymers and C_{60}. Nevertheless the techniques discussed in this chapter can be divided up into specific types of analysis. For example electronic spectroscopy (*i.e.* UV/VIS and Fluorescence) gives details of the optical properties of the sample, the electronic configuration and charge transfers states. Electroabsorption spectroscopy is complementary to electronic spectroscopy and provides information on the excited electronic state and charge transfer of the molecules. Alternatively, information regarding the electronic structure of a system may be obtained through the use of electrical methods such as cyclic voltammetry. In this technique ionic species are produced by electron injection (reduction) or electron removal (oxidation) due to the application of specific voltages. The information, which can be derived from this type of experiment, can allow the estimation of electron affinities, ionisation potentials and diffusion coefficients for a particular molecule. In situ reflectance measurements will provide further information of the effect of electrochemical doping of the polymers. Conductivity measurements will provide an idea of how well the conjugated polymers conduct with and without an acceptor material.

Chapter 4 begins with the experimental exploration of the acceptor material C_{60}. The chapter characterises and clearly shows the difference between C_{60} in its molecular and solid-state form. The first part of the chapter deals with spectroscopic characterisation.

This deals with the optical and electronic properties of the C_{60}. The charge transfer mechanism of C_{60} is then discussed via Electroabsorption and Cyclic voltammetry techniques. The charge transfer technique provides an explanation of why the C_{60} is seen as an idea acceptor material for organic PV cells.

The second part of Chapter 4 deals with the polymeric standard used in this study, MEH-PPV. A full characterisation of MEH-PPV is provided using the methods mentioned throughout this chapter. The results obtained will be used throughout the thesis as a comparison to the new polymers. Ultrafast charge transfer from MEH-PPV onto C_{60} has been very well documented over the past ten years (Sariciftci, 1993 Halls, 1996, Vacar, 1997, Haugeneder A, 1999). Femtosecond spectroscopy has been the main experimental technique employed to observe this charge transfer. However the exact method this charge transfer is still not fully understood. Also the optimum amount of C_{60} required in these composites has also been questionable. This study proposes to use other methods to show this charge transfer. Therefore the third part of Chapter 4 characterises MEH-PPV/C_{60} composites using electronic, fluorescence, and electroabsorption spectroscopy, cyclic voltammetry and conductivity measurements. The indicators of charge transfer shown in these techniques will then be used as markers when investigating if the new polymers are capable of charge transfer with C_{60}.

References:

Aspnes D.E., *"Electric field effects on the dielectric constant of solids"*, Phys. Rev. 153, 972, (1967).

Bard A.J., Faulkner L.R., *"Electrochemical methods, fundamentals and applications"*, John Wiley and Sons: New York, (1980).

Braun D, Heeger A.J., *"Visible light emission from semiconducting polymer diodes"*, *Appl. Phys. Lett.* 58, 1982, (1991).

Bradley D.D.C., *"Conjugated Polymer Electroluminescence"*, Synth. Met, 54, 401, (1993).

Bredas J.L., Street G.B., *"Polarons, Bipolarons, and Solitons in Conducting Polymers"*, Acc. Chem. Res, 18, 309, (1985).

Brown T.M., Kim J.S., Friend R.H., Cacialli F, Daik R, Feast W.J., *"Built-in field electroabsorption spectroscopy of polymer light-emitting diodes incorporating a doped poly(3,4-ethylene dioxythiophene) hole injection layer"*, Appl. Phys. Lett. 75, 1679-1681, (1999).

Bublitz G.U., and Boxer S.G., *"Stark spectroscopy: Applications in chemistry, biology, and materials science"*, Annu. Rev. Phys. Chem. 48, 213, (1997).

Burroughes J.H., Bradley D, Brown A.R., Marks R.N., Mackay K, Friend R.H., Burn P.L, Holmes A.B., *"Light-emitting diodes based on conjugated polymers"*, Nature, 539, 347 (1990).

Cardona M, *"Solid State Physics Supplement 11: Modulation Spectroscopy"*, Academic Press, New York, (1969).

Cervini R, Li X.C., Spencer G.W.C., Holmes A.B., Moratti S.C., Friend R.H., *"Electrochemical and optical studies of PPV derivatives and poly(aromatic oxadiazoles)"*, Synthetic Metals, 84, 359,(1997).

Dittmer J.J., Petritsch K, Marseglia A.E., Friend R.H., Rost H, Holmes A.B., *"Photovoltaic properties of MEH-PPV/PPEI blend devices"*, Synthetic Metals.102, 879, (1999).

Elschner A, Weiser G, *"Electroreflectance studies of the charge-transfer excitons in Anthracene-PMDA"*, Chem. Phys. 98, 465, (1985).

Farrell G, *"Investigation of the electronic properties of organic systems using electroabsorption spectroscopy"*, PhD Dissertation, Dublin Institute of Technology, (2008.)

Halls J.J.M., Pichler K, Friend R.H., Moratti S.C., Holmes A.B., *"Exciton diffusion and dissociation in a poly(p-phenylenevinylene)/C_{60} heterojunction* photovoltaic cell*"*, *Appl. Phys. Lett.* 68 (22), 3120, (1996).

Harrison M.G., Gruener J, Spencer G.C.W., *"Analysis of the photocurrent action spectra of MEH-PPV polymer photodiodes"*, *Phys. Rev. B* 55, 7831, (1997).

Haugeneder A, Neges M, Kallinger C, Spirkl W, Lemmer U, Feldmann J, Scherf U, Harth E, Gügel A, Müllen K, *"Exciton diffusion and dissociation in conjugated polymer/fullerene blends and heterostructures"*, *Phys. Rev. B* 59, 15346, (1999).

Heineman W, Hawkridge F, Blount H, *"Spectroelectrochemistry at Optically Transparent Electrodes"*, Electroanalytical Chemistry, Vol 13, (1986).

Helbig M, and. Horhold H.H., *"Electrochemical studies on poly(pphenylenevinylene)s"*, Makromol Chem, 1607, 194, (1993).

Horvath A, Weiser G, Baker G.L., Etemad S, *"Influence of disorder on the field-modulated spectra of polydiacetylene films"*, Phys. Rev. B 51, 2751, (1995).

Houston W. V., *"Acceleration of electrons in a crystal lattice"*, *Phys. Rev.* 57 184, (1940).

Kosuke I., *"Electrochemistry in Nonaqueous Solutions"*, Ch. 12, John Wiley and Sons: New York, (2002).

Kroto H.W., Heath J.R., O'Brien S.C., Curl R.F., Smalley R.E., *"C_{60} Buckminsterfullerene"*, Nature 318,162, (1985).

Liess M, Jeglinski S, Vardeny Z.V., Ozaki M, Yoshino K, Ding Y, Barton T,*"Electroabsorption spectroscopy of luminescent and nonluminescent π-conjugated polymers"*, Phys. Rev. B 56, 15712, (1997).

Parker I.D., *"Carrier tunneling and device characteristics in polymer light-emitting diodes"*, J. Appl. Phys. 75,1656, (1994).

Petelenz P, *"Non-local polarisabilities in excited states of polyacene crystals"*, Chem. Phys. Lett. 215, 607, (1993).

Petelenz P, *"Electro-absorption spectra of degenerate charge transfer states"*, Chem. Phys. 171, 397, (1993).

Petelenz P, *"Theoretical calculation of the electroabsorption spectra of polyacene crystals"*, J. Chem. Phys. 105, 4427, (1996).

Pope M, Swenberg C.E, *"Electronic Processes in Organic crystals and Polymers"*, Oxford University Press, (1999).

Sariciftci N.S., Braun D, Zhang C, Srdanov V.I., Heeger A.J., Stucky G, Wudl F, *"Semiconducting polymer-buckminsterfullerene heterojunctions: Diodes, photodiodes, and photovoltaic cells"*, *Appl. Phys. Lett.* 62, 585, (1993).

Scott J.C., Kaufman J.H., Brock P.J., DiPietro R, Salem J, Goitia J.A., *"Degradation and failure of MEH-PPV light-emitting diodes"*, J. Appl. Phys. 79, 2745, (1996).

Sebastian L and Weiser G, *"Charge transfer transitions in solid Tetracene and Pentacene studied by Electroabsorption"*, Chem Phys. 61, 125, (1981).

Sebastian L and Weiser G, *"Electroreflectance studies on the excitons in PTS and DCHD single crystals"*, Chem. Phys. 62, 447, (1981).

Sebastian L and Weiser G, *"Charge-transfer transitions in crystalline anthracene and their role in photoconductivity"*, Chem. Phys. 75,103, (1983).

Takase T, Kotani M, *"Charge transfer states in phenothiazine crystal"*, J. Chem. Phys. 94, 2134, (1989).

Turton R, *"The Physics of Solids"*, Oxford University Press, (2000).

Vacar D, Maniloff E.S., McBranch D.W., Heeger A.J., *"Charge-transfer range for photoexcitations in conjugated polymer/fullerene bilayers and blends"*, *Phys. Rev. B* 56(8), 4573, (1997).

Wang J, *"Analytical Electrochemistry"*, VCH Publishers, New York, (1994).

Wayne, R.P., *Photochemistry*, Butterworth and Co. Ltd., London, (1970).

Weiser G, *"Stark effect of one-dimensional Wannier excitons in polydiacetylene single crystals"*, Phys. Rev. B 45, 14076, (1993).

Weiser G and Horvàth A, *"Variation with disorder of absorption and electroabsorption spectra of a π-conjugated polymer: 4BCMU"*, Chem. Phys, 227, 153. (1998).

Weiser G, *"Comparative electroabsorption studies of organic and inorganic solids"*, Journal of Luminescence, Vol 110,189, (2004).

Yang C, Li H, Sun Q, Qiao J, Li Y, Li Y, Zhu D, *"Photovoltaic cells based on the blend of MEH-PPV and polymers with substituents containing C_{60} moieties"*, Solar Energy Materials & Solar Cells 85, 241–249, (2005).

Chapter 4: Characterisation of Reference Materials

4.1 Introduction

This chapter characterises the two reference materials used in this study, that is buckminsterfullerene (C_{60}), which will be used consistently in the work as a generic electron accepting material and poly (2-methoxy-5-(2'-ethylhexyloxy)-1,4 phenylenevinylene) MEH-PPV which will be used as a reference polymer system. It is suggested that MEH-PPV can be used as a reference material as a sizeable body of work exists in the literature on the behaviour of this material in composite systems for PV applications (Sariciftci, 1992, Kraabel, 1994, Halls, 1996, Vacar, 1997). The first part of this chapter will deal with the C_{60}. C_{60} is the smallest and most researched member of the fullerene family (Kroto, 1985). A key point to this work is that it can take on up to six additional electrons (Nalwa, 1999). In 1992 it was shown that photo induced electron transfer from a conducting polymer to C_{60} could be achieved relatively easily (Sariciftci, 1992). This clearly demonstrated that C_{60} could be used as an efficient acceptor material in organic photovoltaic devices.

In terms of the donor material, polymers offer a number of advantages; they are cheap to process on a large scale and can be flexible with a large surface area for applications. This thesis will use a new polymer series (Figure 2.12, Chapter 2) to explore the effect of molecular structure on the electron donor material's charge transfer process in composite systems. In fact the aspect of the structure property relationships with respect to the polymer series is an underlying theme of the work. To explore this adequately however it is crucial that a known reference system be established and characterised. As aforementioned MEH-PPV has been chosen for this purpose. Hence a full

characterisation of MEH-PPV will be provided in the second part of this chapter. The final part of this chapter explores the formation of a MEH-PPV/C_{60} composite. Such composites have been explored intensively in the past and a good understanding has emerged of their photophysical properties and photochemistry. However as mentioned previously in Chapter 2, several gaps in the knowledge still exist in particular to the nature and mechanisms behind the charge transfer from donor to acceptor. The characterisation of the charge transfer states in these composites normally entails the use of femtosecond spectroscopy, namely photoinduced absorption (PIA). Instead of using PIA this study will concentrate on steady state spectroscopic and electrochemical techniques to identify charge transfer indicators within MEH-PPV/C_{60}. These indicators will then be used as markers, for the identification of a charge transfer when investigating the interaction of C_{60} with the new polymer series in later chapters.

4.3 Buckminsterfullerene (C_{60})

C_{60} (Figure 3.3) was first discovered in 1985 by Harold Kroto *et al,* in an attempt to explain anomalous infrared and ultraviolet spectra obtained from red giant carbon stars (Kroto, 1985). C_{60} is a large carbon molecule which contains sixty carbon atoms arranged in 12 five membered rings (pentagons) and 20 six membered rings (hexagons) with an icosahedral symmetry I_h. In the proposed structure for C_{60}, each vertex of the truncated icosahedral (football) is occupied by a carbon atom and each carbon is connected to three other carbon atoms in a sp^2 hybridised bonding arrangement which gives rise to sixty delocalised electrons distributed around the carbon cage. C_{60} can be dissolved in many organic solvents and molecular C_{60} can be sublimed to produce thin films. In the solid state, the C_{60} molecules are bound by weak van der Waals

interactions and at room temperature are packed together in an face centred cubic (fcc) lattice arrangement (Kuzmany, 1994).

4.3 Electronic spectroscopy of C_{60}

Electronic spectroscopy allows us to observe the difference between the molecular and solid-state form of C_{60}. Figure 4.1 shows a typical absorption spectrum for C_{60} in solution and in its solid-state form, recorded between 1.50 eV → 5.50 eV. The solvent used was hexane, as it has little or no absorption in the UV spectrum (Leach, 1994). The high degree of symmetry of the fullerenes renders the HOMO-LUMO transition forbidden, since it has a zero transition dipole moment (Leach, 1994). Nevertheless this HOMO - LUMO transition is weakly visible in the absorption spectrum of C_{60}, as indicated below, around 2.07 eV. The appearance of this band is due to the relaxation of the selection rules, which allow forbidden transitions to occur weakly via Hertzberg-Teller vibrational coupling or Jahn-Teller distortions (Leach, 1994). As a result the broad absorption between 1.90 eV and 3.00 eV has been ascribed entirely to the HOMO-LUMO transition. To date the most detailed analysis of the absorption spectrum of C_{60} has been presented by Leach *et al.* In the work, the absorption spectrum was divided into four regions. Between 6.50 eV and 3.50 eV, there exists three strong bands, and these, in addition to weaker vibronically structured bands in the region of 3.50 eV →2.88 eV, were assigned to nine orbitally allowed singlet-singlet transitions.

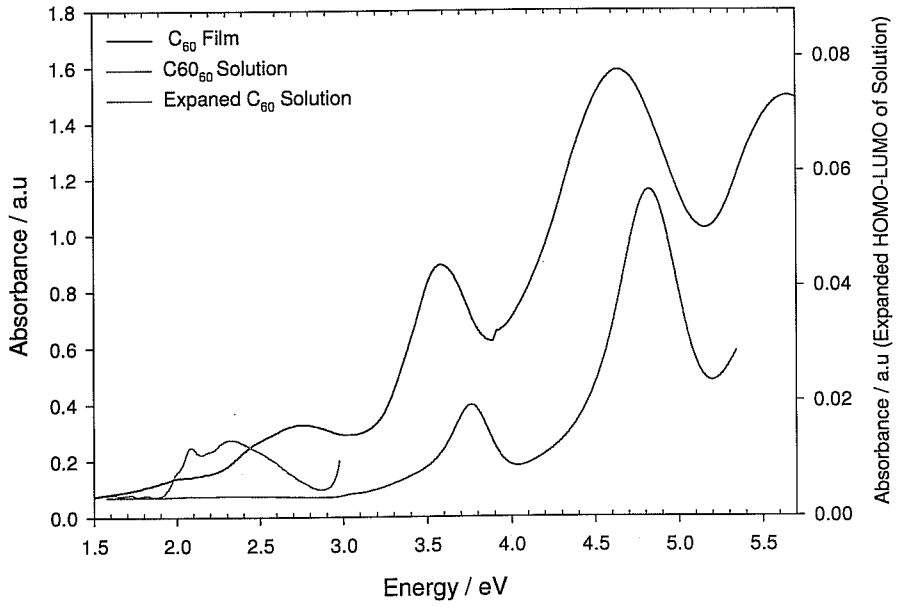

Figure 4.1: Absorption spectra of molecular and solid-state C_{60}.

The vibrational structure has been assigned to the effects of Hertzberg-Teller distortions (Leach, 1994). There are several superimposed peaks and weak shoulders on the HOMO-LUMO background. These bands have been attributed to vibronic transitions in which the excitation of a vibration of suitable symmetry enables the forbidden transition to "steal" intensity from allowed transitions. Leach also identified four extremely weak bands between 1.97 eV and 1.79 eV and assigned them to vibronic features of the spin forbidden singlet to triplet transition. From Figure 4.1 there is one feature which appears strongly in the solid-state spectrum, but not in that of the isolated molecule (solution). The thin film absorption spectrum of C_{60} shows a broad, relatively strong absorption in the range of 2.47 eV→ 2.90 eV with a maximum at 2.77 eV. This feature is absent in the solution absorption spectrum hence suggesting that it is not molecular in origin. Despite this the feature received relatively little attention. However it is now accepted (Farrell, 2005) that this feature is in fact due to the solid state influence on the electronic

properties of the molecule. It is not molecular in character but instead is the result of an intermolecular charge transfer excited state (Kazaoui, 1995). Hence while the solid state of C_{60} appears to behave like a classical molecular solid, there does exist signature charge transfer states which contradict this behaviour. Nevertheless for the purpose of this work it should be noted that the solution spectrum is an indication of molecularly dispersed and the absence of the solid-state feature in the absorption spectrum of any C_{60} composite may be used as an indicator of well dispersed C_{60}, giving the best opportunity for intermolecular charge transfer between the C_{60} and polymer.

4.4 Electroabsorption of C_{60}

In the context of elucidating the excited state properties of any system a thorough understanding of the charge transfer (CT) states is of crucial importance with a special emphasis on the identification of excited states of CT parentage since they serve as precursors for free charge carriers. These states are particularly important when considering physical properties such as electrical conductivity or photoconductivity. It has become evident in recent years that these states are best investigated by electroabsorption (EA) spectroscopy (Sebastian, 1981).

Figure 4.2 shows the electroabsorption of a C_{60} film (200 nm) at room temperature and agrees with the literature for the region studied (Kazaoui, 1995). The electroabsorption spectrum of C_{60} is known to consist of several modulations are observed (Jeglinski, 1992). However the EA spectrum shown in Figure 4.2 only shows modulations at 2.40 eV and 2.70 eV. This is due to instrumentation limitations, as the electroabsorption spectrometer used in this study cannot measure energies above 3.50 eV. Nevertheless

the modulations in Figure 4.2 coincide with those reported in the literature (Kazaoui, 1998).

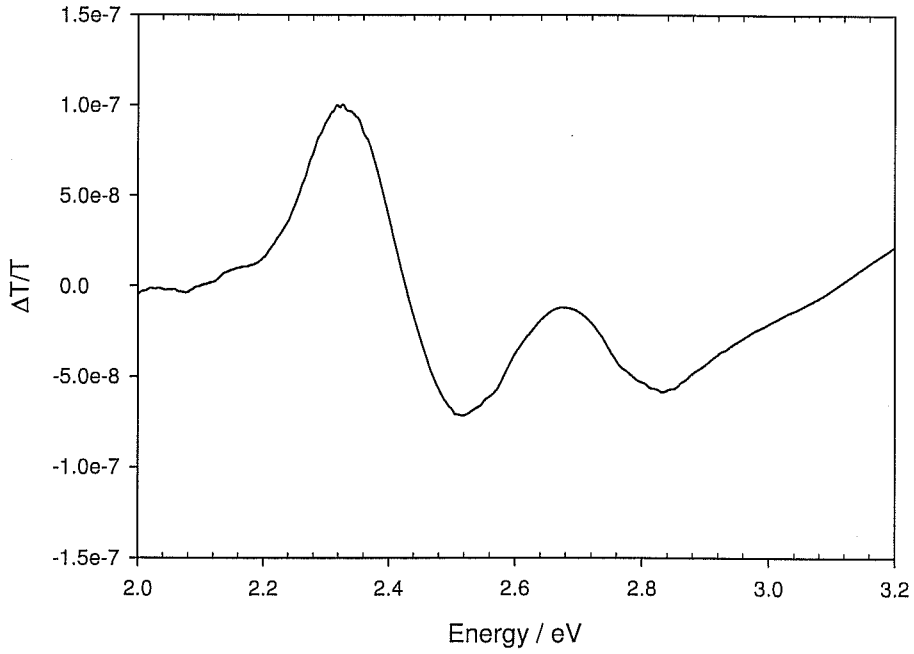

Figure 4.2: Electroabsorption of C_{60} film (200nm) at room temperature.

The EA spectrum of C_{60} can be a combination of first and second order derivatives of the absorption spectrum corresponding to Frenkel and CT excitons respectively. Comprehensive experimental studies (Kazaoui, 1995, Byrne, 1995), supported by detailed theoretical interpretation (Haddon,1986, Averitt,1995) have led to detailed assignment of the observed spectral features in the energy range up to about 4.00 eV. Using a semi empirical model originally proposed by Sebastian *et al* (Sebastian, 1983), Kazaoui *et al.* (Kazaoui, 1995) de-convoluted the EA spectra into a summated series of weighted first and second derivatives of the absorption spectrum. In order to reproduce the EA spectrum of C_{60} they described the EA spectra as being composed of a number of overlapping second derivative type contributions, centred at 2.43 eV and 2.7 eV. The

most significant CT states have been identified at approximately 2.43 eV and 3.50 eV (Haufler, 1990, Kazaoui, 1995).

4.5 Cyclic voltammetry of C_{60}

Cyclic voltammetry was carried out to demonstrate the electron accepting abilities of molecular C_{60}. This method was chosen as it shows a clear difference between molecular and solid states of C_{60} (Jehoulet, 1992), highlighting the need for a good dispersion of C_{60} in any composite system. In addition, CV measurements should provide another method by which the electronic structure of the composite systems can be investigated allowing, for the determination of the band gaps (E_g) and energy levels of these materials to be studied by measuring their oxidation and reduction potentials.

Since the first report on the electrochemical properties of C_{60}, which was over twenty years ago, there has been a steady interest in the electrochemistry of fullerenes and related molecules (Haddon, 1986, Doubois, 1991, Jehoulet, 1991). The interest was stimulated by both theoretical considerations and experimental findings (Pac, 1998) which showed that LUMO of the C_{60} molecule was triply degenerate having the ability to take on up to six additional electrons. Successful detection of the six reduction provided impressive proof of the predicted electronic structure of the molecule (Xie, 1992).

4.5.1 Cyclic voltammetry of C_{60} in solution

The original study of the electrochemical properties of C_{60} was conducted in a methylene chloride electrolyte and showed only two reversible reduction peaks, which

were ascribed to single electron transfers by controlled potential Coulometry measurements (Jehoulet, 1991). Shortly thereafter a third reversible reduction peak was reported in the same electrolyte, after which a succession of reports on the electrochemical reduction of C_{60} were published (Bard, 1980, Cox, 1991, Doubois, 1991). Six reversible reductions of C_{60} were first observed by Xie *et al.* The fact that the C_{60} can take up to six addition electrons (and it is a reversible process), is why it is considered as an ideal acceptor material. The observation of the six reduction peaks reported by Xie *et al* was accomplished by the use of a mixed electrolyte system and low temperature (~-10 °C). The optimal electrolyte composition was between 15 % and 20 % by volume of acetonitrile in toluene. tetrabutylammonium phosphorushexafluoride ($TBAPF_6$) was used as supporting electrolyte. The electrolyte mixture allowed an extremely wide potential window to be examined in comparison to previous studies, extending the region of study down to –3.3 V vs. Fc/Fc^+. The six reversible reduction peaks observed were seen to have half-wave potentials ($E_{½}$) of –0.98 V, -1.37 V, -1.87 V, -2.35 V, -2.85 V, and -3.26 V.vs Fc/Fc^+. In solution the reduction and re-oxidation peaks are reported to occur at approximately the same potential with a peak separation of ΔE_p of ~59 mV (Doubois, 1991). This is characteristic of a single electron transfer.

Figure 4.3 shows a cyclic voltammogram obtained for C_{60} ($8x10^{-4}$ M) in toluene electrolyte, at a gold electrode. In this study tetrabutylammonium perchlorate (TBACIO4) 0.1 M was used as the support electrolyte. The cyclic voltammogram in Figure 4.3 clearly shows four reversible reduction peaks. These peaks have been ascribed to the formation of C_{60}^{-1}, C_{60}^{-2}, C_{60}^{-3} and C_{60}^{-4} anions with $E_{½}$ potentials of –0.908 V, -1.337 V, –1.799 V and -2.273 V.

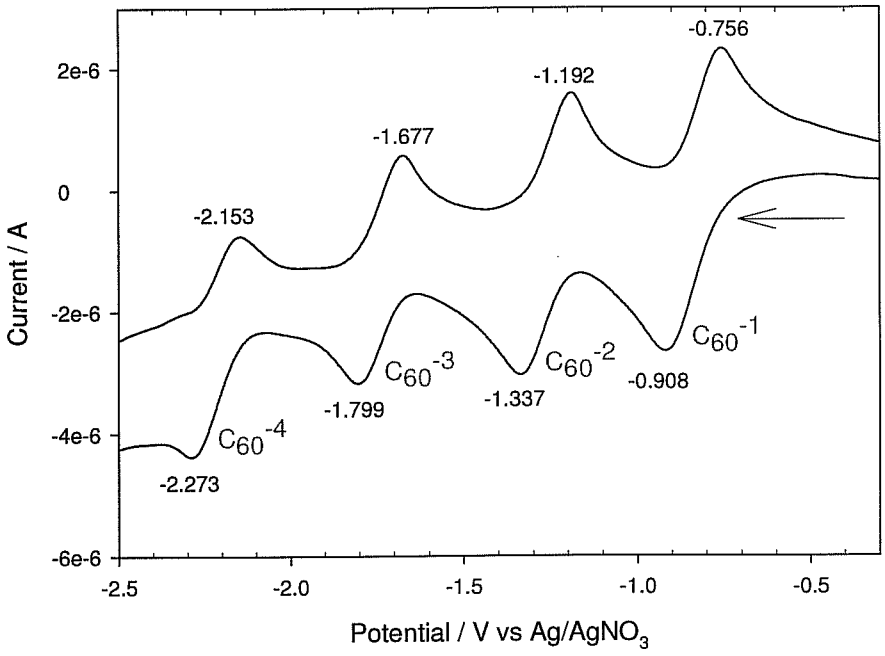

Figure 4.3: Cyclic voltammogram of C_{60} / toluene solution ($8x10^{-4}$ M) @0.1 V/s and 20 °C.

The integrated area of the reduction peaks is approximately equal which suggests a similar process is occurring for all the reduction peaks (Kuzmany, 1994) *i.e.* a single electron reduction. As discussed previously (Section 3.5.1) a single electron that a single electron process should exhibit an ΔE_p value of about 59 mV, the average ΔE_p value obtained for the cyclic voltammogram of C_{60} solution was found to be 63 mV. The 4 mV difference can be attributed to drift within the reference electrode or some impurities in the solution. Only four reductions were achieved because of the range of the gold electrode and due to the fact the scan was taken at standard room temperature.

4.5.2 Cyclic voltammetry of C_{60} films

The electrochemical behaviour of a C_{60} film attached to an electrode via spin coating or drop cast (usually with toluene) is significantly different to that observed for the solution phase. Early voltammetric studies of C_{60} films on platinum electrodes in acetonitrile (MeCN) and ammonium salts such as $TBAPF_6$ reported four reduction peaks with $E_{½}$ potentials of –1.17 V, 1.39 V, -1.88 V and –2.24 V Vs Fc/ Fc^+(Haddon, 1986). The first three peaks closely resemble the first three reduction peaks seen for the solution of C_{60}. However, reported with these half wave ($E_{½}$) potentials was a large potential splitting between the reduction and the re-oxidation whereas in solution the reduction and re-oxidation peaks occur at approximately the same potential with a peak separation ΔE_p of ~59 mV. The variation in peak separation between solution and solid has been attributed to structural rearrangement of the film following the first electron transfer (Haufler, 1990, Jehoulet, 1991, Kuzmany, 1994).

Figure 4.4 shows a typical cyclic voltammogram obtained for a C_{60} drop cast film in this study. The film was prepared by evaporating a two microliters of a C_{60}/toulene solution, on the surface of a glassy carbon electrode (1 mm diameter). The electrolyte used was acetonitrile and the support electrode was tetrabutylammonium tetrafluoroborate ($TBABF_4$). The cyclic voltammogram only shows the first two reduction peaks for C_{60} at -1.10 V and -1.37 V and the corresponding re-oxidation peaks at –0.50 V and –1.10 V respectively.

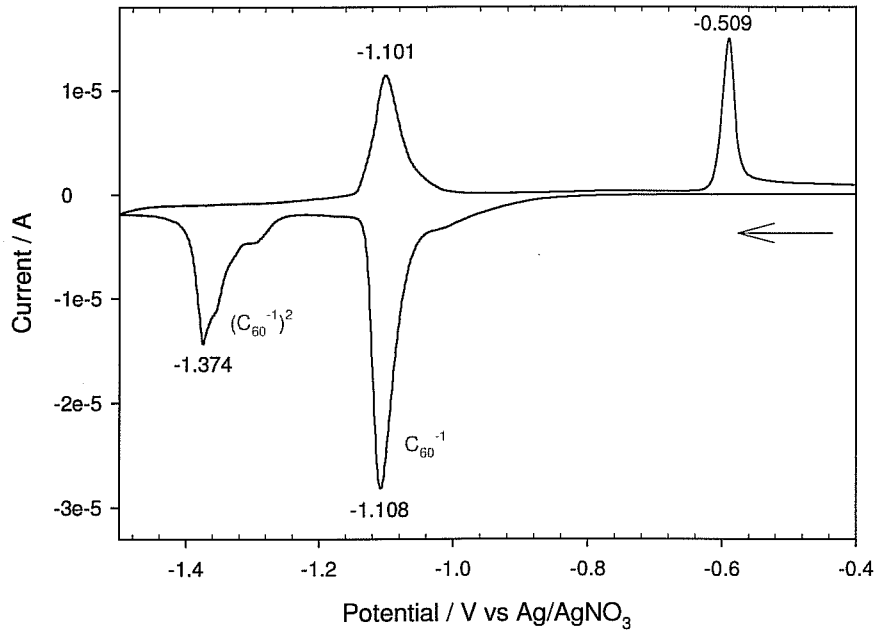

Figure 4.4: Cyclic voltammogram for C_{60} drop cast film@0.1 V/s and 20 °C.

Literature evidence indicates that scanning beyond the second reduction peak can cause irreversible damage to the film (Haddon, 1986, Jehoulet, 1991) hence it was deemed appropriate for this study not to go beyond this feature. As previously observed in literature the peak separation ΔE_p for the both the reduction and re-oxidation couples is quite large *i.e.* approximately 600 mV for the first and 270 mV for the second. This separation is suggested to be due to structural rearrangements that occur during the reduction process. Initially the drop cast film should consist of C_{60} crystallites, each with an fcc packing geometry and a small percentage of toluene, which is trapped in the crystallites during film preparation. Upon reduction, most of the C_{60} in the film reduces to C_{60}^{-1}. The TBA^+ counter ion must then diffuse into the lattice in order to balance the negative charges (Xie, 1992). This counter ion however is comparable in size to the C_{60} molecule and physically cannot intercalate into the spaces of the fcc structure. Therefore

the system rearranges into a new more stable structural configuration, which allows the TBA^+ ion to balance the charges. Figure 4.5 shows the proposed reaction scheme for the first reduction and re-oxidation of C_{60} thin films in $TBABF_4$/ MeCN (Jehoulet, 1991).

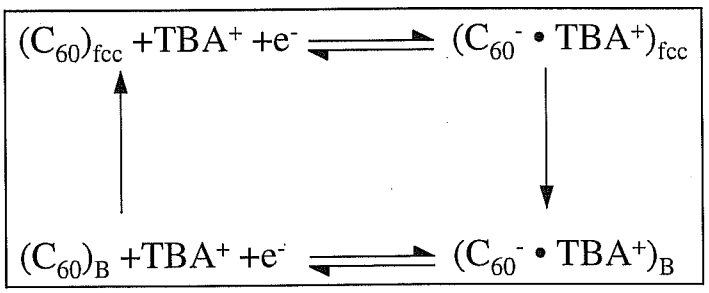

Figure 4.5: Proposed reaction scheme for the first reduction of C_{60} thin films. The molecules are originally in an fcc arrangement and after reduction rearrange in to a new film structure (Jehoulet, 1992).

It is important to note as well that in situ ESR and conductivity measurements reported by Smie and Heinze suggests that the C_{60} is most conductive at the first reduction peak C_{60}^{-1}, which occurs at 50 % charging (Smie and Heinz, 1995). However at the second peak C_{60}^{-2} they found the C_{60} to be less conductive. They attributed this to the formation of a dimeric form or photopolymer form of C_{60}.

4.6 Summary

The ability of C_{60} to accept up to six electrons makes it an ideal acceptor. Another advantage is its size and solubility. C_{60} can be diffused into a polymer solution. The most efficient way of achieving charge separation between C_{60} and conjugated polymers is to prepare devices from a C_{60}/polymer solution. Several studies determined the charge transfer range to be within 5 to 10 nm (Kraabel, 1994, Vacar, 1997, Halls, 1996).

Therefore the C_{60} molecule has to be within ~10 nm of the location of the photoexcitation for the charge transfer to occur. UV/VIS and cyclic voltammetry of composite will provide information on how well dispersed C_{60} is throughout polymer. The next part of this chapter will concentrate on the characterisation of MEH-PPV.

4.7. Characterisation of MEH-PPV

PPV (phenylene vinylene) is an insoluble polymer, which is generally obtained in film form by thermal conversion of a soluble non-conjugated precursor (Martin, 1998). In order to improve its processability derivatives of PPV with solubilising side groups, attached either at the 2 and/or 5 positions on the phenylene ring or on the vinyl linkage have been produced (Martin, 1998). Poly (2-methoxy-5-(2'-ethylhexyloxy)-1,4phenylenevinylene) (MEH-PPV), is the mostly commonly used derivative of PPV and is readily soluble in most organic solvents. For this thesis, solutions were prepared in chlorobenzene unless otherwise stated.

4.7.1 Electronic characterisation

The optical properties of a conducting polymer are important to the development of an understanding of the basic electronic structure of the material. MEH-PPV films were spin coated onto quartz disks (thickness approximately 200 nm). Figure 4.6 shows the solid-state absorbance (black line) and fluorescence spectrum for MEH-PPV (red line). The insert shows the spectral region from 2.00 eV to 2.60 eV. Also included in Figure 4.6 is the UV/VIS absorption spectrum of molecular MEH-PPV (blue line) as measured in a chlorobenzene solution.

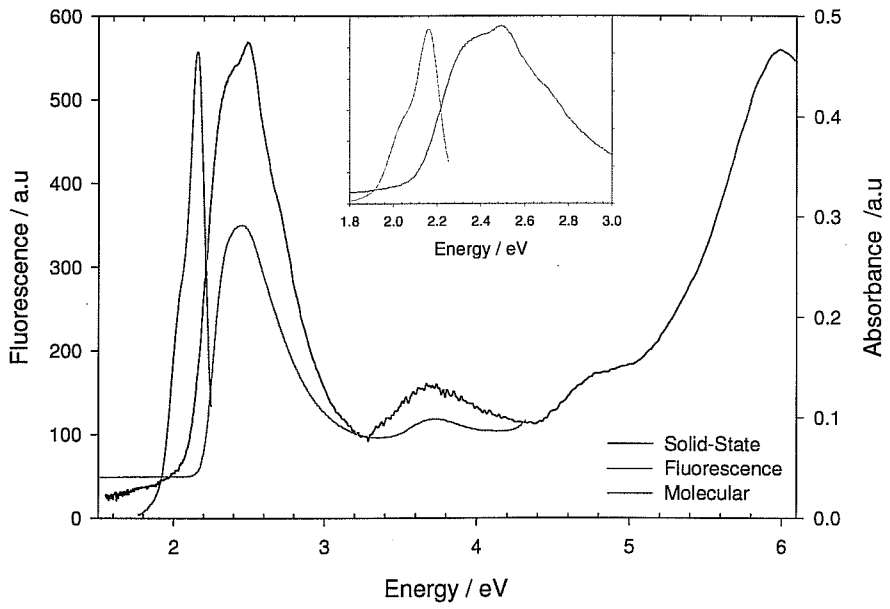

Figure 4.6: Solid-State absorbance (black line), and fluorescence spectrum of MEH-PPV (red line). Inset shows expanded solid-state fluorescence and absorption spectra. The MEH-PPV molecular phase is represented by blue line.

This was done to show that the difference between MEH-PPV in its molecular form and solid-state from is negligible. Therefore it can be said that the solid-state form is of molecular origin and there is little or no aggregation occurring. Aggregation can lead to a red or blue shifting of the $\pi \rightarrow \pi^*$ transition. This will be discussed in greater detail in the next chapter. The solid-state absorption agrees well with previous spectra from literature (Burroughes, 1990, Hagler, 1994). The absorption spectrum has four absorption features. The maximum absorption at 2.44 eV is due to the $\pi \rightarrow \pi^*$ transition of the conjugated backbone. This transition is reported to be confined to the phenyl rings (Martin, 1998). There are two shoulder peaks on either side of the maximum absorption peak at 2.33 eV and 2.64 eV. It has been suggested in literature that these two peaks are due to vibronic transitions. The next peak at 3.73 eV is attributed to a

transition forbidden in the unsubstituted polymer (PPV) but which is allowable in the derivative due to symmetry breaking effects caused by the presence of the additional side chains in MEH-PPV (Martin, 1998). The two other features at 4.75 eV and 5.99 eV are attributed to transitions between delocalised and localised molecular orbitals. The maximum fluorescence occurs at 2.19 eV. Using the maximum absorption and fluorescence a Stokes Shift value of 0.25 eV was calculated. Both the absorption and emission peaks are red shifted compared to PPV due to the electron withdrawing side chains (Burroughes, 1990, Hagler, 1994).

4.7.2 Cyclic voltammetry

The electrochemical properties of MEH-PPV are very well documented (Holt, 2005, Yang, 1999 and Richter, 1994). Figure 4.7 shows the cyclic voltammogram of MEH-PPV. It can be seen from Figure 4.7 that the oxidation potential of MEH-PPV occurs at 0.62 V. It has been suggested that the oxidation (p-doping) shows a quasi- reversible electrochemical response (Yang, 1999, Richter, 1994). A quasi-reversible response means that for higher scan rates, the oxidation peak occurs at higher potential and the current increases (Holt, 2005). Charge transport at this point is facilitated and controlled by the diffusion of counterions in the polymer film (this is the same for all conjugated polymers). It is important to note that for MEH-PPV if the potential is increased beyond the oxidation peak of the polymer (0.62 V), then the polymer can become over oxidised causing the film to degrade hence affecting the reversibility (Richter, 1994).

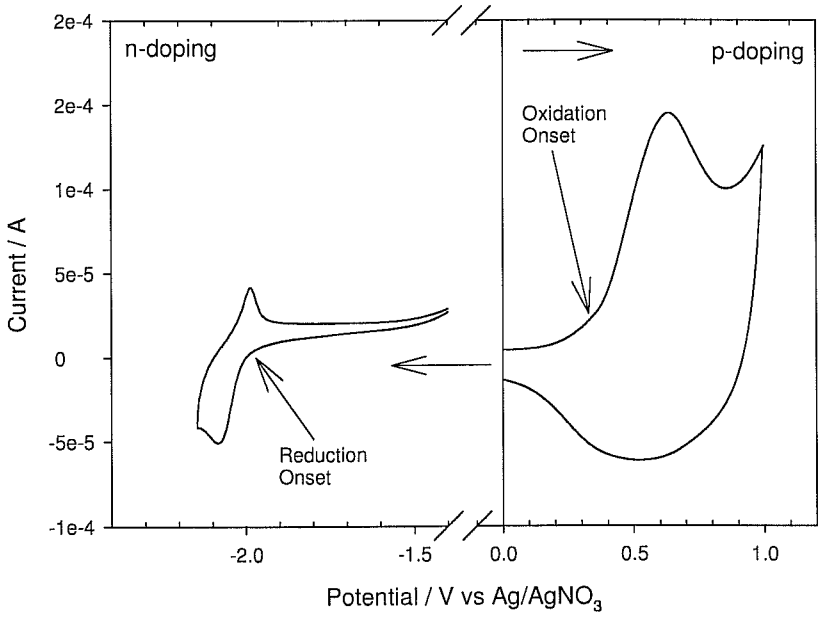

Figure 4.7: Cyclic voltammogram of MEH-PPV in CH_3CN solution of 0.1 M tetrabutylammonium hexafluorophosate @scan rate of 0.1 V/sec.

In comparison in literature reports on the cyclic voltammetry of PPV (Stenger-Smith, 1989) it is seen that the substituent groups affect the overall electrochemical properties. For example electron donating groups (such as the alkyloxy) decrease the oxidation potential of MEH-PPV compared to that of PPV (Gautrot, 2007). This is an important factor which must be considered when exploring the new polymer series in chapter 6. In contrast to the oxidation, MEH-PPV is shown to have fully reversible reduction and reoxidation peaks at -2.08 V and -1.98 V. Reversibility of the n-doping (reduction) scan is a necessity when considering conjugated polymers in optoelectronic devices. In order to maintain a functional device the polymer must be capable of donating electrons to the acceptor material repeatedly. The onset potentials of the p-doping and n-doping scans can be used to determine the LUMO (electron affinity, EA) and HOMO (ionisation potential, IP) energy levels of the polymers and the potential difference can be used to

estimate the band gap of the polymer. These empirical relationships can be mathematically described using the following relations (de Leeuw, 1997):

$$[E_{onset}]^{ox} = \text{Ionisation Potential(IP)} - 4.4 \qquad \text{(Eqn 4.1)}$$

$$[E_{onset}]^{red} = \text{Electron Affinity (EA)} - 4.4 \qquad \text{(Eqn 4.2)}$$

where $[E_{onset}]^{ox}$ and $[E_{onset}]^{red}$ are the onset potentials for the oxidation and reduction of the polymers(de Leeuw, 1997, Cervini, 1997). The on-set potentials may be defined by considering the E_{ox} and E_{red} or the difference between the two in the case of reversible processes. In this study, however, the onset potentials $[E_{onset}]^{ox}$ and $[E_{onset}]^{red}$ were calculated from the intersection of the two tangents drawn at the rising oxidation (reduction) current and background current in the cyclic voltammogram (Li, 1999). The electrode potential of the $Ag/AgNO_3$ (0.10M) reference electrode was calibrated to be -0.01 V Vs $Ag/AgNO_3$. Therefore the -4.40 V in Equation 4.1 and 4.2 is accordingly adjusted to -4.39 V. For MEH-PPV it is found that the oxidation-onset is 0.35 V and reduction-onset is -1.98 V, which results in an ionisation potential (IP) of 4.74 eV and an electron affinity (EA) of 2.41 eV. An electrochemical bandgap of 2.33 eV can thus be derived from the IP and EA values. The calculated bandgap agrees with previous reports in literature (Holt, 2005, Cervini, 1997). It should be noted the electrochemical bandgap is in close approximation with the optical bandgap of 2.44 eV (Holt 2005, Cervini, 1997). Using Equation 4.2 and Figure 4.3 it is also possible to calculate the LUMO level of molecular C_{60}. From Figure 4.3, the reduction onset potential was -0.71 V which results in a LUMO level of 3.68 eV. As there are no oxidation processes in pristine C_{60} the HOMO can't be calculated using Equation 4.1 however by adding the

optical bandgap (1.80 eV) to the calculated LUMO level it is possible to obtain an energy level for HOMO band which is calculated to be 5.48 eV. Therefore it is now possible to redraw Figure 2.11 with greater accuracy. Figure 4.8 shows the shows the energy level diagram for an MEH-PPV/C_{60} device. It is assumed that charge transfer occurs from the LUMO level of MEH-PPV onto that of the C_{60} after photoexcitation. From the energy level diagram it is possible to determine some of the device characteristics. As the HOMO level of MEH-PPV is lower than that of the ITO the device will not possess good hole blocking properties. The other side of the coin is that for electron injection the LUMO level of the C_{60} be higher than that of the aluminium. From Figure 4.8 it can be seen that the C_{60} LUMO level is higher than the aluminium workfunction and hence the device would display good electron injection abilities.

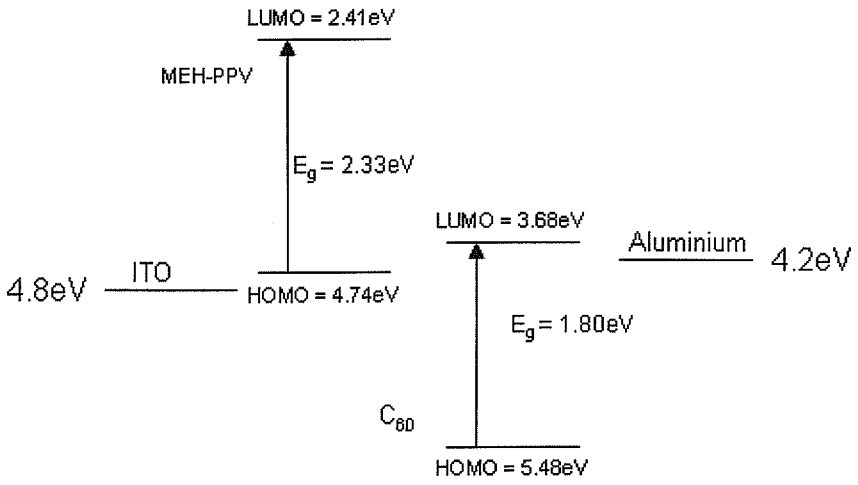

Figure 4.8: Energy level diagram of MEH-PPV and C_{60} device.

The systematic change in the novel polymers will allow investigation of the change in charge transfer when the LUMO level of the polymer is increased or decreased to a higher energy. This higher energy may be more favourable for a charge transfer to

occur. Another question this study could answer is, that if the higher energy (increase in LUMO level) is favourable, how much of an increase will optimise the charge transfer.

4.7.3 Electroabsorption spectroscopy

Figure 4.9 shows the electroabsorption spectrum for MEH-PPV with a first derivative spectrum (the first derivative is of the solid-state optical absorption spectrum in Figure 4.6). In Figure 4.6 the energy range is from 2.00 eV to 5.00 eV. However the electroabsorption spectrometer energy range is from 2.00 eV to 3.50 eV. Therefore the electroabsorption spectrum scan only detects the first absorption band. The electroabsorption spectrum closely matches that of the first derivative line shape. The first feature at 2.20 eV to 2.50 eV is due to the quadratic Stark effect of the lowest exciton (Shimoi, 2000). In between the lowest excitonic feature there is a phonon sideband at 2.30 eV (Liess, 1997). At higher energies (beyond 2.60 eV) the electroabsorption spectrum deviates from the first derivative line shape and there is an induced transition to a forbidden exciton state, which becomes optically allowed by the application of the externally applied field (Martin, 1998).

A lower limit for the exciton binding energy, E_b, may be directly found from the electroabsorption analysis and using Equation 4.3:

$$E_b = E({}_mA_g) - E(1B_u) \qquad \text{(Eqn 4.3)}$$

where ${}_mA_g$ and $1B_u$ are localised excitons with large binding energies, the symmetries of which are restricted to even (${}_mA_g$) or odd parity ($1B_u$).

In the case of this study the exciton binding energy is taken to be the energy separation between the lowest optical exciton level and the banded state. The binding energy of MEH-PPV was calculated to be 0.74 eV (±0.15 eV) from Figure 4.9. This coincides with theoretical values for the binding energy (Martin, 1998, Shimoi, 2000). In fact E_b is normally between 0.50 eV and 0.80 eV for most polymers, (Liess, 1997).

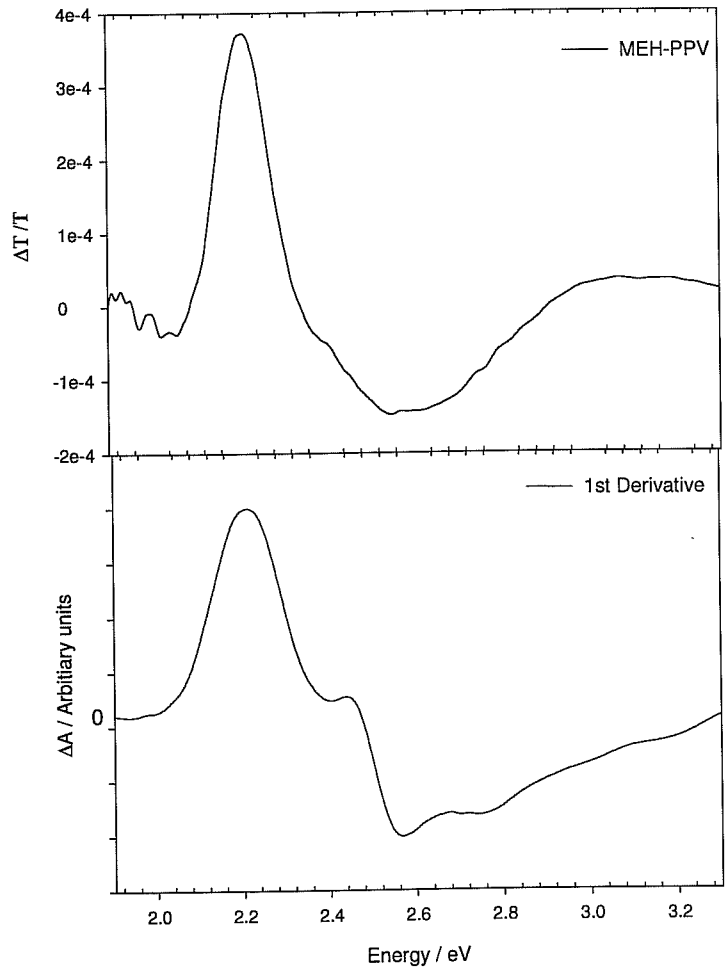

Figure 4.9: Electroabsorption spectrum of MEH-PPV with a first derivative lineshape.

4.7.4 MEH-PPV summary

The first part of this chapter provided an in-depth characterisation of the two reference materials used throughout this study. C_{60} was shown to be an ideal acceptor material due to its size and its ability to acceptor up to six electrons. MEH-PPV is a PPV derivative which, has been shown to charge transfer with C_{60}. The most common way of observing this charge transfer phenomena is to use time resolved photoinduced absorption spectroscopy. The third and final part of this chapter explores evidence of such charge transfer states in MEH-PPV/C_{60} composites using the simpler steady state spectroscopic techniques couple with cyclic voltammetry and conductivity measurements. These methods could mean a faster and less complex way of examining charge transfer between fullerene polymer composites.

4.8 MEH-PPV/ C_{60} composites

The first method used to investigate the MEH-PPV/C_{60} composites was electronic spectroscopy. In literature, the concentration of C_{60} in MEH-PPV/C_{60} composites used varies from 10 % to 100 % (Drees, 2002, Ltaiefa, 2004). A slightly below average value of 52 % was chosen as a starting point in this thesis. A solution of MEH-PPV with 52 % C_{60} was prepared using 1, 2-dichorobenzene. The effect of varying concentration of C_{60} will be further examined using fluorescence measurements in Section 4.8.1. MEH-PPV/C_{60} and MEH-PPV films were fabricated by spin coating onto a quartz disk (thickness approx. 200 nm). Figure 4.10 shows the UV/VIS solid-state absorption spectra of pristine MEH-PPV and MEH-PPV/C_{60} composite. The π-π^* transition of MEH-PPV at 2.45 eV is clearly observed. This is followed by the first dipole allowed

transition in C_{60} at 3.75 eV (Figure 4.1). The spectrum is a simple superposition of the two materials (molecular MEH-PPV and molecular C_{60}, therefore C_{60} is molecularly dispersed) without any indication of states below the π-π^* of the conducting polymer as might arise form interaction between the two materials in the ground state. Even though there is no interaction in the ground state, UV/VIS measurements are important as the addition of C_{60} can effect the π-π^* transition energy of a conjugated polymer. It has been shown that C_{60} can act as a molecular spacer and hence reduce aggregation in polymer systems (Wang, 1997).

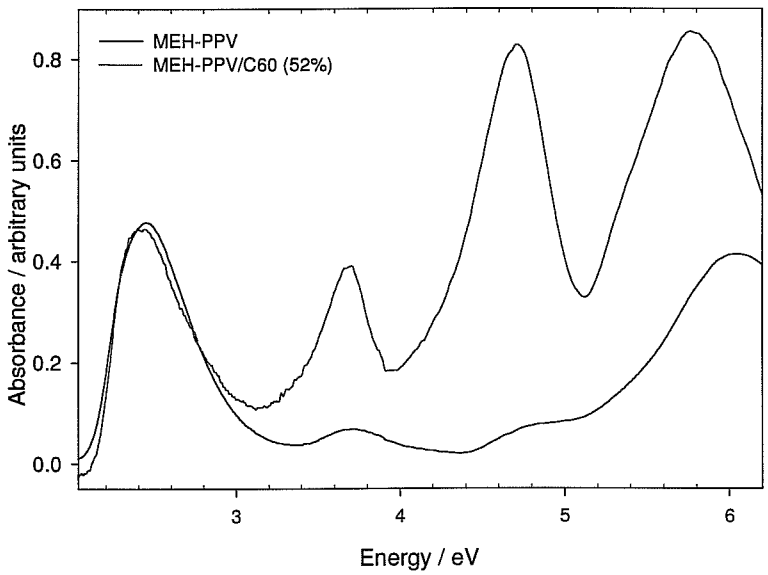

Figure 4.10: UV/VIS absorption spectra of pristine MEH-PPV and MEH-PPV/C_{60} composite.

4.8.1 Fluorescence measurements

Fluorescence measurements are extremely important when investigating charge transfer between donor and acceptor materials. It is one of the most simplest ways of observing charge transfer. Fluorescence quenching in conjugated polymers upon addition of an

acceptor material is consistent with efficient photoinduced charge transfer in polymer/fullerene composites (Morita, 1992, Sariciftci, 1992). The addition of the C_{60} prevents the electron hole pair recombining and hence results in fluorescence quenching. For fluorescence measurements a stock solution of MEH-PPV ($1x10^{-4}$ g/*l* in chlorobenzene) was prepared. This stock solution was divided into nine parts and varying amounts of C_{60} between 0 % and 72 % were added to each of the nine parts to produce a varying loading ratio of C_{60} to MEH-PPV. Fluorescence measurements were then performed on each solution. The excitation wavelength was set at 2.40 eV as to excite at maximum absorbance energy. Figure 4.11 shows the fluorescence spectrum of pristine MEH-PPV and the MEH-PPV/C_{60} composites with different C_{60} loading fractions. As C_{60} does not fluoresce (Catalan J, 1993) the spectrum is that of the pristine polymer.

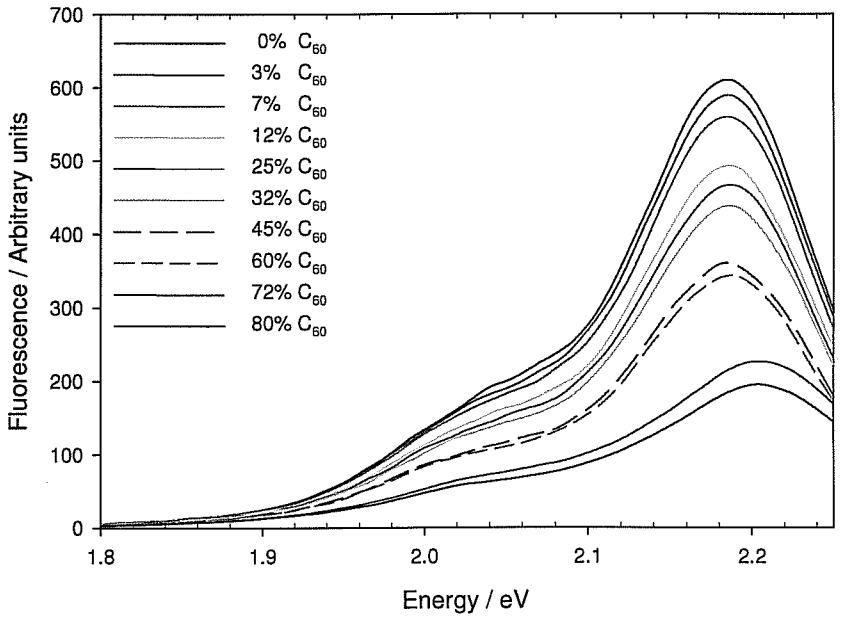

Figure 4.11: Fluorescence of MEH-PPV @ different C_{60} concentrations/ loading fractions.

The first noticeable observation from Figure 4.11 is that the greater the C_{60} percentage the greater the fluorescence quenching. The observed reduction of the fluorescent emission cannot be accounted for by increased absorption by the fullerene in solution. This fluorescence quenching thus provides the first experimental evidence of an interaction between MEH-PPV and C_{60}. It should be noted that a higher concentration the fluorescence maximum is slightly shifted. This may be due to aggregation of the C_{60}.

Figure 4.12 shows a plot of fluorescence intensity against the C_{60} concentration in the MEH-PPV (MEH-PPV concentration was kept constant). As well as providing evidence of charge transfer between the MEH-PPV and C_{60}, the fluorescence measurements allow the calculation of the optimum amount of acceptor material that should be used in a composite. The acceptor material concentration must be optimised as too much can lead to electrical percolation, and the composite properties will become dominated by the acceptor material. The MEH-PPV on its own is highly fluorescent. Fluorescence is a competing process to the formation of an electron-hole pair. The decrease in fluorescence when C_{60} is added is approximately linear from 0 to 45 %. The fluorescence between 45 % and 60 % is approximately constant. At a higher concentration (72 %) the fluorescence is almost completely quenched. This would indicate that the optimum concentration of acceptor material would be between 45 %-60 %. The concentration of C_{60} was thus chosen to be between 50 %-55 %.

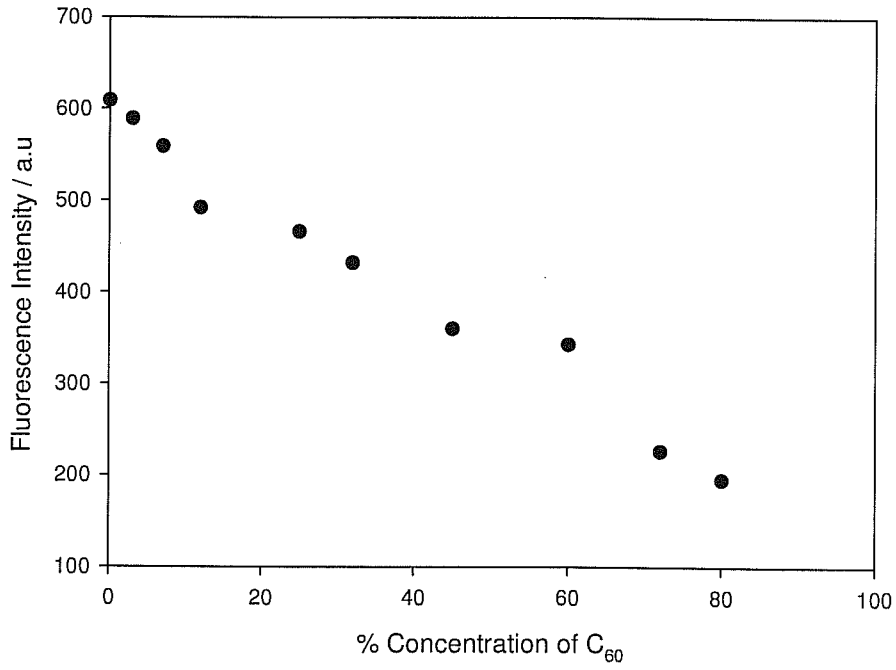

Figure 4.12: Maximum fluorescence against percentage concentration of C_{60}.

4.8.2 Electroabsorption spectroscopy

The Electroabsorption of MEH-PPV in Section 4.7.3 showed it has a first derivative line shape. This implies the electronic states are localised along the polymer backbone. Comprehensive experimental studies on the electroabsorption of C_{60} by Jeglinski *et al* (Jeglinski, 1992) supported by detailed theoretical interpretation (Pac, 1998) have led to detailed assignment of the observed spectral features in the energy range up to about 4.00 eV. In this range, three series of charge transfer states have been detected (Pac, 1998, Kazaoui, 1998). The C_{60} EA spectrum exhibits first and second derivative characteristics indicating both excitonic and charge transfer states as discussed in Section 4.4. When dealing with the electroabsorption of C_{60} in a polymer matrix it is assumed that the C_{60} is dispersed through the film which was also seen in UV/VIS

results. Therefore C_{60} features in the composite spectrum are of molecular C_{60}. Liess *et al* previously reported electroabsorption data on MEH-PPV/C_{60} composites. Liess reported electroabsorption features at 1.18 eV and 1.65 eV which are attributed to bound pairs of C_{60}^- and MEH-PPV. The electroabsorption spectrometer used in this study cannot detect these bands due to the limited spectral range (2.00 eV- 3.60 eV). Figure 4.13 shows the electroabsorption spectra of pristine MEH-PPV and the MEH-PPV/C_{60} composite from 2.00 eV to 3.60 eV. The feature at 2.22 eV is the excitonic transition of MEH-PPV followed by the forbidden state at 3.00 eV (Section 4.5.3).

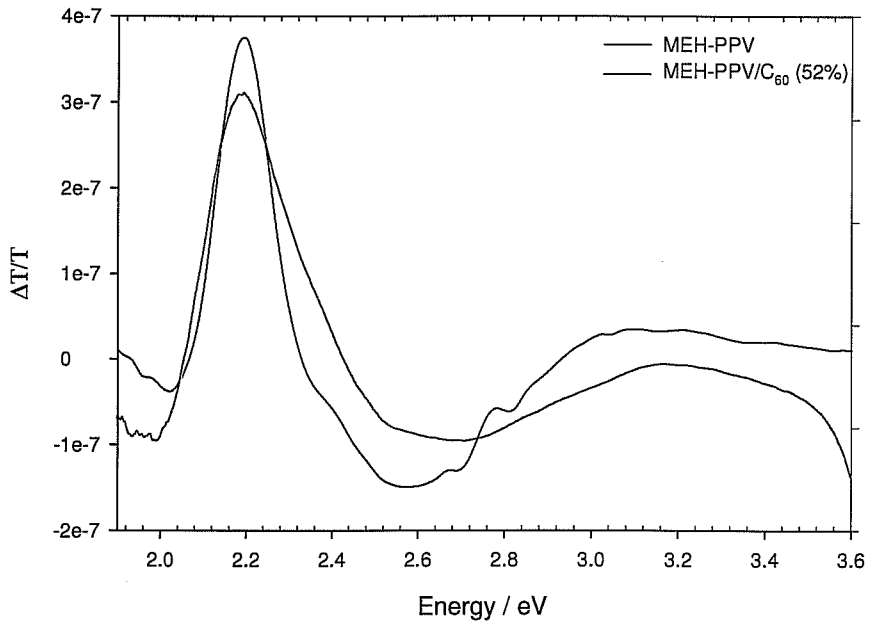

Figure 4.13: Electroabsorption spectra of pristine MEH-PPV and MEH-PPV/C_{60} composite.

The phonon sideband at 2.30 eV is more pronounced in pristine MEH-PPV than in the MEH-PPV/C_{60} composite due to the broadening of the energy states distribution (Liess, 1997). The broadening of the energy state's has been shown to coincide with the appearance of the two features at 1.18 eV and 1.65 eV (Liess, 1997). Therefore although

these features are not visible in Figure 4.13 it can be said that the broadening of the energy states and the loss of the phonon sideband are indicators of an interaction occurring between the MEH-PPV and C_{60}. However it is important to note that although there is evidence of an interaction between the MEH-PPV and C_{60}, the interaction may be due to the morphology of the composite material and not a charge transfer. this could be checked using some microscopy techniques such as atomic force microscopy.

4.8.3 Cyclic voltammetry

Figure 4.14 shows the cyclic voltammetry obtained for the p doping (oxidation) scan of MEH-PPV and MEH-PPV/C_{60}. The composite contains 52 % C_{60}. The films were produced by drop casting onto the electrode. The solvent was then allowed to evaporate under a controlled atmosphere (laminar flow). It can be seen from Figure 4.14 that there are two oxidation peaks visible in composite at 0.63 V and 1.02 V. The p-doping of MEH-PPV showed a quasi-reversible electrochemical response with an oxidation peak at 0.62 V. The first peak in the composite at 0.63 V can thus be attributed to the first oxidation peak of MEH-PPV. Compared to pristine MEH-PPV this peak is shifted slightly to a more positive value. This implies the MEH-PPV is more electronegative when the C_{60} is added. The addition of the C_{60} also leads to an increase in the ionisation potential of the MEH-PPV from 4.74 eV to 4.83 eV (as calculated from Equation 4.2) and hence the composite is more electronegative than the pristine MEH-PPV. The second oxidation peak at 1.02 V is suggested to be a composite feature. Pristine C_{60} has been shown to have no oxidation feature in the positive region (Jehoulet, 1991). It is postulated that when the MEH-PPV loses an electron, the electron is transferred onto the C_{60}, *i.e.* charge transfer occurs and then the C_{60} is charged and can now be oxidised

and hence the evolution of the second oxidisation feature. As pristine C_{60} has been shown to have no oxidation features under p-doping conditions, the new composite feature must be attributed to the MEH-PPV interacting with the C_{60} and not the support electrolyte. However upon cycling the scan past the first oxidation peak of MEH-PPV the film loses its electronegativity.

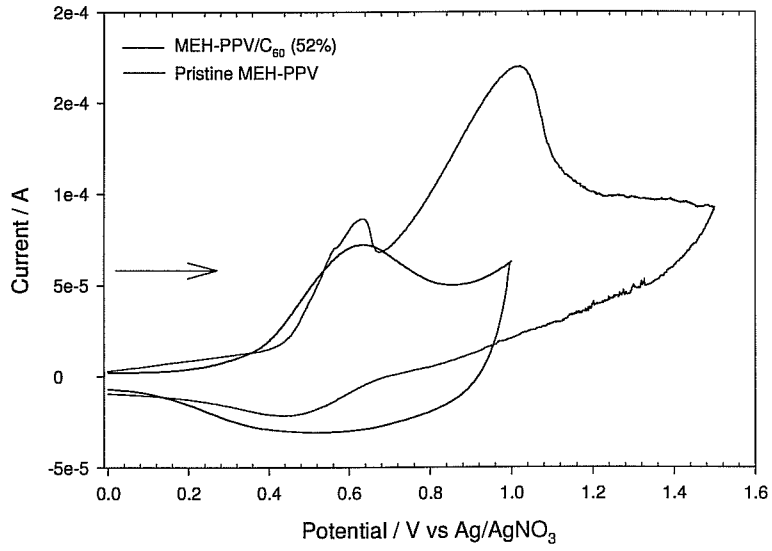

Figure 4.14: Cyclic voltammogram of p-doping of MEH-PPV and MEH-PPV/C_{60} in CH_3CN solution of 0.1 M tetrabutylammonium hexafluorophosate @scan rate of 0.1 V/sec.

The new composite feature occurs at 1.02 V which correlates to the energy difference between the HOMO level of MEH-PPV and the LUMO level of C_{60} (HOMO (MEH-PPV)-LUMO (C_{60}) = 1.06 V). This point reaffirms that there is a charge transfer occurring. However from the energy difference it can also be postulated that the charge transfer is from the HOMO level of the MEH-PPV to the LUMO level of the C_{60}. It has also been reported that varying the amount of C_{60} added will alter the electro induced charge carrier generation (Ding, 2002). A too high concentration of C_{60} leads to

aggregates and phase separation from the MEH-PPV, which results in inhomogeneous films (Ding, 2002). However inhomogeneous films did not result from 52 % concentration which would indicate the concentration obtained from fluorescence measurements was accurate.

Figure 4.15 shows the n-doping scan obtained for the MEH-PPV/C_{60} composite. The scan is a summation of the two materials. The first four peaks at –0.94 V, -1.47 V, -1.76 V and –1.92 V are attributed to the reduction of molecular C_{60}. These peaks are shifted compared to that of the pristine C_{60} (molecular) which could due to the local environment.

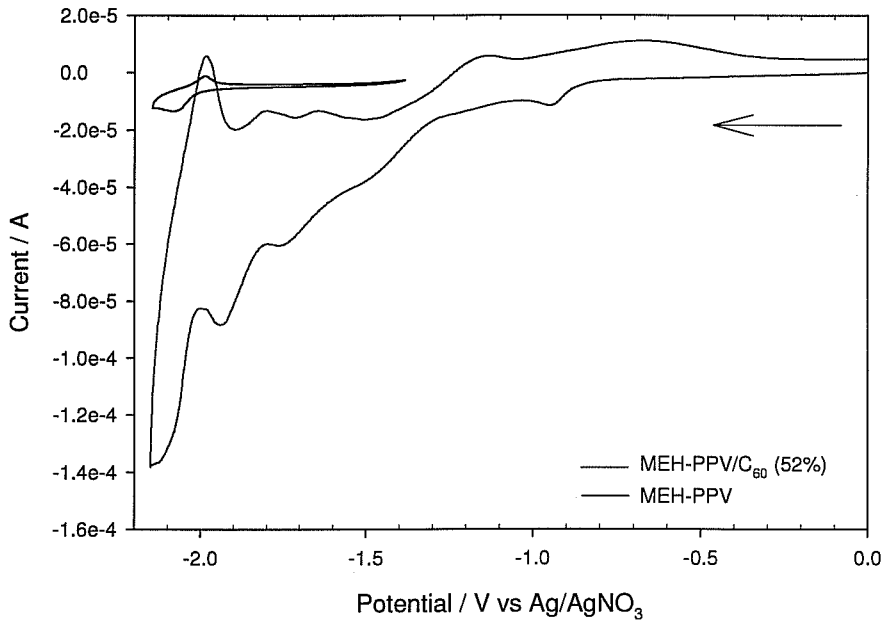

Figure 4.15: Cyclic voltammogram of n-doping of MEH-PPV/C_{60} in CH_3CN solution of 0.1 M tetrabutylammonium hexafluorophosate @scan rate of 0.1 V/sec.

The strongest feature in the graph is the reduction of the MEH-PPV at –2.13 V. For pristine MEH-PPV the current range over which the reduction and oxidation occurs is

less than one order of magnitude. The addition of the C_{60} increases this by two to three orders of magnitude. This would seem practical, as the C_{60} is able to accept the electrons from the MEH-PPV, thus allowing a bigger current intake (in the polymer). This is a clear indication that the addition of an acceptor material has an effect on the polymer.

Previous reports on the addition of a CN group to the MEH-PPV has suggested that the MEH-PPV undergoes a "pre-reduction" (Li, 1999) before its main reduction potential. It is believed that this process favours charge transfer and at the "pre-reduction" potential there is an influx of electrons into the film, e.g. better conduction. The onset of this pre-reduction is taken as the point where the electron affinity of the polymer is measured. If this theory is applied to the MEH-PPV/C_{60} composite, it can be said that a pre-reduction occurs at –0.94 V. Furthermore calculating the electron affinity from the onset of this peak (-0.88 V) it can be seen that the electron affinity is found to be 3.51 eV compared to 2.41 eV in pristine MEH-PPV. The addition of the C_{60} therefore raises the LUMO level of pristine MEH-PPV. This increase of the LUMO level coupled with the increase in conductivity is evidence of an interaction between MEH-PPV and C_{60}. Conductivity measurements were performed next to clarify the increase in current with the addition of the C_{60}.

4.8.4 Electrical conductivity measurements

To further support the electrochemical measurements an electrical conductivity study was performed on a MEH-PPV single layer device and on MEH-PPV/C_{60} single layer device. It could be said that conductivity measurements are similar to electrochemically p-doping measurements; the obvious difference is that p-doping is a chemical process.

A sandwich structure geometry was used as explained in Section 3.7.1. Figure 4.16 (A) shows the I-V characteristic curve for a MEH-PPV single layer device and (B) the I-V characteristic curve for a MEH-PPV single layer device and MEH-PPV/C_{60} single layer device obtained using 237 Keithley programmable electrometer and current voltage power sources. Films were placed in a Linkam microscope cooling stage which was purged with nitrogen so as to keep the films under an inert atmosphere.

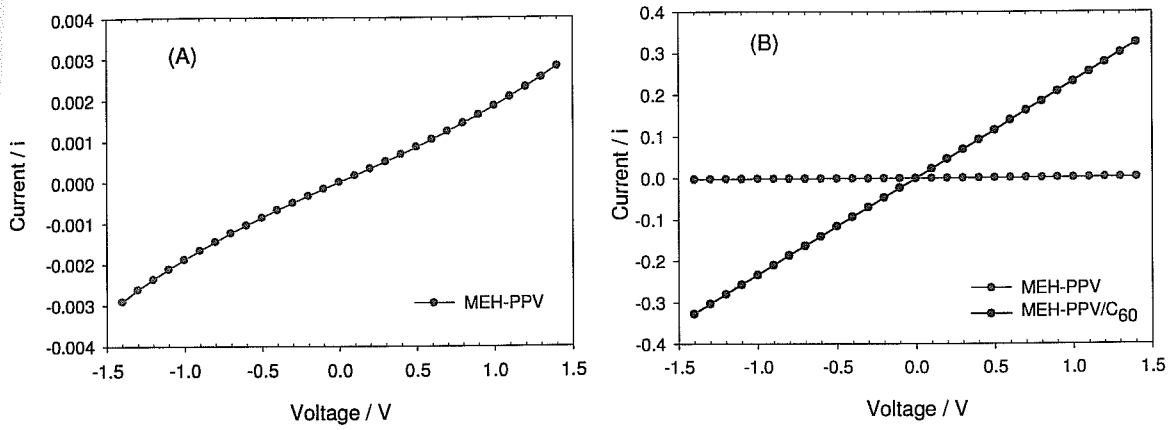

Figure 4.16: I-V characteristic curve for (A) MEH-PPV single layer and (B) MEH-PPV single layer device and MEH-PPV/C_{60} single layer device.

The short circuit current (I_{sc}) of the MEH-PPV/C_{60} device at ±1.5 V is 2 orders of magnitude larger than the MEH-PPV single layer device. The addition of the C_{60} enhances the transport of electrons and holes through the acceptor and donor material respectively in a preferred direction to the extracting electrodes. The conductivity measurements confirmed that the addition of an acceptor material into the MEH-PPV increases the conductivity of the polymer. This result is important as it reaffirms the previously discussed cyclic voltammetry measurements. As the C_{60} has been shown to be molecular dispersed it can be assumed that the percolation threshold has not been

surpassed. The percolation threshold will be surpassed if there is enough C_{60} in the composite to create a conducting path from the anode to cathode.

4.9 Summary

The first two parts of this chapter described the characteristics of C_{60} and MEH-PPV which where chosen as the electron acceptor material to be used throughout the study and an electron donating reference material respectively. The information gained from the characterisation of these materials provides an insight not only into the individual properties of each material but as how well the energy levels of each are matched together, Figure 4.8.

A detailed characterisation of the composite of these materials in an optimised 52 % loading fraction was also carried out with the specific task of identifying any indicators of charge transfer using simple steady state techniques. The identification of such indicators would alleviate the need for the costly techniques such as femtosecond spectroscopy to study charge transfer processes in polymer based PV devices, thus making the area more accessible to researchers

UV/VIS measurements of the composite indicate that the C_{60} is molecularly dispersed. The absence of any new spectral features leads to the conclusion that there is no charge transfer in the ground state's between the MEH-PPV and C_{60}. Fluorescence quenching provided the first indication of the photoinduced charge transfer in MEH-PPV and C_{60}. It also allowed determination of the optimum concentration of acceptor material that can be used without totally dominating the composite.

Electroabsorption studies indicate that a charge transfer could take place in the composite. The addition of C_{60} results in a broadening of the energy states distribution

in MEH-PPV. The phonon sideband at 2.30 eV in pristine MEH-PPV was absent in the composite. The two occurrences are known to coincide with a charge transfer between the two materials.

The cyclic voltammetry measurements first showed a new composite feature in the p-doping scan. It is believed that this feature is due to the addition of an electron to the C_{60}. Further evidence of this was the voltage correlation between the HOMO (MEH-PPV)-LUMO (C_{60}) and the potential of the composite feature.

In contrast the n-doping scan was a summation of the two materials. The addition of the C_{60} increases the electron affinity thus reduces the bandgap of the composite. The conductivity range of the reduction potential of MEH-PPV was increased by two orders of magnitude with the addition of the C_{60}. Conductivity measurements confirmed that the addition of the C_{60} increases the conductivity of the polymer.

In conclusion, clear and identifiable signatures of charge transfer between MEH-PPV and C_{60} are evident from steady state measurements, cyclic voltammetry and conductivity measurements. These techniques should therefore also be capable of detecting similar signatures of charge transfer in the new novel polymer/fullerene composites.

The next chapter starts the exploration and characterisation of the conjugated polymers mentioned in Chapter 3 (Section 3.2). Chapter 5 deals with the electronic characterisation of the polymers. Using the results obtained from the electronic characterisation, two of the polymers will be chosen and used to produce composites with C_{60}. This composite will also be characterised using electronic spectroscopy.

References:

Averitt R.D., Pippenger P.M., Papanyan V.O., Dura J.A., Nordlander P, Halas N.J., *"Photoluminescence Spectra of Epitaxial Single Crystal C_{60}"*, Chem. Phys. Lett. 242, 592, (1995).

Bard A.J., Faulkner L.R., *"Electrochemical methods, fundamentals and applications"*, John Wiley & Sons, New York, NY, (1980).

Braun D, Heeger A.J., *"Visible light emission from semiconducting polymer diodes"*, Appl. Phys. Lett, 58, 1982, (1991).

Burroughes J.H., Bradley D, Brown A.R., Marks R.N., Mackay K, Friend R.H., Burn P.L., Holmes A.B., *"Light-emitting diodes based on conjugated polymers"*, Nature, 539, 347 (1990).

Byrne H.J., in *"Physics and Chemistry of Fullerenes and Derivatives"*, Kuzmany H, Fink, J, Mehring M, Roth S eds., World Scientific Singapore, p183, (1995).

Cervini R, Li X. C, Spencer G.W.C., Holmes A.B., Moratti S.C., Friend R.H., *"Electrochemical and optical studies of PPV derivatives and poly(aromatic oxadiazoles)"*, Synthetic Metals, 84, 359,(1997).

Cox D.M., Behal S, Disko M, Gorun S.M., Greaney M, Hsu C.S, Kollin E.B., *"Characterisation of C_{60} and C_{70} clusters"*, J. Am. Chem. Soc. 113, 2940, (1991).

de Leeuw D.M., Simenon M.M.J., Brown A.R., Einerhand R.E.F., *"Stability of n- type doped conducting polymers and consequences for polymeric microelectronic devices"*, Synthetic Metals 87, 53, (1997).

Ding H, Bertoncello P, Ram M.K, Nicloni C, *"Electrochemical investigation on MEH-PPV/C_{60} nanocomposites Langumir-Schaefer films"*, Electrochemical Communications 4, 503, (2002).

Doubois D, Kadish K.M., Flanagan S, Wilson L.J., *"Electrochemical detection of fulleronium and highly reduced fulleride (C605-) ions in solution"*, J. Am. Chem. Soc. 113, 7773, (1991).

Drees M, Davis R.M., Marciu D, Premaratne K, Miller M, Heflin J.R., *"Improved polymer- fullerene interface in photovoltaic devices by thermally-controlled interdiffusion"* Polymer Preprints (American Chemical Society, Division of Polymer Chemisrty) 43(2), 506, (2002).

Farrell G, Chambers G, Byrne H.J., *"Electroabsorption studies of structurally modified fullerene thin films"*, Journal of Luminescence, 112, 291, (2005).

Haddon R.C., Brus L.E., Raghavachari K, *"Electronic Structure and Bonding in Icosahedral C_{60}"*, Chem. Phys. Lett. 125, 459, (1986).

Hagler T.W., Pakbaz K, Heeger A.J., *"Polarization anisotropy, the off-axis dipole moment, and excited-state delocalization"*, Phys. Rev. B 49, 10968, (1994).

Halls J.J.M., Pichler K, Friend R.H., Moratti S.C., Holmes A.B, *"Exciton diffusion and dissociation in a poly(p-phenylenevinylene)/C_{60} heterojunction* photovoltaic cell", Appl. Phys. Lett. 68 (22), 3120, (1996).

Haufler R.E., Conceicao J, Chibante L.P.F., Chai Y, Byrne N.E., Flanagan S, Haley M.M., O'Brien S.C., Pan C, Xiao Z, Billups W.E., Ciufolini M.A., Hauge R.H., Margrave J.L., Wilson L.J., Curl R.F., Smalley R.E., *"Efficient production of C_{60} (buckminsterfullerene), $C_{60}H36$, and the solvated buckide ion"* ,J. Phys. Chem. 94, 8634, (1990).

Holt A.L., Leger J.M., Carter S.A., *"Electrochemical and optical characterization of p- and n-doped Poly[2-methoxy-5-(2-ethylhexyloxy)-1,4-phenylenevinylene]"*, Journal of Chemical Physics, 123, 044704, (2005).

Gautrot J, Hodge P, *"Poly(dibenzo[a,c]phenazine-2,7-diyl)s- Synthesis and characterisation of a new family of electron-accepting conjugated polymers"*, Polymer, 48, 7065, (2007).

Jeglinski S, Vardeny Z.V., Moses D, Srdanov V, Wudi F, *"Electroabsorption studies of undoped C_{60} films"*, Synth. Meth., 49, 557, (1992).

Jehoulet C. Brad A.J., Wudl F, *"Electrochemical Reduction and Oxidation of C_{60} films"*, J Am. Chem. Soc 113, 5456, (1991).

Kazaoui S, Minami N, Tanabe Y, Byrne H.J., Elimes A, Petelenz P, *"Comprehensive analysis of intermolecular charge-transfer excited states in C_{60} and C_{70} film"*, Phys Rev B. 58, 7689, (1998).

Kraabel B, McBranch D, Sariciftci N.S., Moses D, Heeger A.J., *"Ultrafast spectroscopic studies of induced electron transfer from semiconducting polymers* to C_{60}*"*, Phys. Rev. B, 50(24), 18543, (1994).

Kroto H.W., Heath J.R., O'Brien S.C., Curl R.F., Smalley R.E., *"C_{60} Buckminsterfullerene"*, Nature 318,162, (1985).

Kuzmany H, Matus M, Pichler T, Winter J, *"Physics and Chemistry of Fullerenes"*, World Scientific London, (1994).

Leach S, *"Physics and Chemistry of Fullerenes"*, World Scientific London, (1994).

Li Y, Cao Y, Gao J, Wang D, Yu G, Heeger A.J., *"The synthesis, optical and charge transport properties of poly (aromatic oxadiazole)s"*, Synthetic Metals 99, 243, (1999).

Liess M, Lane P.A., Vardeny Z.V., Kafafi Z.H., *"Electro modulated induced absorption of C_{60} doped MEH-PPV"*, Synthetic Metals 84, 683, (1997).

Liess M, Jeglinski S, Vardeny Z.V., *"Electroabsorption spectroscopy of luminescent and nonluminescent π-conjugated polymers"*, Phys. Rev. Lett, Vol 56, 2415, (1997).

Ltaiefa A, Bouazizia A, Davenasb J, Ben Chaabanea R, Ben Ouadaa H, *"Electrical and optical properties of thin films based on MEH-PPV/fullerene blends"*, Synthetic Metals 147, 261. (2004).

Martin S.J., Mellor H, Bradley D, Burn P.L., *"Electroabsorption studies of PPV and MEH-PPV"*, Optical Materials, Vol 9, 88, (1998).

Morita S, Zakhidov A.A., Yoshino K, *"Doping effect of buckminsterfullerene in conducting polymer: Change of absorption spectrum and quenching of luminescence"*, Sol. State Commun, 82, 249, (2002).

Nalwa H.S., *"Handbook of Organic Conductive Molecules and Polymers. Volume 1 Charge transfer salts, Fullerenes and Photocinductors"*, (1997).

Pac B, Petelenz P, Slawik M, Munn R.W., *"Theoretical interpretation of the electroabsorption spectrum of fullerene films"*, Chem. Phys. 109, 7932, (1998).

Richter M.M., Fan R.F., Klavetter F, Heeger A.J., Bard A.J., *"Electrochemistry and electrogenerated chemiluminescence of films of the conjugated polymer 4-methoxy-(2-ethylhexoxyl)-2,5-polyphenylenevinylene"*, Chem Phys Lett, 226(1-2), 115-120, (1994).

Sariciftci N.S., Smilowitz L, Heeger A.J., Wudl F, *"Photoinduced electron transfer from a conducting polymer to buckminsterfullerene"*, *Science* 258, 1474-1476 (1992).

Smie A and Heinze J, "*Physics and Chemistry of Fullerenes and Derivatives*", World. Scientific Singapore, (1995).

Shimoi Y, Murata K, Abe S, Noguchi T, Ohnishi T, "*Electroabsorption of electroluminescent polymer poly (p-phenylene vinylene) in a wide spectral region*", Journal of Luminescence, 87, 753. (2000).

Stenger-Smith J.D., Lenz R.W., Wegner G, "*Spectroscopic and cyclic voltammetric studies of poly(p-phenylene vinylene) prepared from two different sulphonium salt precursor polymers*", Polymer, Volume 30, 6, 1048, (1989).

Vacar D, Maniloff E.S., McBranch D.W., Heeger A.J., "*Charge-transfer range for photoexcitations in conjugated polymer/fullerene bilayers and blends*", Phys. Rev. B 56(8), 4573 (1997).

Wang H.L., Grigorova M, Maniloff E.S., McBranch D.W., Mates B.R., "*Variation in the optical properties of poly (3-hexythipohene)/C_{60} blends and poly (3-hexylthiophene)/sol-gel composites*", Synthetic Metals, 84, 7681-782. (1997).

Xie Q, Pérez-Cordero E, Echegoyen L, "*Electrochemical detection of C_{60} and C_{70} fullrides in solution*", J.Am. Chem. Soc. 114, 3978, (1992).

Yang C, He G, Wang R, Li Y, "*Solid-state electrochemical investigation of poly [2-methoxy, 5-(2'-ethyl-hexyloxy)-1,4-phenylene vinylene]*", Journal of Electroanalytical Chemistry, 471, 32-36, (1999).

Chapter 5: Electronic Characterisation of Conjugated Polymers and Composites

5.1 Introduction

The previous chapter detailed the characterisation of the reference materials and attempted to isolate simple indicators of the known charge transfer processes between C_{60} and MEH-PPV. Florescence spectroscopy clearly highlighted an interaction via fluorescence quenching; the evidence however was less convincing from absorption spectroscopy. Nevertheless electroabsorption spectroscopy and cyclic voltammetry measurements showed considerably more promise with the evidence suggesting that they could indeed be used as indicators of charge transfers as well as assisting in the matching of energy levels for the efficient design of PV devices. The establishment of these crucial facts will thus allow the remainder of the thesis to focus upon the application of the aforementioned techniques to the characterisation of the new polymer series discussed in Chapter 2 (Section 2.11) and their respective composites with C_{60}.

The work presented in this chapter will thus begin the characterisation of the new polymer series by using electronic spectroscopy. Absorption spectroscopy will be presented first and was employed to probe the ground state interaction of the conjugated polymers and polymer composites in both their solution and solid-state form. Fluorescence measurements were also used to investigate the decay of the polymers to the ground state by radiative emission. As mentioned in Section 4.7.1, fluorescence is extremely important as it is regarded as one of the simplest indicators of charge transfer between two materials without the need for transient spectroscopy (Sariciftci, 1992, Smilowitz, 1993 and Morita, 1992). Throughout the chapter the evolution of new solid-state characteristics, will be compared to the molecular form of the polymers.

5.2 Absorption spectroscopy of conjugated polymers series

The optical properties of conducting polymers are important in order to develop an understanding of the basic electronic structure of the material. As described in Section 2.11 (Chapter 2) the solution properties of the polymer series for this study have been well defined (O'Neill, 2007). In contrast little is known about the behaviour of these materials in the solid state. The characterisation presented in this thesis therefore is the first to explore their solid-state properties and will, were appropriate draw comparisons to the solution or molecular state. The polymer series was originally designed to investigate what the effects of introducing systematic changes to a materials structure was on the final molecular properties of the material *i.e.* the structure property relationships. Such studies are important for elucidating the processes which governed molecular design or tailoring (O'Neill, 2007). The previous studies however focused solely upon the molecular properties. It is thus important that the remaining knowledge gap be closed by establishing whether the well defined structure property relationships established for the molecular form of the polymers is preserved in the solid-state. This is a fortunate aside for the work presented in this thesis, nevertheless it must be emphasised that it is an important concept in the design of any polymer based device which requires the matching of energy levels. The primary purpose however of this chapter is to investigate if the indicators of a charge transfer from Chapter 4 with respect to electronic spectroscopy reveal any degree of interaction when used to examine composites produced using the new polymers. To do this the polymers were spin coated onto quartz disks giving polymer films with thicknesses of approximately 200 nm. The first polymer in the series to be studied was (poly (para-2,5-bis-(n-octyloxy)- phenylenevinylene), POPV. Figure 5.1 shows the absorption spectra of

POPV in its solid-state and molecular form. The insert shows the structure of POPV as previously presented in Chapter 2. The two spectra are normalised for clarity and therefore the absolute absorbance values are not relevant.

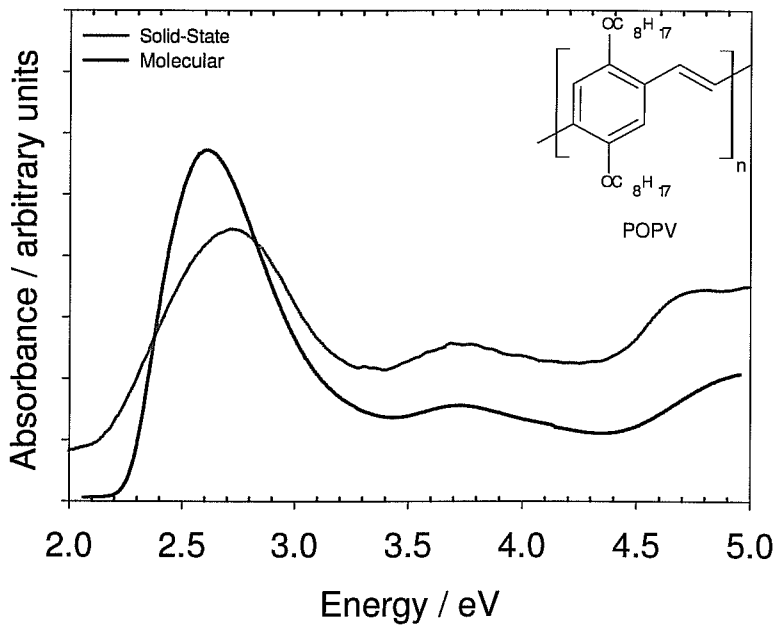

Figure 5.1: Molecular structure and UV/VIS absorption spectra of solid-state and molecular POPV.

Three absorption peaks are visible in both the solution and solid-state spectrum. The relatively weak features at 3.73 eV, 4.71 eV are due to the n→ π^* transition. These are attributed to a transition forbidden in the unsubstituted polymer that is made allowable by the charge conjugation symmetry breaking effects of the substituents (Pope, 1999). The n→ π^* transitions occur at the same energy level in both forms. Although the lowest energy absorption maximum appears at 2.51 eV, the lowest energy feature of the solution form of POPV occurs at 2.41 eV (O'Neill, 2007) and originates from an electron transition between the HOMO and LUMO levels (the band is associated with the $\pi \rightarrow \pi^*$ transition of the conjugated backbone). The double featured nature of the

$\pi \rightarrow \pi^*$ transitions is consistently observed throughout the series although the structure is better resolved in some of the polymers. This transition is excitonic in nature and is also confined to the phenyl rings (Martin, 1998). At 2.71 eV the lowest energy feature in the solid-state shows a hypsochromic shift (blue shift) compared to that of the molecular feature. This shift may indicate that a significant degree of aggregation is occurring within the polymer (Franck, 1938). An aggregate is formed when two or more single molecules interact strongly enough that mixing of the energy levels occurs. The probability of this interaction is concentration dependent (Fleming, 2003). In the solid-state the number of isolated molecules is reduced in favour of aggregation.

A ground-state aggregate is a dimer of cofacially aggregated conjugated molecules with ground-state chain interactions. Therefore, a ground-state aggregate forms a new chromophore that is directly excitable. The understanding of the ground-state aggregation, in the case of small molecules, has been well established due to the manageable intermolecular orientation and packing, in addition to straightforward theoretical modelling (Kim, 2002). When two chromophores form a card pack-like orientation known as an H-aggregate, the resulting excitonic splitting produces a forbidden lower-energy band and an allowed higher-energy band, consequently inducing a blue-shift in the absorption spectrum. In contrast, a J-aggregate (end-to-end orientation of chromophores) produces a red-shift due to the resulting allowed lower-energy band and a forbidden higher-energy band (Cornil, 2001 and Whitten, 1993). Figure 5.2 shows a schematic representation of the relationship between chromophore arrangement and spectral shift based on the molecular exciton theory (Franck, 1938).

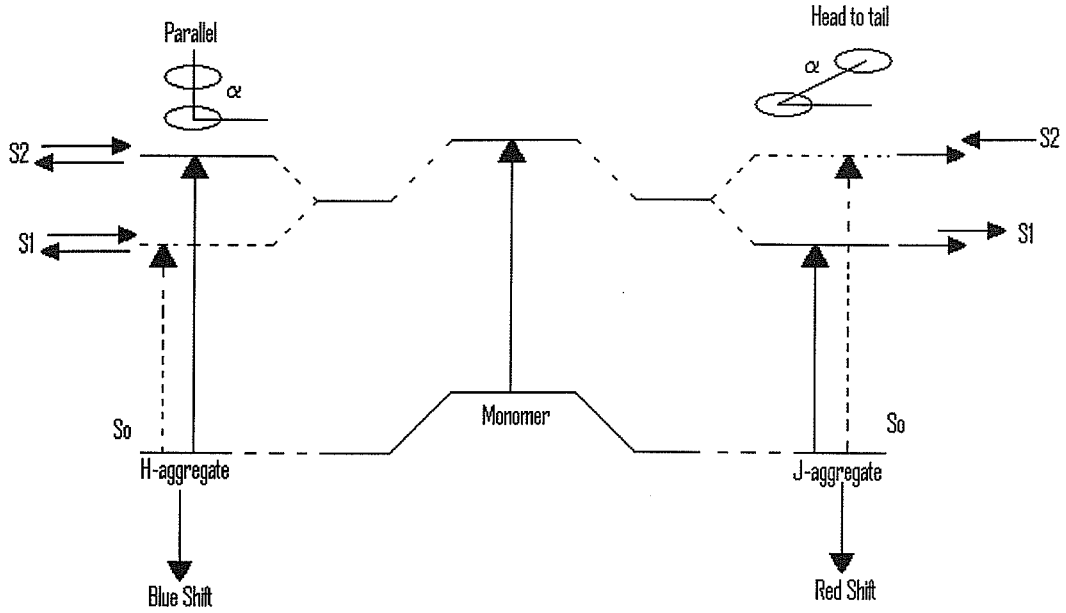

Figure 5.2: Schematic representation of the relationship between chromophore arrangement and spectral shift (Franck, 1938).

The ambiguity in defining chromophores, the amorphous character and the large molecular weight have prevented a systematic definition of aggregates in conjugated polymers. Experimentally it is not possible to directly deduce what type of aggregation was occurring within the polymers (electron spin resonance measurements could potentially provide some indication of the type of aggregation). However as the POPV shows a blue shift it is assumed that a card pack-like orientation is favourable in the solid-state.

The first structural change made to the POPV was to replace alternate phenyl units with substituted naphthyl units (POPV-ONV). Figure 5.3 shows the structure of POPV-ONV along with the absorption spectra in its solid-state and molecular form.

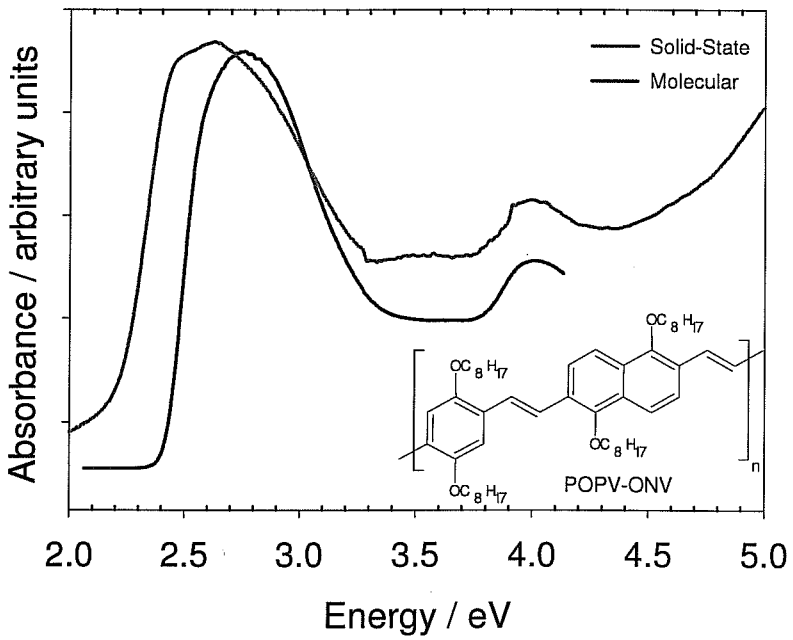

Figure 5.3: Molecular structure and UV/VIS absorption spectra of solid-state and molecular POPV-ONV.

The n→ π^* transitions occur at 3.97 eV and 5.15 eV in the solid-state. The 3.97 eV transition also appears in the molecular spectrum. These peaks are attributed to the naphthyl units (Bai, 2006). The HOMO-LUMO transition occurs at 2.62 eV for the solid-state form. Again it shows a hypsochromic shift compared to that of the molecular feature (2.58 eV). This shift is not as large as in the POPV, but it still indicates a degree of aggregation. The introduction of the naphthyl groups seems to reduce the interchain stacking causing the aggregation.

The second structural variation made to the POPV was the replacement of the substituted phenyl units with substituted anthryl units (POPV-OAV). Figure 5.4 shows the structure of POPV-OAV along with the absorption spectra in its solid-state and molecular form.

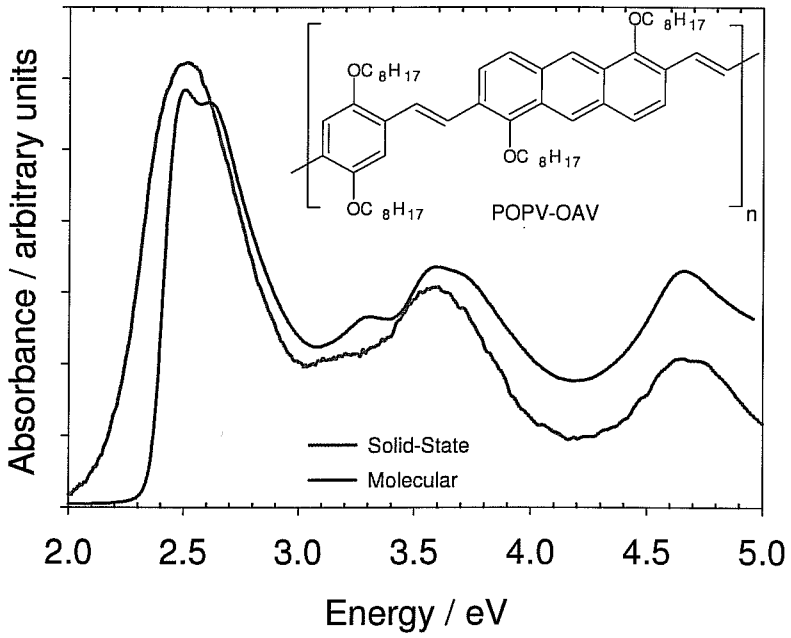

Figure 5.4: Molecular structure and UV/VIS absorption spectra of solid-state and molecular POPV-OAV.

The introduction of the anthryl group results in a hypsochromic shift of the $\pi \rightarrow \pi^*$ transition relative to POPV (solid-state) and a decrease in the bandgap to 2.50 eV. The POPV-OAV has two less intense peaks at 3.58 eV and 4.68 eV in both forms due to n $\rightarrow \pi^*$ transitions. These can be attributed to the anthryl substituents (Swager, 1995). The optical bandgap for the molecular state occurs at 2.48 eV. The double feature nature of the $\pi \rightarrow \pi^*$ transition is clearly resolved here in comparison to POPV and POPV-ONV. The anthryl groups therefore have a greater effect than the naphthyl groups in restricting aggregation.

The next step taken was to replace all phenyl units producing a fully conjugated naphthalene polymer, PONV. Figure 5.5 shows the structure of PONV along with the absorption spectra in its solid-state and molecular form. The solid-state PONV (2.78 eV) shows a bathochromic shift compared to molecular POPV (2.81 eV). This large

shift can be explained due to the steric interaction of the octyloxy side chains which force the polymer to assume a more planar geometry (Collison, 2001).

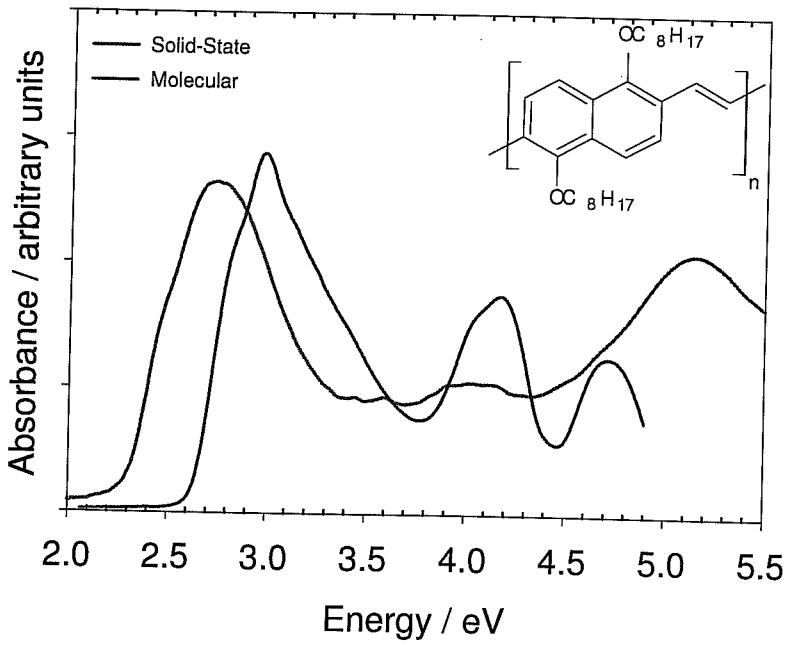

Figure 5.5: Molecular structure and UV/VIS absorption spectra of solid-state and molecular PONV.

The octyloxy side chain interaction restricts torsional freedom and thus allows for an increase in the conjugation of the system. The n $\rightarrow \pi^*$ transitions at 3.97 eV and 5.15 eV are attributed to the naphthyl units (Bai, 2006). These features also appear in the POPV-ONV spectrum. However unlike the other polymers these features are shifted from solid-state to the molecular state, which is an indication of significant aggregation.

Anthryl groups were then added to produce PONV-OAV. Figure 5.6 shows structure of PONV-OAV along with the absorption spectra in its solid-state and molecular form. The addition of the anthryl groups reduces the optical bandgap slightly to 2.76 eV compared to that of PONV (2.78 eV).

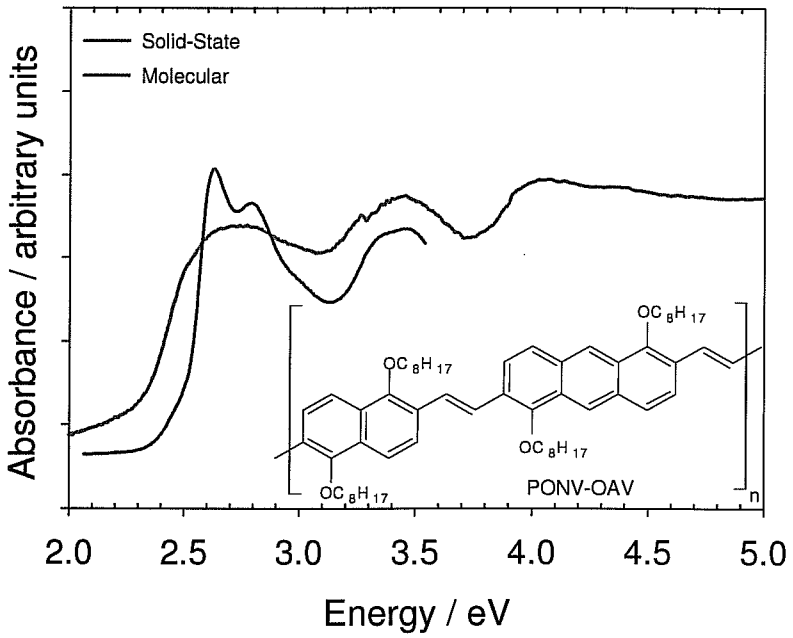

Figure 5.6: Molecular structure and UV/VIS absorption spectra of solid-state and molecular PONV-OAV.

Although the molecular absorption spectrum of the polymers has been shown to have a clear structural relationship, in general the solid-state optical absorption of the polymers shows no discernable trends. The comparison of the isolated molecule to the solid-state form shows that there is significant aggregation occurring within the polymers. Therefore the electronic properties of the two forms are different and the structure property relationships determined for the molecular forms do not apply to the solid-state.

For the composites, two of the polymers were chosen. The first polymer chosen was POPV-OAV. POPV-OAV shows the smallest degree of aggregation and the solid-state absorption spectrum closely resembles the molecular spectrum. The maximum absorption of POPV-OAV lies at 2.51 eV, which is the same absorption bandgap as MEH-PPV, the model material used for ultrafast charge transfer to C_{60} discussed in Chapter 4. The second polymer used was PONV, which has an optical bandgap of 2.78

eV. PONV absorbs in the blue region of the solar spectrum whereas POPV-OAV absorbs more towards the red region. Also PONV is known to have greater stability towards photo-oxidation then any of the other polymers (Lynch, 2008). The development of photovoltaic devices using organic materials has somewhat been limited by the degeneration of the active material (Atreya, 1999). The choice of a more photostable polymer is therefore appropriate for this study.

5.3 Absorption spectroscopy of composites

A solution of POPV-OAV/PONV with 52% C_{60} was prepared using 1,2-dichorobenzene. Thin films of ~200 nm were fabricated by spin coating. Figure 5.7 shows the optical absorption spectrum of solid state POPV-OAV and POPV-OAV/C_{60} composite (52% C_{60}). The spectra are offset for clarity. Examining the composite spectrum it is possible to assign the $\pi \rightarrow \pi^*$ transition of POPV-OAV to the feature at 2.58 eV assuming that the C_{60} is close to being molecularly dispersed and having only a minor contribution in this spectral region. Similarly the first dipole allowed transition of C_{60} appears to dominate the feature at 3.75 eV. Finally the feature at 4.84 eV has also been attributed primarily to the C_{60}. The spectrum is a simple superposition of the two components (molecular POPV-OAV and molecular C_{60}) without any indication of the states below the $\pi \rightarrow \pi^*$ transition gap of the POPV-OAV as might arise from interaction between the two materials in the ground state (Ltaiefa, 2004). One noticeable difference in the $\pi \rightarrow \pi^*$ transition of the POPV-OAV/C_{60} composite is that it is slightly blue shifted compared to that of the pristine solid-state POPV-OAV spectrum which indicates a reduction in aggregation and hence it can be said it is of molecular origin.

Similar results were observed by Wang *et al* using poly (3-hexlythiophene) (Wang, 1997). This effect was shown to be concentration dependant.

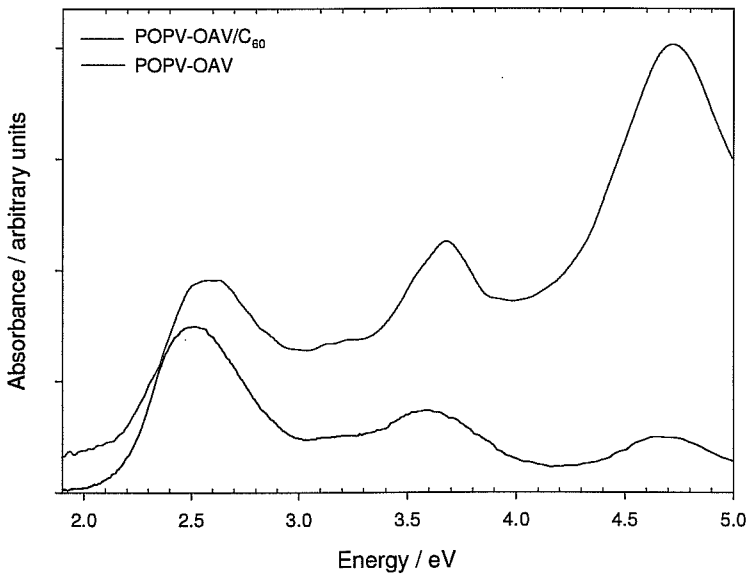

Figure 5.7: UV/VIS absorption spectrum of pristine POPV-OAV and POPV-OAV/C_{60} Composite.

Figure 5.8 shows the solid-state optical absorption spectra of PONV and PONV/C_{60}. It can be seen that the composite spectrum is not a simple summation of the individual materials (solid-state PONV and molecular C_{60}). The lowest energy feature in the composite is comprised of two peaks at 2.72 eV and 2.90 eV. There is also a very weak feature at 3.03 eV. The entire ensemble of features most likely originate from the maximum intensity peak in the PONV molecular spectrum. It is proposed that the introduction of the C_{60} reduces the effects of aggregation in the PONV and resolves the lowest energy feature into individual components. Indeed close examination of the PONV molecular spectrum (Figure 5.5) does reveal some weak unresolved features in the 2.70 eV $\rightarrow$ 3.10 eV region. The two other features at 3.60 eV and 4.70 eV are attributed to the C_{60}. The features are red shifted compared to those of pristine solid-

state C_{60}, indicating the C_{60} is dispersed sufficiently to begin approaching a molecular like spectrum. The composite spectrum shows a peak at 2.90 eV. If this is compared to the maximum absorbance of the pristine PONV (solid-state), then it can be said that it is blue shifted indicating reduced aggregation.

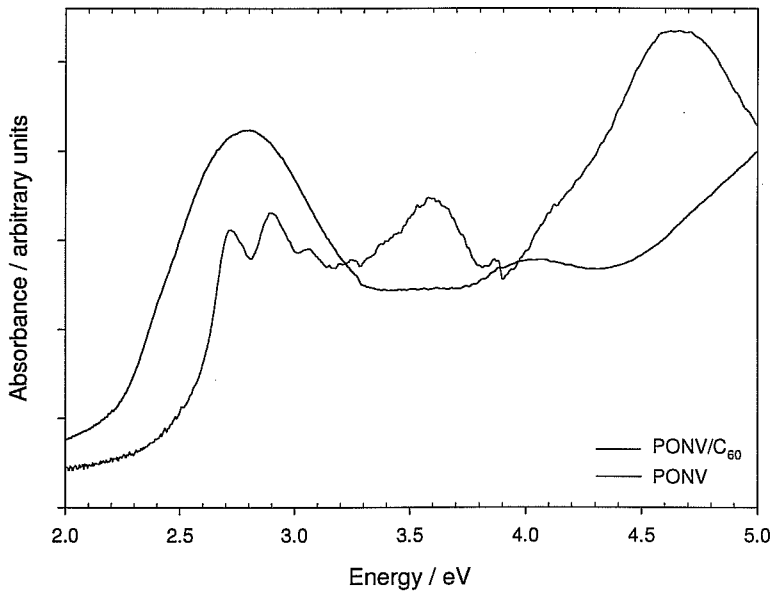

Figure 5.8: UV/VIS absorption spectrum of pristine PONV and PONV /C_{60} Composite.

The 2.72 eV peak may be a more resolved version of the shoulder peak of the pristine PONV solid-state absorption spectrum, which occurs at 2.42 eV, also blue shifted. Therefore it can be said that this is the formation of a PONV/ C_{60} composites similar to that described previously for POPV-OAV. The introduction of the C_{60} reduces the effects of aggregation in the PONV and resolves the lowest energy feature into individual components. The interaction is not that of a charge transfer, the C_{60} intercalates in the polymer thus reducing aggregation.

In conclusion there is no indication of charge transfer occurring in the ground state, as expected. However the interaction of the C_{60} with the two polymers is very different. The POPV-OAV/C_{60} spectrum is a simply summation of the two materials although there is a slight blue shift, as a result of the interaction with the C_{60}. However the same cannot be said for the PONV/C_{60} spectrum. The lowest energy transition is split and structured. The introduction of the C_{60} in both polymers induces a blue shift an indication of reduced aggregation. To further investigate the solid-state interaction of the pristine polymers and the interaction of the C_{60} with the POPV-OAV and PONV fluorescence measurements were carried out.

5.4 Fluorescence characterisation of polymers

Fluorescence spectroscopy is important in conjugated polymers due to their potential applications in organic light emitting diodes and photovoltaic cells. In the case of pristine conjugated polymers fluorescence can provide information when going from ground state to excited state. It can also be used to probe changes in the environment and the sensitivity of the decay processes to the molecular structure and the environment (Lakowicz, 1999).

Figure 5.9 shows the fluorescence spectra of the conjugated polymers POPV, POPV-ONV, POPV-OAV, PONV and PONV-OAV in their film form. The spectra are all normalized for clarity and therefore the y-axis values are not relevant. Although clear structure property relationships have been identified in their molecular (solution) form (O'Neill, 2007) the energy positioning of the solid-state fluorescence spectra shows no systematic trend with regard to the structural changes. As in the case of the absorption spectroscopy this is assumed to be a result of polymer aggregation in the solid-state.

This aggregation can affect the emission energy and weakly emissive interchain species can be formed. These interchain species lead to fluorescence red shift and reduced quantum yield (Jenekhe, 2004, Conwell, 1997 and Samuel, 1996).

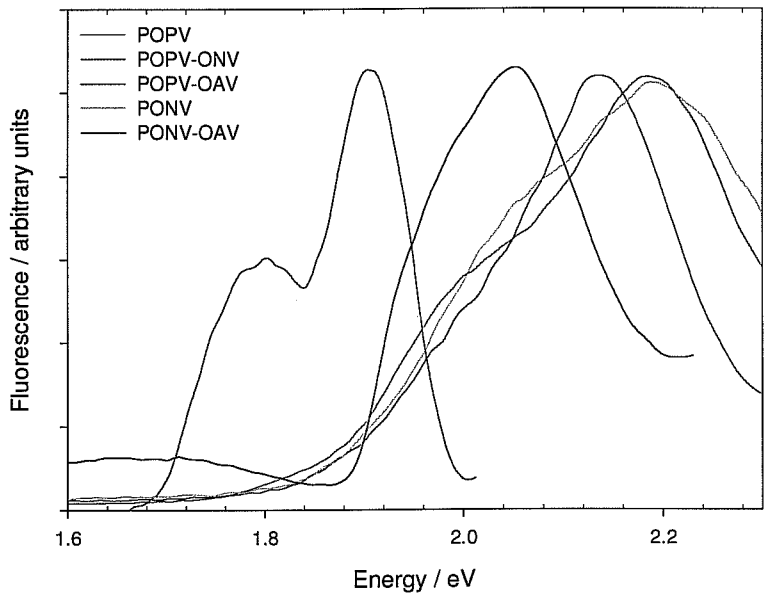

Figure 5.9: Fluorescence spectra of Polymer series.

The solid-state emissions of the polymers were all seen to be red shifted compared to those of their isolated molecular form. The fluorescence yield was also low, which confirms that there are aggregates within the polymers in their solid-state form. The degree of shifting from the solution spectrum varies from polymer to polymer, indicating a different degree of aggregation. The nature of these aggregates within conjugated polymers is still debatable. However it is believed that due to the strong intermolecular interactions "(aggregates), the emission properties of the polymers deteriorate". The shift in both optical and emission spectrum leads to an increase in Stokes shift for each polymer. The emission energies and Stokes shifts for the polymers

are shown in Table 5.1. The Stokes shift is taken to be the difference in energy between the initial absorption and the final emission photon energies.

Table 5.1: Emission energies of polymers in solid-state form.

Polymer	Optical Bandgap Solid-State / eV	Emission Energy Solid-State / eV	Stokes Shift / eV
POPV	2.71	2.13	0.58
POPV-ONV	2.62	2.18	0.44
POPV-OAV	2.51	1.90	0.61
PONV	2.78	2.19	0.59
PONV-OAV	2.76	2.05	0.71

5.5 Fluorescence characterisation of composites

In order to probe the interaction of the C_{60} and the polymers, as in the case of MEH-PPV, the fluorescence characteristics of the composite solutions were compared to those of the polymers. Figure 5.10 shows the fluorescence spectrum of molecular POPV-OAV ($1x10^{-5}$ M) and molecular POPV-OAV/C_{60} (52%). POPV-OAV has two emission peaks at 2.19 eV and 2.36 eV. The maximum fluorescence yield taken from the y-axis (Fluorescence) is 870 (arbitrary units). The addition of the C_{60} leads to a quenching of the fluorescence yield by over 50 %. This strong quenching in solution indicates the existence of a charge transfer, *e.g.* subpicosecond electron transfer (Sariciftci, 1992, Smilowitz, 1993 and Morita, 1992). One other interesting feature from the spectrum is that although the peak at 2.36 eV has decreased the peak at 2.19 eV has increased and is shifted to a lower energy. This may be further evidence of the morphological or electronic effects that the C_{60} is having on the polymer.

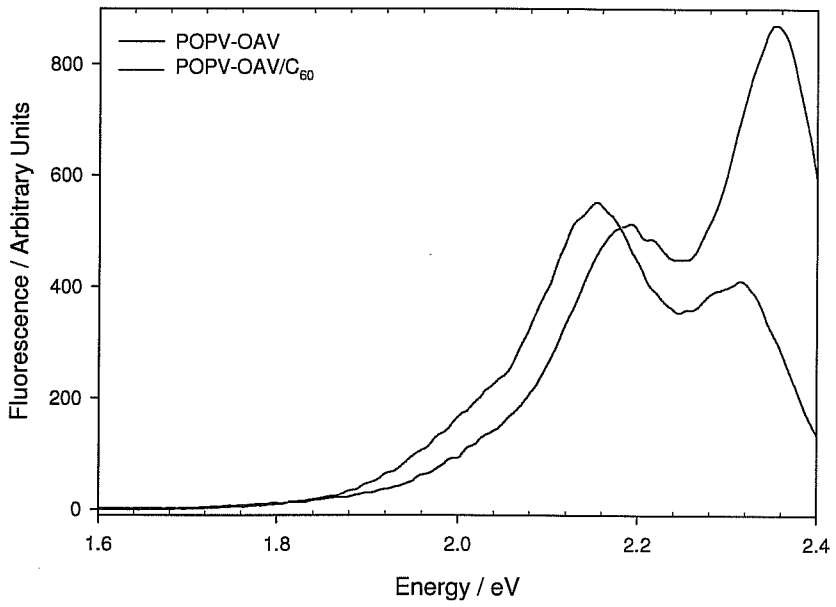

Figure 5.10: Fluorescence spectra of POPV-OAV and POPV-OAV/C_{60}.

However as the feature at 2.19 eV in the composite spectrum has become more intense, it could be assumed that re-absorption of the light emission by the C_{60} could be occurring and not quenching. To fully ensure that the results seen were a quenching, the fluorescence spectrum of the pristine polymer was normalised for re-absorption by the C_{60}. In order to achieve this, the absorption spectrum obtained for molecular C_{60} (Figure 4.1) was changed to a transmission spectrum. Once the transmission spectrum of C_{60} was determined, the spectrum was multiplied by the original fluorescence spectrum of POPV-OAV (Figure 5.10). Figure 5.11 shows the fluorescence spectrum of molecular POPV-OAV ($1x10^{-5}$ M) and molecular POPV-OAV/C_{60} (52%) along with the calculated spectrum of POPV-OAV/C_{60}. From Figure 5.11 it can be seen that the calculated spectrum is similar to the pristine fluorescence. The ratio of the two fluorescence peaks is the same. As the calculated spectrum is not comparable to the

fluorescence spectrum of POPV-OAV/C_{60} the possibility of re-absorption of the C_{60} occurring can be ruled out.

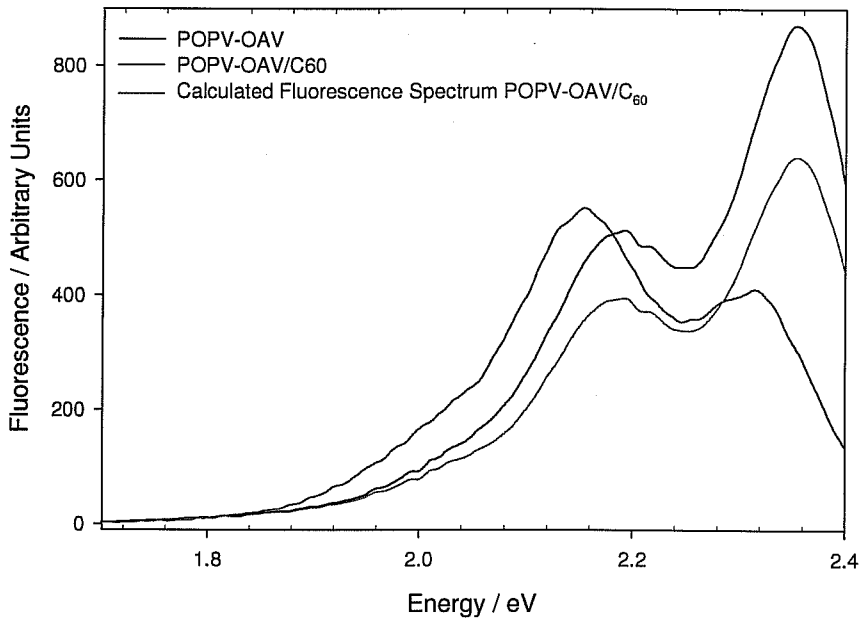

Figure 5.11: Fluorescence spectra of POPV-OAV and POPV-OAV/C_{60} and calculated fluorescence spectrum for POPV-OAV/C_{60}.

Similar results are seen for the PONV. Figure 5.12 shows the fluorescence spectrum of PONV ($1x10^{-5}$ M) and PONV/C_{60} (52 %). The pristine PONV has an emission energy of 2.63 eV and a fluorescence yield of 770 (arbitrary units). The fluorescence yield is almost completely quenched with the addition of the C_{60}. Again this is strong evidence that charge transfer is occurring between the two materials (Sariciftci, 1992, Smilowitz, 1993 and Morita, 1992).

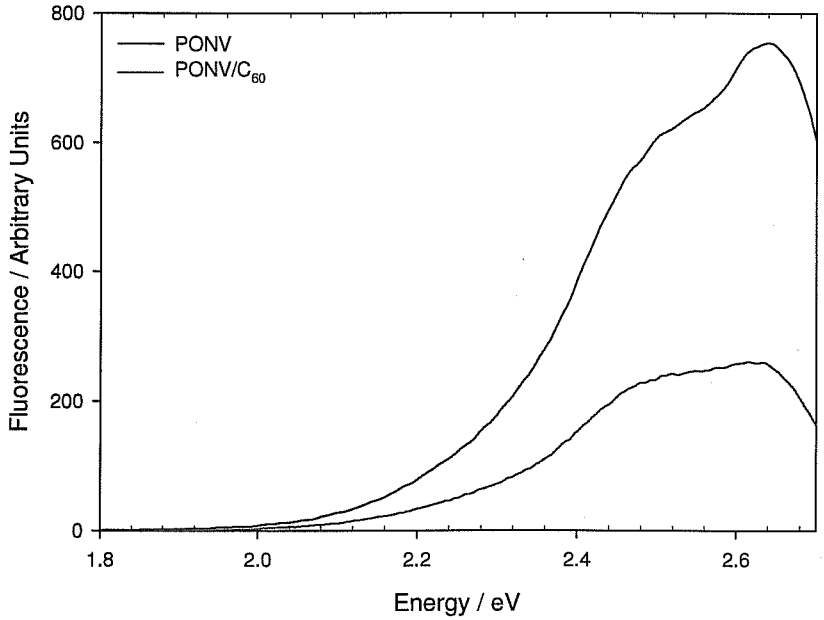

Figure 5.12: Fluorescence spectra of PONV and PONV/C_{60}.

5.6 Summary

This chapter described the first reported case of the electronic behaviour of the polymer series in their solid-state form. On comparison of the solid-state absorption to the isolated molecular absorption it was found that new interchain species had occurred within the solid-state. These aggregates are due to the stacking formation of the polymers. The absorption spectra of POPV, POPV-ONV, POPV-OAV and PONV-OAV were all shown to blue shift compared to that of their isolated form. It could be said that the stacking arrangement of these polymers is a card pack-like orientation (H-aggregates). PONV showed a red shift and is therefore believed to form an end-to-end orientation of chromophores (J- aggregates). POPV-OAV and PONV were then used to form a composite material with C_{60}. Absorption spectra of the two composites showed

no evidence of charge transfer in the ground state, which is as expected. The POPV-OAV/C_{60} spectrum was a direct summation of the molecular POPV-OAV and molecular C_{60}. However the PONV/C_{60} composite was not a direct summation, which is unusual. The introduction of the C_{60} resolved the $\pi \rightarrow \pi^*$ transition into three individual features. Also the addition of the C_{60} led to a blue shift in the $\pi \rightarrow \pi^*$ transition of the conjugated backbone of each polymer. This is consistent with a reduction of the aggregation observed in the solid-state.

Fluorescence measurements confirmed that there was aggregation within the solid-state of the polymers but showed no systematic trend that could be related back to the absorption spectrum or to the isolated form of the polymers. Fluorescence quenching was observed within the two composite materials in solution. This was the first evidence of charge transfer between the two polymers and the C_{60}. The PONV showed a higher degree of fluorescence quenching.

The next chapter deals with the cyclic voltammetry and in-situ reflectance measurements of the polymers and the composites. Cyclic voltammetry is a useful tool as its can be used to obtain precise values for the HOMO-LUMO levels in conjugated polymers. It is also used to show the conductivity capabilities of conjugated polymers. In-situ measurements will provide additional information on the electronic nature of the polymers and composites as they are probed using cyclic voltammetry.

References:

Atreya M, Li S, Kang E.T., Neoh K.G., Ma Z.H., Tan K.L., Huang W, *"Stability studies of poly(2-methoxy-5-(2'-ethyl hexyloxy)-p- (phenylene vinylene) [MEH-PPV]"*, Poly. Degr. And Stability, 65, 287, (1999).

Bai H, Wu X, Gaoquan S, "Synthesis and characterization of poly(1,5-naphthylene vinylene) and its copolymers with poly(2-methoxy-5- (2-ethylhexyloxy)-p-phenylene vinylene)", Polymer, 47, 1533, (2006).

Collison C.J., Rothberg L.J., Treemaneekarn V, Li Y, *"Conformational effects on the photophysics of conjugated polymers: A two species model for MEH-PPV spectroscopy and dynamics"*, Macromolecules, 34 (7): 2346-2352 (2001).

Conwell E, *"Mean free time for excimer light emission in conjugated polymers"*, Trends Polym. Sci. 5, 218– 222. (1997).

Cornil J, Beljonne D, Calbert J.P., Bredas J.L., *"Interchain Interactions in Organic π-Conjugated Materials: Impact on Electronic Structure, Optical Response, and Charge Transport"*, Adv. Mater. 13, 1053–1067 (2001).

Fleming A.J., Coleman J.N., Dalton A.B., Fechtenko1tter A, Watson M.D., Mullen K, Byrne H.J., Blau W.J., *"Optical Spectroscopy of isolated and aggregate Hexabenzocoronene derivatives: a study of self-assembly molecular nanowires"*, J. Phys. Chem B, 107, 37-43, (2003).

Franck J, Teller E, J,*"Migration and photochemical action of. excitation energy in crystals"*, Chem. Phys. 6 (1938).

Jenekhe S.A. and Osaheni J.A., *"Excimers and Exciplexes of Conjugated Polymers"*, Science 265, 765–768 (1994).

Kim J, *"Assemblies of comjugated polymers. Intermolecular and intramolecular effects on the photophysical properties of conjugated polymers"*, Pure Appl. Chem., Vol. 74, No. 11, pp. 2031–2044, (2002).

Lakowicz J.R., *"Principles of Fluorescence Spectroscopy"*, 2nd edition, NY Kluwer. Academic Publishers, (1999).

Ltaiefa A, Bouazizia A, Davenasb J, Ben Chaˆabanea R, Ben Ouadaa H, *"Electrical and optical properties of thin films based on MEH-PPV/fullerene blends"*, Synthetic Metals 147, 261. (2004).

Lynch P, *"Synthesis and characterisation of conjugated polymers with a view to developing an understanding of structure property relationships"*, PhD Dissertation, Dublin Institute of Technology, (2008.)

Morita S, Zakhidov A.A., Yoshino K, *"Doping effect of buckminsterfullerene in conducting polymer: Change of absorption spectrum and quenching of luminescence"*, Sol. State Commun, 82, 249, (2002).

Martin S.J., Mellor H, Bradley D, Burn P.L., *"Electroabsorption studies of PPV and MEH-PPV"*, Optical Materials, Vol 9, 88, (1998).

O'Neill L, Lynch P, McNamara M, Byrne H.J., *"Spectroscopic Characterisation of Novel Polycyclic Aromatic Polymers"*, J. Phys.Chem A, 111 (2), 299-305, (2007).

Pope M, Swenberg C.E., *"Electronic Processes in Organic crystals and Polymers"*, Oxford University Press, (1999).

Samuel D.W, Rumbles G, Collison C.J., Crystall B, Moratti S.C., Holmes A.B., *"Luminescence efficiency and time dependence in a high electron affinity conjugated polymer"*, Synthetic Metals. 76, 15–18 (1996).

Sariciftci N.S., Smilowitz L, Heeger A.J., Wudl F, "*Photoinduced electron transfer from a conducting polymer to buckminsterfullerene*", Science 258, 1474-1476 (1992).

Smilowitz L, Sariciftci N.S., Wu R, Gettinger C, Heeger A.J., Wudl F, *"Photoexcitation spectroscopy of conducting-polymer–C60 composites: Photoinduced electron transfer"*, Science. 258, 1474. (1992).

Swager T.M., Gil C.J., Wrighton M.S., *"Fluorescence Studies of Poly(-phenyleneethynylene)s: The Effect of Anthracene Substitution "* J. Phys. Chem., *99,* 4886,(1995).

Wang H.L., Grigorova M, Maniloff E.S., McBranch D.W., Mates B.R., *"Variation in the optical properties of poly (3-hexythipohene)/C_{60} blends and poly (3-hexylthiophene)/sol-gel composites"*, Synthetic Metals, 84, 7681-782. (1997).

Whitten D.G., *"Photochemistry and photophysics of trans-stilbene and related alkenes in surfactant assemblies"*, Acc. Chem. Res. 26, 502–509 (1993).

Chapter 6: Electrochemical Characterisation and In-situ UV/VIS Spectroelectrochemistry of Conjugated Polymers and Composites

6.1 Introduction

Chapter 4 outlined a number of experimental techniques which showed promise for the determination and assessment of charge transfer species between C_{60} and MEH-PPV. It was suggested that these techniques may offer an alternative to femtosecond spectroscopy when assessing to the potential of other materials undergo a charge transfer with C_{60}. Chapter 5 examined the used of electronic spectroscopy with respect to meeting this requirement for a set of recently developed PPV polymer derivatives. It reported the first solid state investigation into the electronic properties of these materials and revealed a number of interesting facts regarding aggregation as the material moved from solution to solid. Absorption spectroscopy showed no evidence of charge transfer states, although there was evidence to suggest that the C_{60} disrupted the aggregation process. In contrast fluorescence spectroscopy, as expected showed clear signs of a charge transfer with significant quenching in the composites studied. In addition to electronic spectroscopy Chapter 4 proposed a number of electrical methods such cyclic voltammetry, spectroelectrochemistry, conductivity based measurement and electroabsorption which could aid in the identification of charge transfer species. This chapter presents the data obtained from electrochemical measurements of the polymers and their composites, while Chapter 7 will deal specifically with electroabsorption.

Electrochemical methods like cyclic voltammetry help in understanding the redox behaviour of materials as well as the generation of charge carriers and when coupled with optical spectroscopy can provide significant insights into the generation and origin

of excited states. As with the solid state electronic spectroscopy in Chapter 5 this chapter will present for the first time a detailed study of the electrical properties of the polymer series under investigation. This information will yield valuable details regarding the electronic structure of these polymers under doping conditions.

6.2 Cyclic voltammetry characterisation of polymer series

The first part of this chapter deals with the basic cyclic voltammetric measurements performed on the polymer series. As aforementioned these are the first such studies performed on these materials. The films were produced by drop casting the solution onto the electrode. The solvent (chlorobenzene) was then allowed to evaporate under a controlled atmosphere (laminar flow). The electrolyte that was used was acetonitrile and the supporting electrolyte was 0.1 M of tetrabutylammonium hexafluorophosphate. Figure 6.1 shows the cyclic voltammogram of POPV. The p-doping (oxidation) scan in Figure 6.1 shows a quasi-reversible electrochemical response with an oxidation potential of 0.86 V. There is a slight bump before the oxidation peak in the scan which can be attributed to the glassy carbon electrode as it also appears in the rest of the voltammograms of the polymer series. The n-doping (reduction) scan is also a quasi-reversible process with a reduction potential of -2.30 V. As discussed in Chapters 3 and 4, a reversible electrochemical process has a peak separation (ΔE_p) of 59 mV, while POPV has an ΔE_p value of 76.50 mV. A quasi-reversible response occurs if the electron transfer processes are 'slow' (relative to the voltage scan rate). In other words the ΔE_p is larger than 59 mV for a quasi-reversible response. The reduction potential of all conjugated polymers also depends on mesomeric effects, which could explain slight

deviations from ideal behaviour (Janietz and Schulz, 1996) although slight changes in the film morphology during the cycle are a more likely origin.

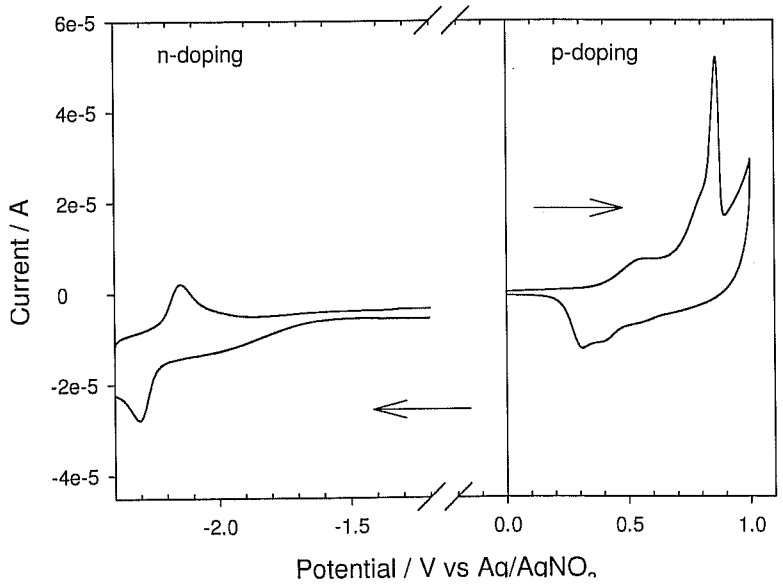

Figure 6.1: Cyclic Voltammogram of POPV in CH_3CN solution of 0.1 M tetrabutylammonium hexafluorophosate @scan rate of 0.1 V/sec.

The reduction potential of POPV (-2.30 V) is more negative compared to that of MEH-PPV, which has a reduction potential of -1.98 V. In other words the POPV is harder to reduce than the MEH-PPV. The MEH-PPV has an electron withdrawing group (alkoxy side groups) which helps it to reduce at a less negative potential.

Figure 6.2 shows the cyclic voltammogram of POPV-ONV. The p-doping (oxidation) scan shows a quasi-reversible electrochemical response. Oxidation occurs at 1.09 V. The introduction of the naphthyl units increases the oxidation potential. The increase in the oxidation potential implies that in a solid-state device the polymers should possess good hole blocking properties as discussed in Chapter 2, Section 2.9 (Li, 1996). The n-doping (reduction) scan indicates that POPV-ONV reduction is quasi-reversible as the

ΔE_p is 82.50 mV. The current peaks are much narrower than those of POPV, which means that the amount of charge consumed is less than that of the POPV (Li, 1999). The reduction potential of POPV-ONV is -2.22 V and is shifted towards a more positive value than that of POPV.

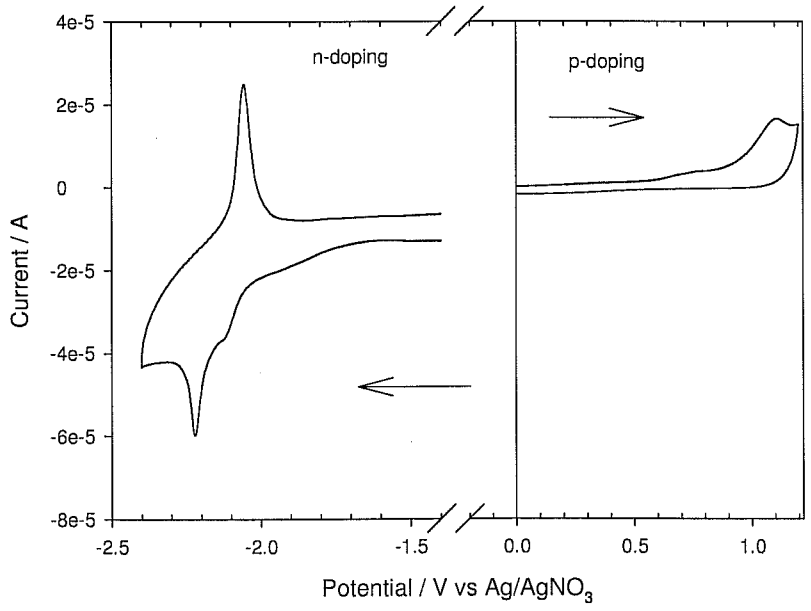

Figure 6.2: Cyclic Voltammogram of POPV-ONV in CH_3CN solution of 0.1 M tetrabutylammonium hexafluorophosate @scan rate of 0.1 V/sec.

Figure 6.3 shows the cyclic voltammogram of POPV-OAV. The p-doping (oxidation) scan showed a quasi-reversible electrochemical response. The oxidation potential of POPV-OAV was found to be 0.89 V. The oxidation potential is greater than that of POPV. The addition of the anthryl also results in an increase of oxidation potential but not as much as the naphthyl groups. The n-doping (reduction) scan showed the reduction of POPV-OAV to be a reversible (ΔE_p is 59 mV). The reduction potential of

POPV-OAV occurs at -2.17 V which is a more positive reduction potential compared to that of POPV and POPV-ONV.

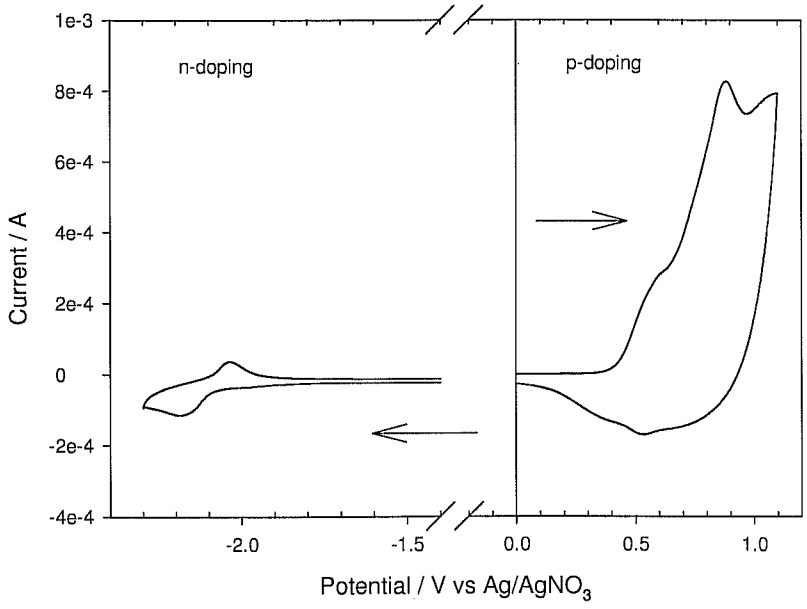

Figure 6.3: Cyclic Voltammogram of POPV-OAV in CH_3CN solution of 0.1 M tetrabutylammonium hexafluorophosate @scan rate of 0.1 V/sec.

Figure 6.4 shows the cyclic voltammogram of PONV. The p-doping (oxidation) scan again showed a quasi-reversible electrochemical response. Oxidation was found to occur at 0.74 V. The oxidation potential is the lowest of all the conjugated polymers. The reduction process (n-doping) of PONV is a reversible process (ΔE_p is 56 mV), the 3 mV difference compared to the ideal value of 59 mV can be attributed to drift within the reference electrode. The reduction potential of PONV is -2.23 V. The reduction potential is decreased compared to POPV, but is increased compared to POPV-OAV having a similar reduction potential to that of POPV-ONV *i.e.* -2.24 V.

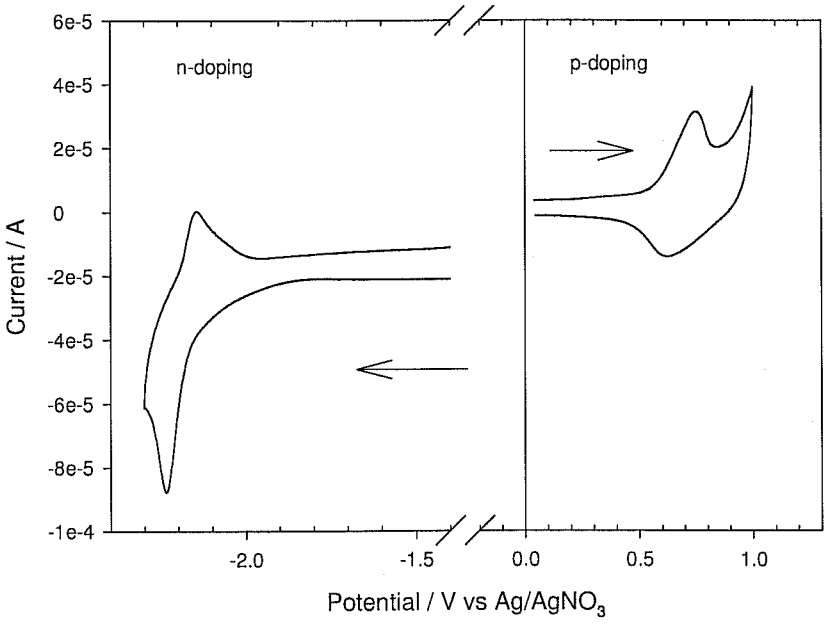

Figure 6.4: Cyclic Voltammogram of PONV in CH_3CN solution of 0.1 M tetrabutylammonium hexafluorophosate @scan rate of 0.1 V/sec.

Figure 6.5 shows the cyclic voltammogram of PONV-OAV. Oxidation of PONV-OAV occurs at 0.97 V. The introduction of the anthryl units to the naphthyl shifts the oxidation to a higher potential than that of PONV. The n-doping (reduction) scan indicates that PONV-OAV reduction is quasi-reversible with an ΔE_p value of 89 mV. The reduction potential of PONV-OAV was found to be -2.25 V.

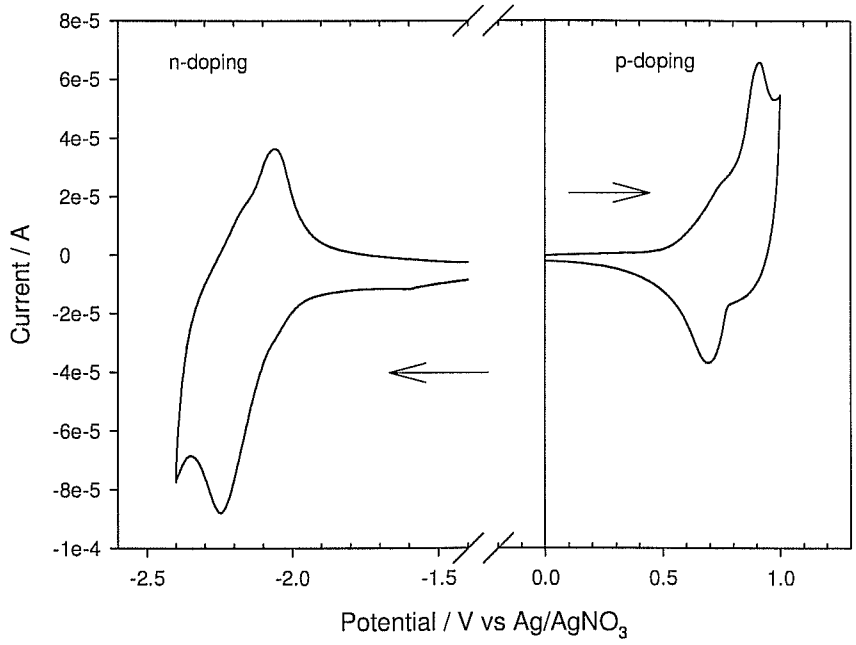

Figure 6.5: Cyclic Voltammogram of PONV-OAV in CH_3CN solution of 0.1 M tetrabutylammonium hexafluorophosate @scan rate of 0.1 V/sec.

6.3 Discussion and analysis of cyclic voltammograms

All the polymers displayed quasi-reversible processes in the p-doping scans. The increase in the oxidation potential compared to that of MEH-PPV implies that in a solid-state device the polymers should possess good hole blocking properties. The greater the increase in the oxidation potential the better the hole blocking ability. An increase in oxidation is a result of an increase in the HOMO level of the polymer, which implies the HOMO level will be greater than the ITO (Figure 2.11) and hence it will be more difficult to generate hole carriers. As mentioned in Chapter 4, the onset potentials of the p-doping and n-doping scans can be used to determine the electron affinity (LUMO) and ionisation potential (HOMO) of the polymers using Equations 4.1 and 4.2 (de Leeuw, 1997) and subsequently the electrochemical bandgap of the polymer

(Cervini, 1997). Applying these equations to the previously discussed cyclic voltammograms (Figure 6.1 to Figure 6.5), an estimation of the HOMO-LUMO levels of the polymers can be obtained and the bandgap derived. This value should be comparable to that of the optical bandgaps previously discussed in Chapter 5. Table 6.1 shows the calculated p and n doping onset potentials, HOMO-LUMO levels and the electrochemical and optical bandgaps for the MEH-PPV and the polymer series. From Table 6.1 it can be seen that the electrochemical and solid-state bandgaps are comparable (within 0.2 eV of each other).

Table 6.1: p and n doping onset potentials, HOMO-LUMO levels, estimated LUMO levels, electrochemical bandgaps and solid-state optical bandgaps for MEH-PPV and polymer series

Polymer	Reduction Potential (Volts)	Oxidation Potential (Volts)	p-onset (Volts)	n-onset (Volts)	HOMO (eV)	LUMO (eV)	Electrochemical Bandgap (eV)	Optical Bandgap (eV)
MEH-PPV	-2.08	0.62	0.35	-1.98	4.74	2.41	2.33	2.44
POPV	-2.30	0.86	0.681	-2.21	5.07	2.18	2.89	2.71
POPV-ONV	-2.22	1.09	0.607	-2.08	4.99	2.30	2.69	2.62
POPV-OAV	-2.17	0.89	0.426	-2.06	4.81	2.32	2.49	2.50
PONV	-2.23	0.74	0.564	-2.00	4.95	2.38	2.56	2.48
PONV-OAV	-2.25	0.97	0.815	-1.94	5.20	2.45	2.75	2.77

The electronic properties of the homologous polymer series have been shown to be a balance of the increased electron density of the aromatic substituents and their communication across the vinyl bond. The phenyl units have been shown to have a strong electron affinity of -1.12 eV, compared to that of the naphthyl (electron affinity = -0.19eV) units and the anthryl units (electron affinity = +0.53 eV) (Rienstra-Kiracofe,

2001). The addition of the naphthyl units to the phenyl units (POPV-ONV) results in a depletion of the π electron density of the vinyl bond which has been shown to be manifest for example in a systematic softening of the vinyl stretch band in the Raman spectrum (O'Neill, 2007). This governs the systematic variation of the optical bandgap and should therefore govern the systematic variation in the LUMO. The electron density of the vinyl bridging unit has been quantified in terms of the parameter EA_{vinyl} (O'Neill, 2007). Figure 6.6 shows a plot of the LUMO levels of the polymers against the EA_{vinyl} parameter.

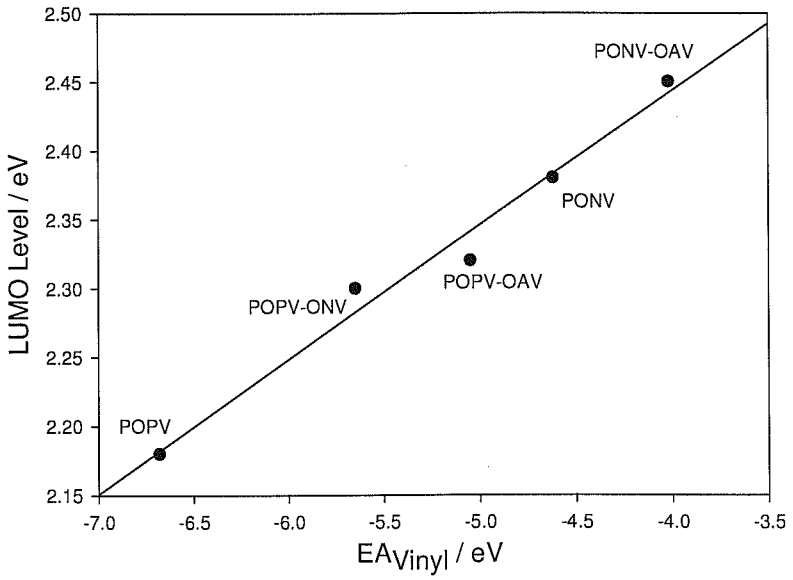

Figure 6.6: Plot of LUMO levels of polymers against calculated EA_{vinyl} parameter

EA_{vinyl} is an accurate variation of the vinyl bond as the larger, higher electron affinity units, are substituted into the chain. A polymer, being a chain-like structure, will be limited by the weakest link and thus the limiting of the conjugation across the vinylene bond will hinder the electron-phonon coupling being distributed across the entire polymer back-bone. From Figure 6.6 a linear relationship can be drawn between the

EA_{vinyl} parameter and the LUMO levels. Further comparison can be made between the calculated HOMO levels of the polymers and the optical bandgap. Figure 6.7 shows a plot of the calculated HOMO levels for the polymers against their optical bandgap. Although an exact linear dependence is not inferred, a correlation is clearly evident and a line is plotted as a guide to observe the trend. Although an increase in HOMO level is favourable for hole blocking properties in a device structure (Figure 2.11), it can also be seen from Figure 6.7 that the increase in HOMO level results in an increase in the bandgap of the polymers.

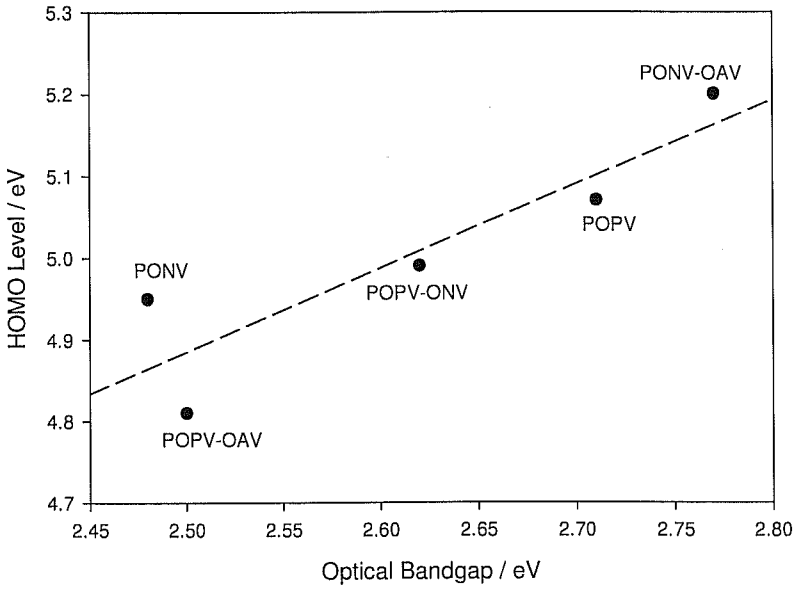

Figure 6.7: Plot of HOMO levels of polymers against optical bandgaps

It has been shown previously by Bonesi *et al* (Bonesi, 2000) that is it possible to construct a relationship between the electrochemical bandgap and the reduction potential of the polymers. With reference to the Bonesi approach the electrochemical bandgap obtained from Table 6.1 can be considered as

$$\Delta E = E_{HOMO} - E_{LUMO} \qquad \text{(Eqn. 6.1)}$$

It should be noted that the approach used here differs slightly from the model proposed by Bonesi due to the fact that he used a theoretical model to calculate the reduction potential and ΔE values of a polyhalomethane series. Bonesi used the Rehm-Weller equation (Rehm and Weller, 1970) to obtain the reduction potential of each polymer. The Rehm-Weller equation estimates the free energy change between a donor (D) and an acceptor (A) as

$$\Delta G^o = e\left[E_D{}^o - E_A{}^o\right] - \Delta E^* + w \qquad \text{(Eqn. 6.2)}$$

where e(Coulombs) is the unit electrical charge, $E_D{}^o$ and $E_A{}^o$ are the reduction potentials of the electron donor and electron acceptor respectively, ΔE is the energy of the singlet or triplet excited state and *w* is the work required to bring the donor and acceptor to within the electron transfer distance (Bonesi, 2000, Croney, 2003) (Rehm-Weller equation is generally not used for polymer/fullerene composites; instead the charge separation is calculated using Marcus theory, Sariciftci, 2000). The HOMO-LUMO energy level values of the polyhalomethanes were calculated from their optimised geometries by using *ab initio* computational methods and hence the ΔE was calculated according to Equation 6.1 (Bonesi, 2000). Bonesi found a linear relationship between the reduction potential and the HOMO-LUMO energy difference ΔE of the polyhalomethane series. In the case of this study it is not necessary to use theoretical calculations as direct experiment methods were available. Figure 6.8 shows a plot of HOMO-LUMO energy difference (ΔE) against the reduction potentials of polymer

series. As shown in Figure 6.8, a plot of ΔE against reduction potential yields an approximate linear relationship (linear is plotted as a guide to observe trend). This is a similar trend to the one observed by Bonesi for the polyhalomethane series. The reduction potential can be related to the electrochemical bandgap. A decrease in reduction is constituent with a decrease in the electrochemical bandgap.

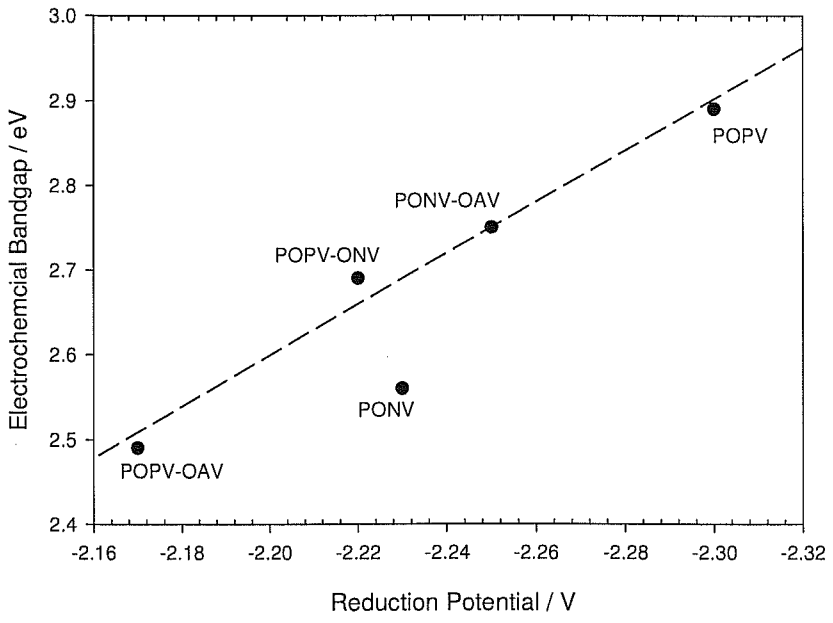

Figure 6.8: Correlation between the HOMO-LUMO energy difference (ΔE) and reduction potentials of polymer series.

From Figures 6.6-6.8 it can be seen that the electrochemical properties, optical properties and to an extent the vibrational properties can all be related to each other, and hence can be further related back to the structural changes made to each polymer, demonstrating the benefits of the systematic approach of the analysis of the systems.

Using Table 6.1 is it now possible to draw an energy level diagram for the polymer series. Figure 6.9 shows the calculated HOMO-LUMO levels in the polymer series.

This diagram can be further expanded to include the excited energy levels within each polymer using spectroelectrochemical techniques. The precise energy levels of the HOMO-LUMO are important when considering device fabrication and charge transfer mechanisms with the C_{60}.

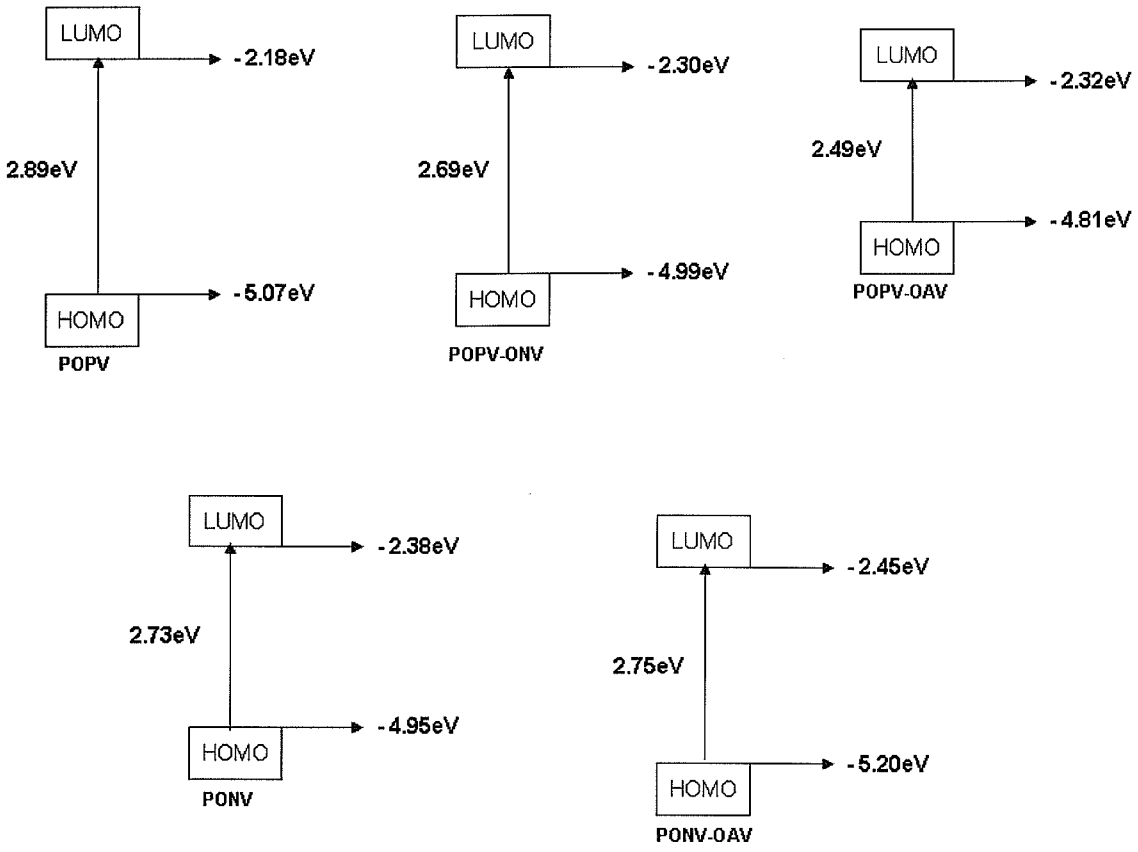

Figure 6.9: Calculated HOMO-LUMO levels in the polymer series.

Also from Figure 6.9 the effective change in HOMO-LUMO can be seen with respect to the different structural change made. The exact HOMO-LUMO levels are of importance when considering the polymers for device design. Ideally the HOMO level should be greater than the workfunction of the ITO (4.8 eV) and the LUMO level should be grater than that of the aluminium top electrode (4.2 eV). From Figure 6.9 it can be seen that all

the polymers should possess good hole blocking properties due to the positioning of the HOMO levels of each polymer. As the PONV-OAV has the higher HOMO level it should possess the best hole blocking properties. The LUMO levels of the polymers are higher than that of aluminium. There further away the LUMO levels from the aluminium the greater the electron injection barrier.

6.4 Cyclic voltammetry of composites

Figure 6.10 shows the p-doping cyclic voltammogram obtained for POPV-OAV/C_{60} composite (52% C_{60}) and pristine POPV-OAV. The pristine scan showed a quasi-reversible electrochemical response (Figure 6.3) in which oxidation occurs at 0.86 V. In the composite spectrum two oxidation peaks are seen to occur. Firstly there is a very weak oxidation at 0.87 V, which could almost be referred to as a pre-oxidation (Section 4.8.3). This peak can be attributed to the pristine polymer. The peak at 1.15 V is the main oxidation peak of the composite. This peak could be an indication of a charge transfer between the polymer and C_{60} and is similar to the results seen for MEH-PPV/C_{60}. When the polymer is oxidised, it then has an extra electron which the C_{60} accepts and under the CV conditions is forced to give the electron up, hence the second oxidation peak. The process was seen to be irreversible as scanning past this peak potential (1.15 V) resulted in the composite losing its electronegativity (composite becomes over oxidised). The significance of this is that the composite cannot be subject to a potential greater than that of the second oxidisation peak. From the calculated HOMO-LUMO (Figure 6.9) levels it can seen that the energy difference between the HOMO level of POPV-OAV and the LUMO level of C_{60} is 1.13 eV. This can be correlated to the new feature at 1.13 eV. Therefore it can be proposed that a charge

transfer from the HOMO of the POPV-OAV to the LUMO of the C_{60} is occurring. Therefore it may be possible to predict the potential of the charge transfer peak.

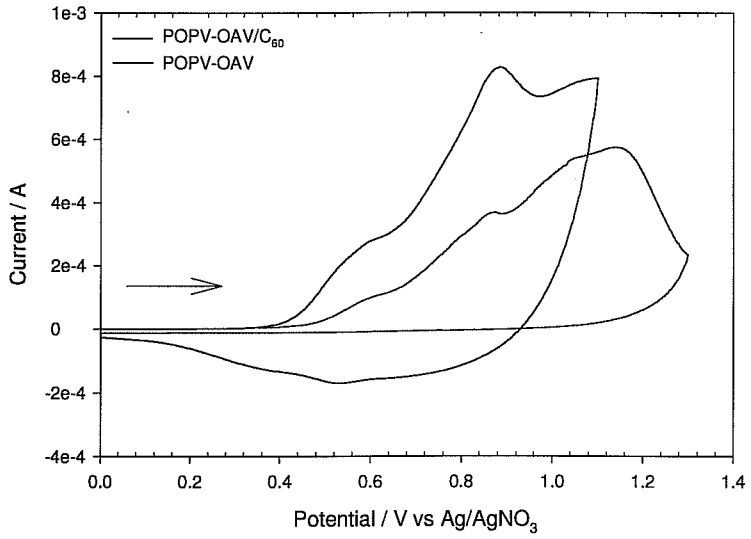

Figure 6.10: p-doping Cyclic Voltammogram of POPV-OAV/C_{60} and POPV-OAV in CH_3CN solution of 0.1 M tetrabutylammonium hexafluorophosate @scan rate of 0.1 V/sec.

Figure 6.11 shows the n-doping cyclic voltammogram obtained for POPV-OAV/C_{60} composite (the scan also contains the reduction scan for pristine POPV-OAV for clarity). The insert shows the potential window from 0 V-1.1 V so as to observe the first C_{60} reduction potential. The composite spectrum is a summation of the two materials. The composite spectrum has three reduction features. The first three reduction peaks at -0.98V, -1.29 V and -1.70 V can be attributed to molecular C_{60} with the re-oxidation peaks occurring at -0.52 V,-0.89 V and -1.67 V. These three C_{60} features are also seen in the molecular C_{60} cyclic voltammogram in Chapter 4, Section 4.5.1. Therefore it can be said the C_{60} is molecularly dispersed. The reduction peak at -0.98 V is masked by the current range of the other peaks in the graph. The peak separation is significantly

greater than 59 mV for the two C_{60} reductions which indicates it is not a standard one electron transfer. The fourth reduction peak at -2.24 V is attributed to the reduction of the POPV-OAV. The composite current range is a factor of five larger than that of the pristine POPV-OAV. This increase in current is consistent with C_{60} acting as an acceptor material allowing the polymer to accept or channel more charge. Similar results were observed for the MEH-PPV/C_{60} composite in Chapter 4. For calculation of the LUMO level of the composite the onset of the reduction was taken just before the first C_{60} reduction. The LUMO level of the composite was calculated to be 3.17 V (an increase of 0.85 eV over the pristine PONV-OAV). This increase will make charge transfer between the two materials more favourable (Ding, 2002) and leads to a lower electrochemical bandgap of 1.64 eV.

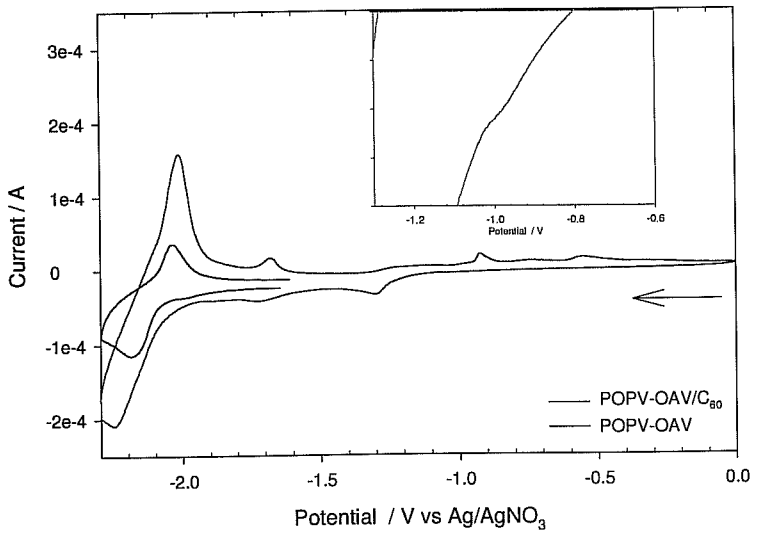

Figure 6.11: n-doping Cyclic Voltammogram of POPV-OAV/C_{60} and POPV-OAV in CH_3CN solution of 0.1 M tetrabutylammonium hexafluorophosate @scan rate of 0.1 V/sec. Insert shows the first reduction process of the composite.

Figure 6.12 shows the p-doping cyclic voltammogram for PONV/C_{60} and pristine PONV. The PONV/C_{60} composite shows two oxidation peaks. The first peak occurs at a very low potential of 0.10 V and the second occurs at a potential of 0.69 V. The second peak can be attributed to the oxidation of the PONV. In the previous case the POPV-OAV was oxidised and this process was followed by a new oxidation feature which was assumed to be a charge transfer feature of the composite. However in this case there is no electron transfer after the oxidation of the polymer. Instead the new peak occurs before the oxidation of the pristine PONV. This new peak could be due to a new excited state produced in the composite.

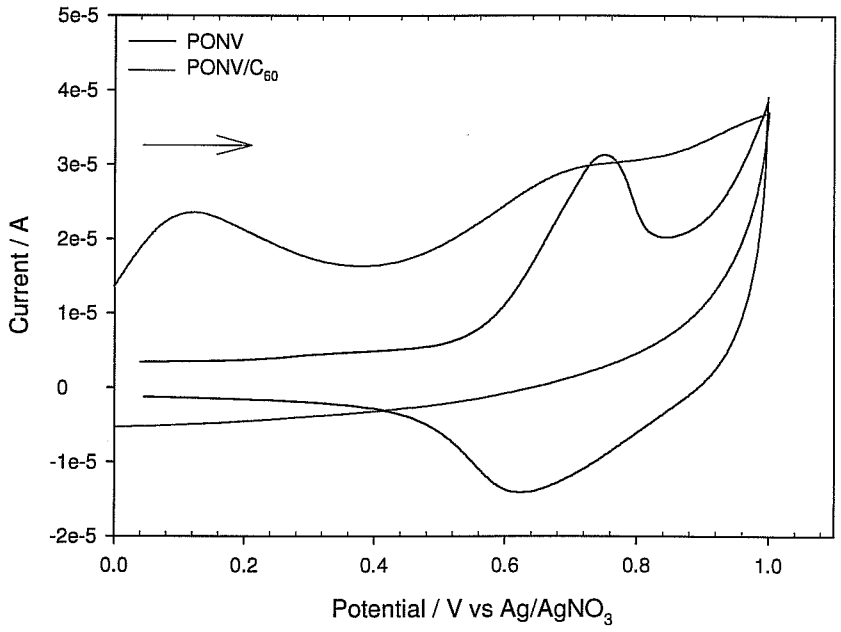

Figure 6.12: p-doping Cyclic Voltammogram of PONV/C_{60} and PONV in CH_3CN solution of 0.1M tetrabutylammonium hexafluorophosate @scan rate of 0.1V/sec.

However applying the same theory to the PONV/C_{60} that was applied to the POPV-OAV/C_{60} and the MEH-PPV/C_{60} composites it is possible to predict where a charge transfer peak would occur. The difference between the HOMO level of PONV and the

LUMO level of C_{60} is 1.27 eV. This is quite a high potential and therefore the absence of the charge transfer peak may be due to the limits of the polymer and C_{60} under CV conditions.

The onset of the peak at 0.10 V occurs in the negative part of the cyclic voltammogram. This onset results in a HOMO level of 4.27 eV. When the C_{60} was added to the POPV-OAV the HOMO level was increased whereas with the PONV the HOMO level was reduced. The structures and the stacking arrangements of the polymers in the solid-state affect the charge transfer between themselves and the C_{60}. As mentioned earlier H type and J-type aggregates result in different stacking arrangements. The different stacking arrangement of the polymers may result in the C_{60} being better dispersed throughout the film.

Figure 6.13 shows the n-doping cyclic voltammogram obtained for PONV/C_{60} composite. The insert shows the scan from -0.5 V – 1.1 V for observation of the first reduction process of molecular C_{60}. The composite spectrum is a summation of the two materials. The composite spectrum has three reduction features. The first three reduction peaks at, -0.98 V, -1.35 V and -1.82 V can be attributed to molecular C_{60} with the re-oxidation peaks occurring at -0.82 V, -1.66 V and -1.08 V. The fourth reduction peak at -2.21 V is attributed to the reduction of the PONV. The difference in the reduction potential of the pristine PONV and the PONV in the composite is negligible and can be attributed to drift within the reference electrode. The noticeable difference again is the increase in the current range of the polymer reduction. The composite current range was a factor of 2 larger than that of the pristine PONV. As mentioned previously this is consistent with the C_{60} acting as an acceptor material and hence the polymer can accept more charge. The current peaks are much broader in the PONV/C_{60} composite than those of POPV-OAV/C_{60} composite, which means that the amount of

charge consumed is greater in the PONV/C_{60} composite (Li, 1999). The LUMO level of the composite was calculated to be 3.24 V. This increase will make charge transfer between the two materials more favourable (Ding, 2002). This increase in LUMO level and the decrease in HOMO level leads to an electrochemical bandgap of 1.03 eV (bandgap of composite is lower than that of pristine polymer).

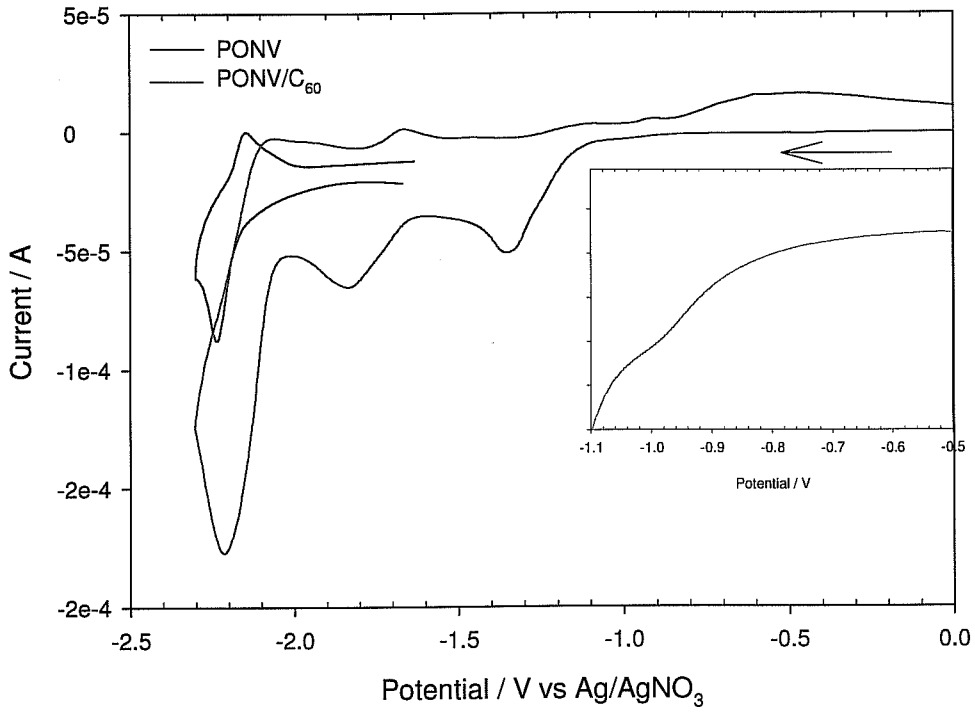

Figure 6.13: n-doping Cyclic Voltammogram of PONV/C_{60} and PONV in CH_3CN solution of 0.1 M tetrabutylammonium hexafluorophosate @scan rate of 0.1 V/sec. Insert shows the first reduction process of the composite.

In general the cyclic voltammetry of the two composite materials provided evidence of an interaction between the polymers and the C_{60}. This further supports the suggestion of an interaction seen in the fluorescence quenching. Thus the two methods have provided

evidence of a charge transfer between the polymers and the C_{60}. However there a still some questions left open by the cyclic voltammetry results of the polymers and composites. In order to fully understand what is occurring, in situ reflectance measurements were carried out. In situ measurements were first performed to probe the effect and changes (if any), on the optical properties of the polymers and composites when subject to cyclic voltammetric conditions.

6.5 Introduction to spectroelectrochemistry in conjugated polymers

As described in Chapter 3, the combination of electrochemical and optical methods can be employed to provide vital information on the excited properties of the polymers. A number of optical methods have been coupled with electrochemical techniques (Brett, 1993). The approach used in this study was reflectance mode absorption spectroelectrochemistry (Chapter 3).

The doping process in conjugated polymers as currently understood introduces deformations known as solitons, polarons and bi-polarons into the polymer system causing new levels to form in the bandgap, increasing the amount of possible energy transitions (Bredas, 1985, Baeriswyl, 1992). Conjugated polymers can be divided into two types, degenerate and nondegenerate. Solitions are considered to be the important excitations in degenerate polymers. For example polyacetylene is one of the most commonly known polymers with a degenerate ground state (the double and single bonds can be interchanged with no energy cost) (Patil, 1988). Polythiophene, poly (p-phenylene) and polypyrrole are examples of polymers with a nondegenerate ground state (the polymers used in this study are nondegenerate). The ground state degeneracy is lifted so that polarons and bipolarons are the important excitations and the dominant

charge storage configurations (Patil, 1988). Polarons and bipolarons describe localised charge distributions that accompany a distortion along a polymer chain. The lattice relaxation stretches over the repeat units of the polymer chain. Polarons and bipolarons are considered quasiparticles because they are mobile on the polymer chain. Upon p-doping an electron is removed form the π system of the polymer backbone, leaving behind a positive spinless charge and a free radical. This spin ½ combination, called a polaron, creates two energy levels inside the bandgap, one singly occupied, symmetrically placed around the centre of the gap. That single electron can be removed creating a spinless bipolaron with localised energy states further from the band edges than the polaron states because of the stronger lattice relaxation (Bredas, 1985, Patil, 1988, Holt, 2005). Figure 6.14 shows the energy levels suggested for these quasiparticles as well as the possible energy transitions. In the electron-phonon-coupled model utilised by Fesser *et al* ω_1 and ω_2 are the dominant transitions for a polaron and ω_1 for the bipolaron (Fesser, 1983). In previous theories and past experiments it has been suggested that polarons are dominant at low doping levels whereas bipolarons are more favourable at high doping levels (Patil, 1988). Polymers are inherently disordered so it is difficult to characterise the fundamental roles of these quasi-particles in the doping process. One of the most common was of exploring dopant deformations is to apply in-situ spectroscopic techniques such as Raman, infrared absorption and UV/VIS absorption (Bredas, 1985, Holt, 2005).

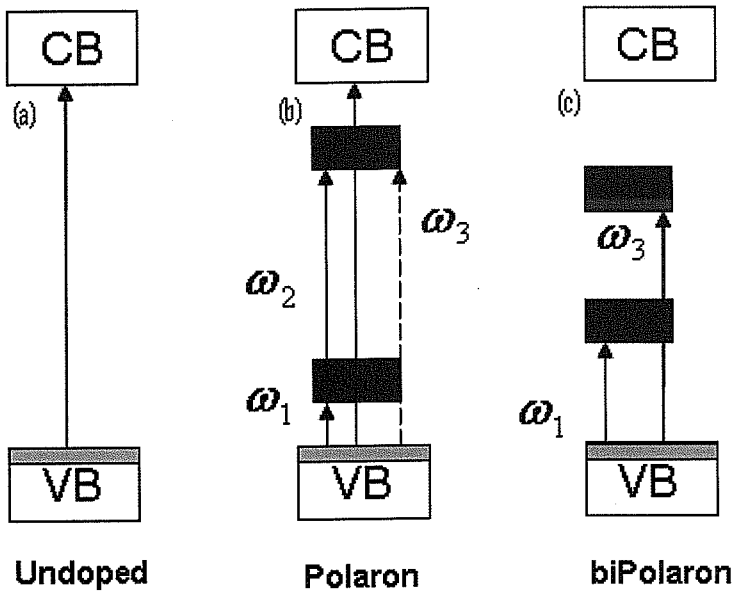

Figure 6.14: Illustration of the energy transitions for (a) an undoped polymer, (b) a positive polaron, (c) a positive bipolaron (Bredas, 1985, Patil, 1988 Holt, 2005).

6.6 Spectroelectrochemistry of polymer series

The spectroelectrochemical technique is described in Chapter 3 (Section 3.5.3). A description of the specific experimental details are described are provided here. The in-situ measurements were carried out in the dark to prevent stray light from reaching the cell. Prior to the spectra being collected, the detector dark spectral response and reference spectra were recorded. The dark response was measured by disconnecting the fibre optic from the light source. The reference spectrum was taken of the bare glassy carbon electrode in electrolyte. The polymer films were then deposited onto the electrode. Due to the spectral limits of the Ocean Optics S2000 spectrometer, spectra were recorded in the range of 1.50 eV to 3.50 eV. The scans were performed in reflectance mode as a high reflectance is equal to a high transmission. Each of the

polymers was reduced (n-doping) using the potentiostat. The sensitivity of the potentiostat did not allow the scans to be stopped at exact potentials. For each polymer four absorption spectra were obtained at different potentials of 0 V, -0.5 V, -1.0 V, and -1.5 V and at the reduction onset potential for each polymer.

Figure 6.15 shows the in-situ UV/VIS spectra obtained for PONV. At 0 volts there is one peak apparent in the spectrum at 2.95 eV. This peak is attributed to the $\pi \rightarrow \pi^*$ transition of the polymer backbone. As the applied voltage is increased from low doping to high doping there is a change in the spectrum. The highest doping occurs at -2.10 volts, which is just after the onset potential. At this potential there is a reduction in the intensity of the $\pi \rightarrow \pi^*$ transition (LUMO population is increased as the polymer is being reduced, reducing the number of states to which an optical transition can occur) and an evolution of a new peak at 2.48 eV. The second feature at 2.48 eV is attributed to the effect of the doping and can be said to be a polaron or bipolaron as it represents absorption to or from a state which is slightly offset from the band edge (Figure 6.14). It is assumed that the excited energy levels in all polymers are bipolarons from previous results and reports in literature (Bredas, 1985, Patil, 1998, Pope, 1999, Holt, 2005). The other bipolaronic transition is occurring outside the spectral limits of the spectrometer. However as the first transition is visible it is possible to calculate the second transition. From Figure 6.14 it can be deduced that the sum of ω_1 and ω_3 should be equal to the calculated electrochemical bandgap. Therefore if the first bipolaron transition is subtracted from the electrochemical bandgap (2.73 eV-2.48 eV) a value for the second bipolaron transition can be obtained. The second bipolaron transition can be said to be approximately around 0.25 eV. Also from Figure 6.15 it can be seen that as the doping level is increased from -1.5 V to -2.10 V there is a blue shift in the bandgap, which has

also been shown to accompany the formation of bipolaron bands which occur within the bandgap for heavy doping (Holt, 2005).

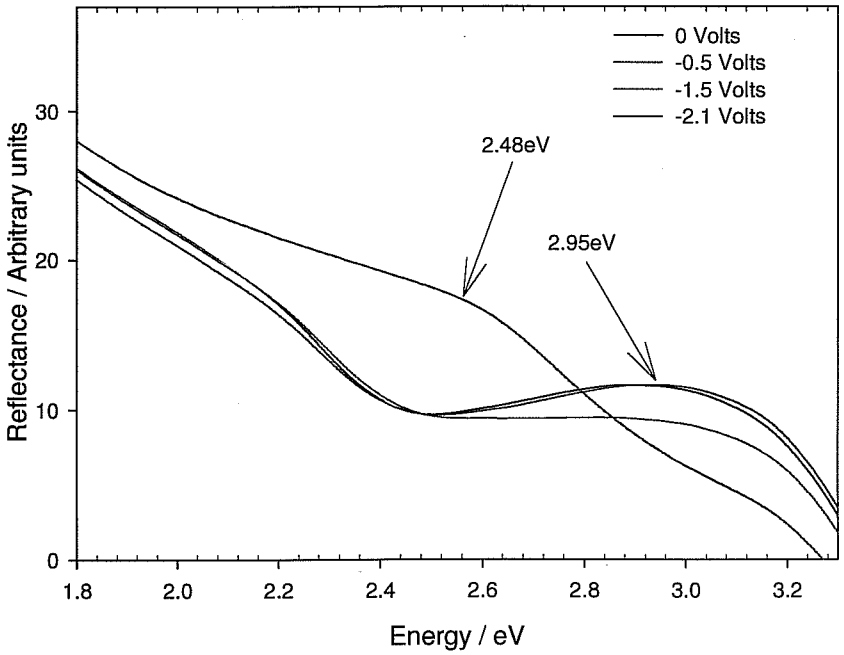

Figure 6.15: In situ reflectance spectra for POPV at various doping potnetials.

The same experimental procedure and calculations were also performed on the rest of the polymer series. Using the data obtained form the cyclic voltammetry and the in-situ spectroscopic measurements a schematic illustration of the energy levels within the polymers can be depicted. Figure 6.16 is an illustration of the bandgap energy levels and the suggested bipolaron energy levels in all of the polymers. In general the spectroelectrochemistry provides a representation of the charged states within the polymer series. There is no clear trend observed for these interband states with regard to the systematic structural changes made to the polymers. However it is important to have

a knowledge of polaron and bipolaron energy levels as they are one of the charge transfer mechanisms that can occur between donor and acceptor materials.

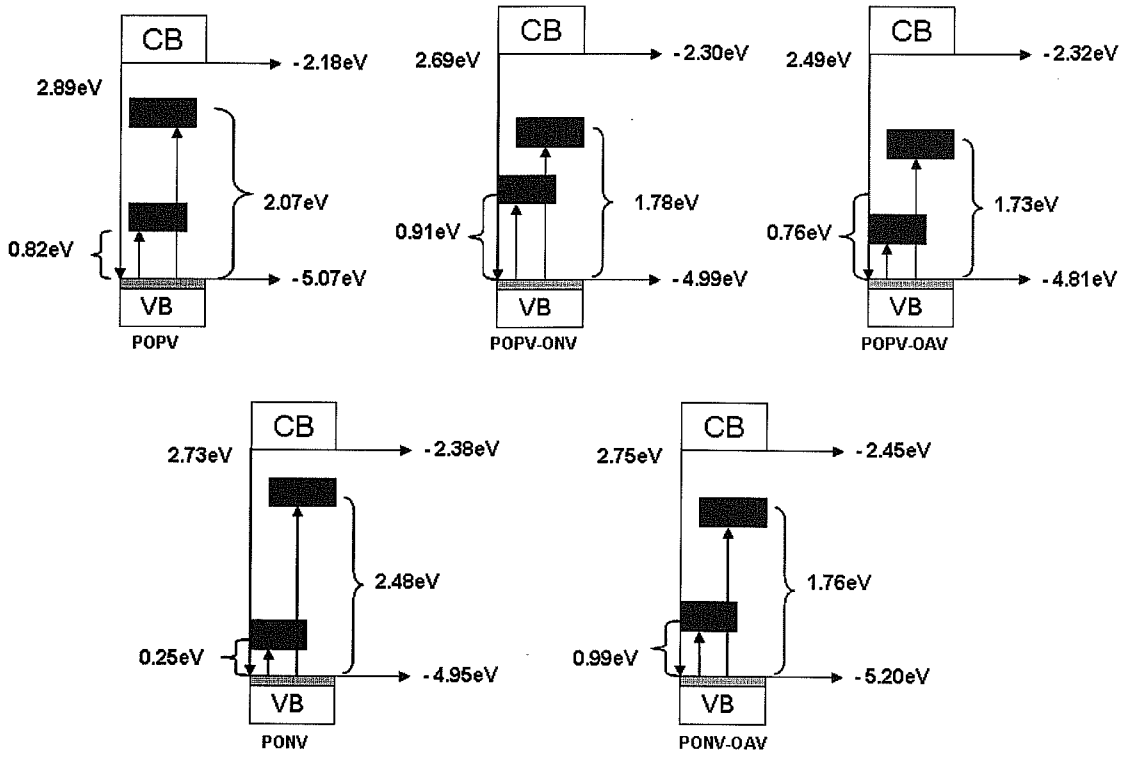

Figure 6.16: Illustration of HOMO-LUMO levels and bipolaron levels in polymer series.

6.7 Spectroelectrochemistry of composites

Although the p-doping scan gave more conclusive evidence of a charge transfer, the in-situ reflectance measurements were performed on the n-doping scans because as the n-doping scans were a summation of the two materials it was thought best to try and observe the changes (if any) to the C_{60} upon reduction. Figure 6.17 shows the UV/VIS reflectance spectra obtained for POPV-OAV/C_{60}. The spectrum is a summation of the two materials. At 0V, three peaks are seen at 1.57 eV, 2.20 eV and 2.45 eV. The peak at

2.45 eV can be attributed to the $\pi \rightarrow \pi^*$ transition of the POPV-OAV. The two other peaks at 1.57 eV and 2.20 eV can be attributed to the C_{60} (Leach, 1994, Kazaoui, 1998) as shown in the UV/VIS absorption spectra of C_{60} (Figure 4.2). As the doping potential is increased from 0 V to -1.22 V there is little or no change in the spectrum. At the next doping potential of -1.64 V the spectrum starts to change and there is a small spectral shift. At -1.80 V the spectral shift is increased and is more noticeable, especially for the two C_{60} peaks at 1.57 eV and 2.20 eV.

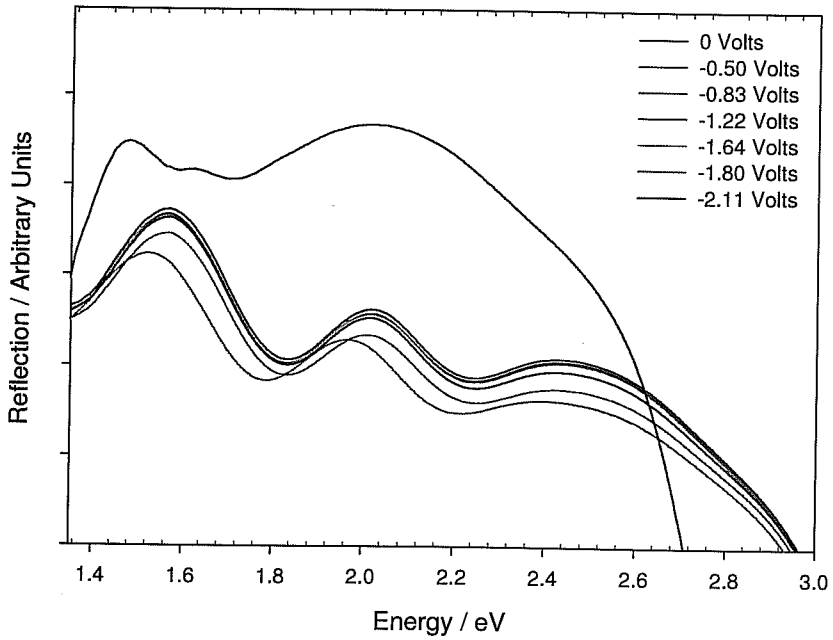

Figure 6.17: In-situ reflectance spectra for POPV-OAV/C_{60} at various doping potentials.

This spectral shift could be due to the third C_{60} (Figure 6.9) reduction peak (C_{60}^{-3}) and not an interaction between the two materials. The next doping potential at -2.11 V is just before the reduction potential of the POPV-OAV (Figure 6.11). The peak at 1.57 eV has

decreased (but can still be seen) and a new feature has appeared at 1.48 eV. This peak is attributed to a charge transfer between the POPV-OAV and the C_{60}. More evidence for this is the absence of the $\pi \rightarrow \pi^*$ transition at 2.45 eV. The width of the peak at 2.20 eV has increased and is spectrally shifted. The increase in width could be a broadening of the energy states of the C_{60} which is further evidence of an interaction. The spectroelectrochemistry result reaffirms the cyclic voltammetry proposals that there is an interaction between the polymer and the C_{60}. However there is no evidence of an interaction until the composite is exposed to heavy doping potentials.

Figure 6.18 shows the in-situ UV/VIS reflectance results obtained for PONV/C_{60} at different potentials. As in the case of the UV/VIS absorption spectrum, Figure 5.8, the spectrum is not a direct summation of the two materials. The peak at 2.76 eV can be attributed to the $\pi \rightarrow \pi^*$ transition of the PONV. There is a shoulder peak just before the $\pi \rightarrow \pi^*$ transition at 2.64 eV. As the doping potential is increased from 0V through to -1.08V the change is negligible. At the next doping potential of -1.24 V (-1.24 V is approximately at the onset of the first C_{60} reduction peak in the CV scan of PONV/C_{60}, Figure 6.9) the $\pi \rightarrow \pi^*$ transition of the PONV disappears and the shoulder peak at 2.64 eV becomes more dominant and undergoes a spectral shift from 2.64 eV to 2.50 eV. The absence of the peak at 2.76 eV and the emergence of the peak at 2.50 eV, indicates an interaction between the two materials; it may be that a new excited state energy level has emerged as the doping levels are increased further to -2.15 V. This new peak at 2.50 eV starts to decrease and the feature at 1.36 eV becomes more intense. The decrease of these peaks could be another indication of charge transfer. There is evidence of an interaction between PONV and C_{60}. There seems to be no need to proceed to high doping levels as the charge transfer appears to occur at a low doping level of -1.50 V,

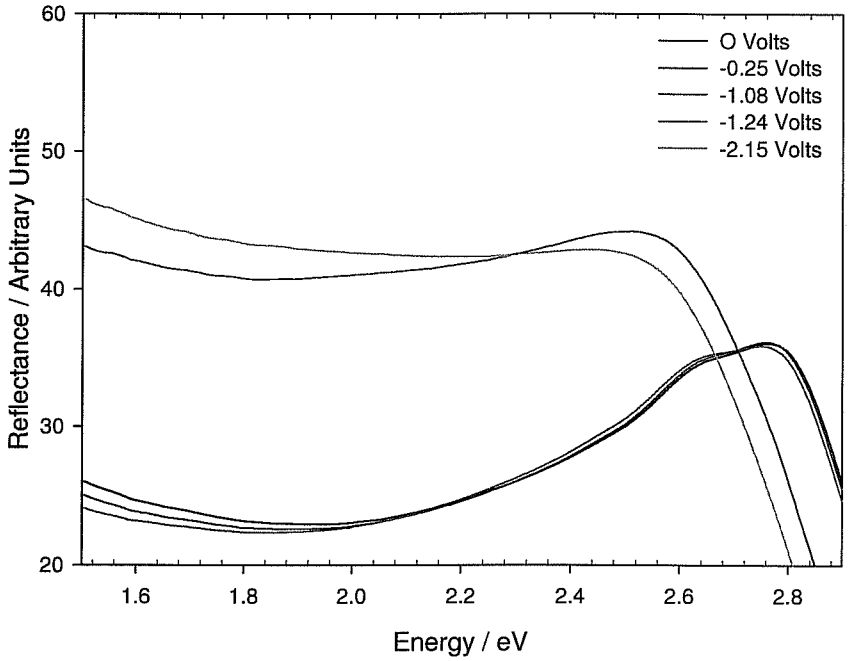

Figure 6.18: In-situ reflectance spectra for PONV/C_{60} at various doping potentials.

6.8 Summary of cyclic voltammetry and spectroelectrochemical measurements

Electrochemical measurements provided an insight to the redox behaviour of the polymers. All the polymers were capable of being oxidised and reduced electrochemically. The electrochemical properties, optical properties and vibrational properties were all found to correlate and be related back to the structural changes made to each polymer. The cyclic voltammetry and the spectroelectrochemical results enabled a visualisation of the bandgaps and excited state levels within the polymer series. Electrochemical bandgaps were in close accordance to the optical bandgaps. Some of the structural changes made to the polymers could be quantified with the different changes to the HOMO-LUMO levels of the polymers. The HOMO-LUMO levels of the polymers were all shown to match up with the HOMO-LUMO levels of the C_{60}.

Cyclic voltammetry measurements on the composites provided evidence of a charge transfer between the polymer and the C_{60}. In the p-doping scan a new feature which was attributed to a charge transfer was seen in the POPV-OAV/C_{60} composite. This result was similar to that seen for MEH-PPV. The PONV/C_{60} p-doping scan did show a new feature but this was before the oxidation of the polymer and is attributed to anew excited state formed between the PONV and C_{60}. The n-doping spectra were summations of the composite materials. The main evidence of an interaction in the n-doping scans was the increase in current range between the reduction and re-oxidation peaks. The addition of the C_{60} allows the polymer to accept more charge as it can donate it to the C_{60}. The PONV/C_{60} composite showed a larger current than the POPV-OAV/C_{60} composite. In-situ spectroscopic measurement reaffirmed that there is an interaction between the polymer and the C_{60} in the composites. Only with heavy doping did the UV/VIS spectrum of POPV-OAV show a significant change indicative of a potential charge transfer.

The PONV/C_{60} did show what appeared to be a charge transfer, which occurred at lower doping levels. It is important to note at this stage that the above results are new and novel. The last part of this chapter focuses on conductivity measurement. The conductivity should be able to reaffirm the above measurements and conclude that there is an interaction between the polymers and the C_{60}.

6.9 Current voltage characteristics of POPV-OAV and PONV

Figure 6.19 shows the current voltage characteristics of POPV-OAV and PONV. I-V curves were obtained using a 237 Keithley programmable electrometer and current voltage power sources. Films were placed in a Linkam microscope cooling stage and

purged with nitrogen so as to keep the films under an inert atmosphere. Both polymer devices displayed diode behaviour. As the voltage is increased, the polymers become conductive and allow charge to flow at which point, it can be said that the polymer diode is turned on (turn on voltage) (Liang, 2005). The turn on voltage of POPV-OAV is 2.3 volts. The turn on voltage for PONV occurs at a lower potential of 1.7 volts. As mentioned previously, it could be said that conductivity measurements are similar to electrochemically p-doping measurements.

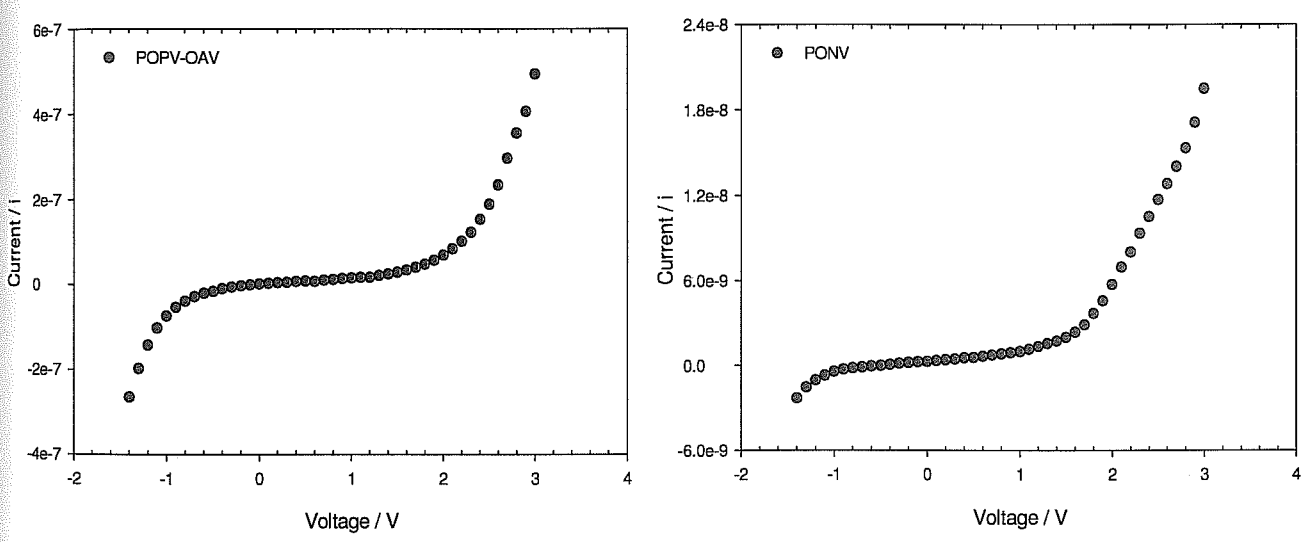

Figure 6.19: I-V characteristic curve for POPV-OAV and PONV single layer devices.

However if we compare the turn on voltages to the oxidation potential it can be seen that in both cases PONV has a lower turn on potential and a lower oxidation potential compared to that of POPV-OAV. The PONV also has a higher HOMO level and a lower LUMO which provide a better hole blocking properties and a lower electron injection barrier. Another point of importance is that the short circuit current (I_{sc}) at 1.5 V of POPV-OAV is one order of magnitude larger than that of PONV. Again if this is compared this to the electrochemical p-doping results it can be seen that the current

intake in the p-doping scan of POPV-OAV is also one order of magnitude larger than that of PONV.

6.10 Current voltage characteristics of composites

Figure 6.20 shows the current voltage characteristics of a POPV-OAV and a POPV-OAV/C_{60} single layer device (pristine POPV-OAV curve is shown for clarity). The films were spin coated from a solution of POPV-OAV with 52% C_{60}. Therefore the active layer can be said to be combination of the two materials.

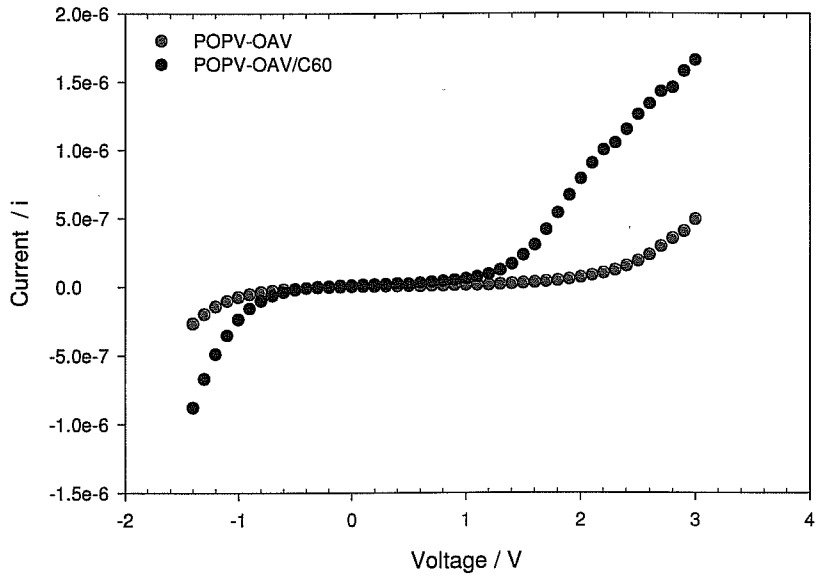

Figure 6.20: I-V characteristic curve for POPV-OAV/C_{60} and POPV-OAV single layer devices.

As mentioned in Chapter 2 diffuse devices have been to shown to increase current by over two orders of magnitude (Yu, 1995, Sariciftci, 1993, Shaheen, 2001). The addition of the C_{60} to the POPV-OAV results in a decrease in the turn on voltage to 1.4 volts

compared to that of 2.3 volts of POPV-OAV single layer device. The short circuit current of the POPV-OAV/C_{60} device at 1.4 V is a factor of 1.5 larger than the POPV-OAV single layer device. The addition of the C_{60} enhances the transport of electrons and holes through the acceptor and donor material respectively in a preferred direction to the extracting electrodes.

Figure 6.21 shows the I-V characteristics for the PONV/C_{60} composite along with the pristine PONV. The composite has a turn on voltage of 0.5 volts compared to a turn on voltage of 1.7 volts for the pristine PONV. This is quite a significant shift in turn on potential.

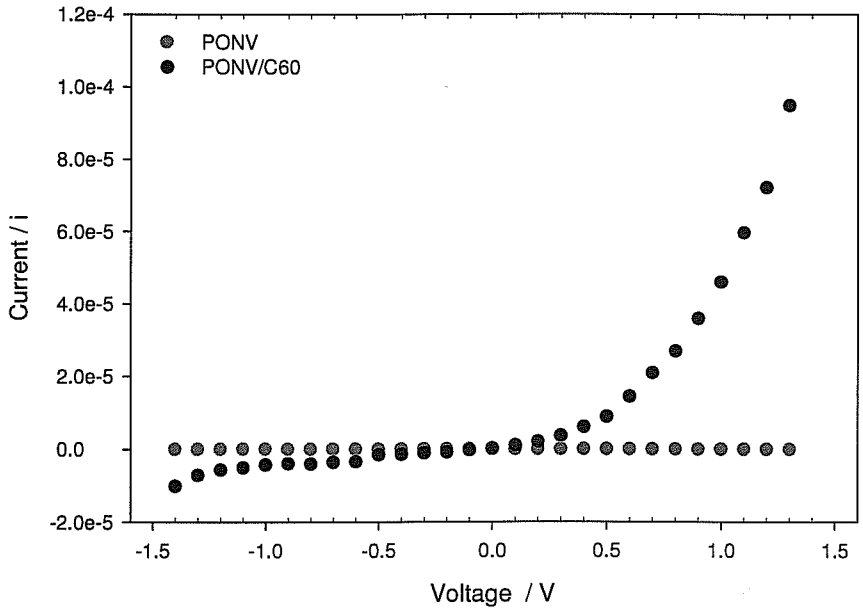

Figure 6.21: I-V characteristic curve for PONV/C_{60} and PONV single layer devices.

The I_{sc} at 1.5 volts in the composite is a factor of 10,000 larger than that of the pristine PONV. This large increase in current proves that the C_{60} is affecting the conductivity of

the composite. The conductivity of MEH-PPV has been shown to increase by two to three orders of magnitude with the addition of C_{60} (Drees, 2002). This was also seen in Figure 4.16 for the MEH-PPV/C_{60} composite. It is important to note that in the spectroelectrochemical and conductivity measurements, the PONV was seen to have a more profound effect with the C_{60} than the POPV-OAV. At this moment it appears that the interaction of C_{60} with PONV is more compatible for device fabrication due to the lower turn on voltage and the larger increase in conductivity. The logical explanation for this is due to positioning of the HOMO-LUMO levels of the PONV relative to that of the C_{60} and electrodes.

6.11 Summary of conductivity measurements

The pristine polymers displayed diode behaviour. The turn on voltage of both POPV-OAV and PONV were obtained. The addition of the C_{60} leads to a lower turn on voltage and also to an increase in conductivity. The increase reaffirms the cyclic voltammetry results that the addition of the C_{60} allows for a greater current intake. The current voltage characteristics show that the increase in current is larger in the PONV than the POPV-OAV. Although it has been shown throughout this study that both polymers have the potential to charge transfer with C_{60}, it may be that this charge transfer is more favourable with the PONV. However the exact charge transfer mechanism with donor acceptor materials (e.g. polymer-fullerene) is still not fully understood. The energy levels of PONV could make charge transfer more favourable as they seem to align better with energy levels of the C_{60}.

In general summing up, fluorescence spectroscopy, cyclic voltammetry, spectroelectrochemical and conductivity measurements have all provided evidence of an

interaction in the same two new novel composites, which at this stage of the study make a clear case for replacement of time resolved spectroscopy with the already mentioned techniques.

The next chapter focuses on electroabsorption spectroscopy. EA spectroscopy will provide information on the excited electronic states and charge transfer in the polymer series (Liess, 1997, Weiser, 1998).

References:

Baeriswyl D, Campbell I.D., Mazumdar S, *"Conjugated Conducting Polymers"*, Springer-Verlag Series, (1992).

Bonesi S.M., Balsells R.E., *"Outer-sphere electron transfer from carbazoles to halomethanes. Reduction potentials of halomethanes measured by fluorescence quenching experiments"*, J. Chem. Soc, Perkin Trans. 2, 1583, (2000).

Bredas J.L., Street G.B., *"Polarons, Bipolarons, and Solitons in Conducting Polymers"*, Acc. Chem. Res, 18, 309, (1985).

Brett C.M, Brett A.M.O, *"Electrochemistry Principles, Methods and Applications"*, Oxford University Press, (1993).

Burroughes J.H., Bradley D, Brown A.R., Marks R.N., Mackay K., Friend R.H., Burn P.L., Holmes A.B.," *Light-emitting diodes based on conjugated polymers"*, Nature, 539, 347 (1990).

Cervini R, Li X. C, Spencer G. W. C., Holmes A. B., Moratti S. C., Friend R. H., *"Electrochemical and optical studies of PPV derivatives and poly(aromatic oxadiazoles)"*, Synthetic Metals, 84, 359-369,(1997).

Croney J.C., Helms M.K., Jameson D.M., Larsen R.W., *"Conformational Dynamics and Temperature Dependence of Photoinduced Electron Transfer within Self-Assembled Coproporphyrin:Cytochrome c Complexes"*, Biophysics Journal, Vol 84, 4135, (2003).

de Leeuw D.M., Simenon M.M.J., Brown A.R., Einerhand R.E.F., *"Stability of n- type doped conducting polymers and consequences for polymeric microelectronic devices"*, Synthetic Metals 87, 53-59. (1997).

Ding H, Bertoncello P, Ram M.K., Nicloni C, *"Electrochemical investigation on MEH-PPV/C_{60} nanocomposites Langumir-Schaefer films"*, Electrochemical Communications 4, 503, (2002).

Drees M, Davis R.M., Marciu D, Premaratne K, Miller M, Heflin J.R., *"Improved polymer-fullerene interface in photovoltaic devices by thermally-controlled interdiffusion"* Polymer Preprints (American Chemical Society, Division of Polymer Chemisrty) 43(2), 506, (2002).

Fesser K, Bishop A.R, Campbell D.K, *"Optical absorption from polarons in a model of polyacetylene"*, Phys. Rev. B, 27, 4804, (1983).

Holt A.L., Leger J.M., Carter S.A., *"Electrochemical and optical characterization of p- and n-doped Poly[2-methoxy-5-(2-ethylhexyloxy)-1,4-phenylenevinylene]"*, Journal of Chemical Physics, 123, 044704, (2005).

Janietz S and Schulz B, *"Electrochemical Investigations on Poly(arylene-1,3,4-oxadiazoles)s"*, Eur. Poly. J. Vol. 32(4), 465, (1996).

Kazaoui S, Minami N, Tanabe Y, Byrne H.J., Elimes A, Petelenz P, *"Comprehensive analysis of intermolecular charge-transfer excited states in C_{60} and C_{70} film"*, Phys Rev B. 58, 7689, (1998).

Leach S, *"Physics and Chemistry of Fullerenes"*, World Scientific London, (1994).

Li X.C., Spencer G.C.W., Holmes A.B., Moratti S.C., Cacialli F, Friend R.H, *"The synthesis, optical and charge transport properties of poly(aromatic oxadiazole)s"* Synthetic Metals 76, 153, (1996).

Li Y, Cao Y, Gao J, Wang D, Yu G, Heeger A.J., *"Electrochemical properties of luminescent polymers and polymer light-emitting electrochemical cells"*, Synthetic Metals 99, 243, (1999).

Liang F, Pu Y.J., Kurata T, Kid J, Nishide H, *"Synthesis and electroluminescent of poly(p-phenylenevinylene)s"*, Polymer, 46, 3767,(2005).

Liess M, Jeglinski S, Vardeny Z.V., Ozaki M, Yoshino K, Ding Y, Barton T, *"Electroabsorption spectroscopy of luminescent and nonluminescent π-conjugated polymers"*, Phys. Rev. B 56, 15712, (1997).

O'Neill L, Lynch P, McNamara M, Byrne H.J., *"Vibrational Characterisation and Fluorescence Optimisation of Polycyclic Polymers"*, Journal of Physical Chemistry A, 111, 7999, (2007).

Patil A.O., Heeger A.J., Wudl F, *"Optical Properties of Conducting Polymers"*, Chem. Rev. 88, 183, (1988).

Pope M, Swenberg C.E., *"Electronic Processes in Organic crystals and Polymers"*, Oxford University Press, (1999).

Rehm D and Weller A. *"Kinetics of fluorescence quenching by electron and H-atom transfer"*, J. Chem. 8:259, (1970).

Rienstra-Kiracofe J.C., Barden C.J., Brown S.T., Schaefer H.F., *"Electron Affinities of Polycyclic Aromatic Hydrocarbons"*, J, Phys. Chem. A, 105, 524, (2001).

Sariciftci N.S., Smilowitz L, Heeger A.J., Wudl F, *"Semiconducting Polymers (as donors) and Buckminsterfullerene (as acceptor) - photoinduced electron-transfer and heterojunction devices"*, Synthetic Metals 59, 333, (1993).

Sariciftci N.S., *"Optical and Electronic Properties of Fullerenes and Fullerene-Based Materials"* edited by Shinar J, Vardeny Z.V, Kafafi Z, 362, (2000).

Shaheen S.E., Brabec C.J., Sariciftci N.S., Padinger F, Fromherz T, Hummelen J.C., *"2.5 % Efficient Organic Solar Cells"*, Appl. Phys. Lett. 78, 841, (2001).

Weiser G, Horvath A, *"Variation with disorder of absorption and electroabsorption spectra of a π-conjugated polymer: 4BCMU"*, Chem. Phys. 227, 153, (1998).

Xiao Y, Yu W.L., Chen Z.K., Lee N.H.S., La Y.H., Huang W, *"Synthesis and characterisation of a novel light emitting copolymer with improved charge-balancing property"*, Thin Solid Films, 363, 102, (2000).

Yu G, Gao J, Hummelen J.C, Wudl F, Heeger A.J., *"Polymer photovoltaic cells: enhanced efficiencies via a network of internal donor-acceptor heterojunctions"*, Science, 270, 1789, (1995).

Chapter 7: Electroabsorption Spectroscopy

7.1 Introduction

As discussed in Chapter 3 the electroabsorption spectrum of organic/inorganic materials can be dominated by first or second derivatives of the absorption spectrum. In the case of solid-state C_{60}, it is dominated by a second derivative and hence a number of charge transfer states have been assigned to C_{60} in the energy range up to 4.00 eV (Kazaoui, 1995, Byrne, 1995) (Chapter 4, Section, 4.4). Most organic polymers are dominated by the intramolecular excited states (or Frenkel Exciton). This was seen the electroabsorption spectrum of MEH-PPV also in Chapter 4, Section 4.7.3. At energies between 2.00 eV→3.00 eV the electroabsorption spectrum of MEH-PPV closely resembled that of a first derivative absorption fit. However at higher energies the electroabsorption spectrum of MEH-PPV was shown to deviate due to the induced transition to a forbidden exciton state, which becomes optically allowed by the application of the externally applied field (Martin, 1998). Therefore it can be expected that the electroabsorption of the polymer series should be dominated by the quadratic Stark effect (Weiser, 2004) (Section 3.6.3). The binding energies of the polymer series should also be comparable to that of MEH-PPV.

The electroabsorption of the MEH-PPV/C_{60} composite did show a broadening of the lowest excitonic electroabsorption transition, which was reported to coincide with a reported charge transfer between the two materials (Liess, 1997). However in the new polymer/C_{60} composites this deduction will not be valid as a broadening of the lowest exciton feature could be due to the morphology of the composite material and not a charge transfer, as the optical transition has been seen to be strongly influenced by

aggregation phenomena. Therefore the observation of second derivative contributions of the absorption spectrum in the electroabsorption spectra could be pivotal in determining charge transfer signatures.

7.2 Electroabsorption spectroscopy of polymer series

Figure 7.1 shows the electroabsorption spectrum of POPV along with a first derivative of the solid-state absorption.

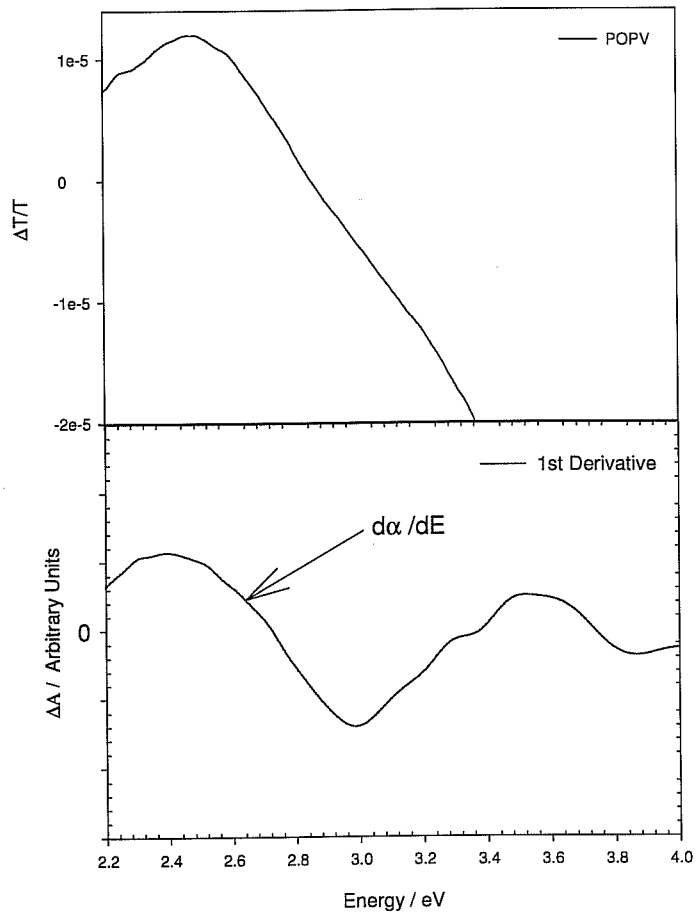

Figure 7.1: Electroabsorption spectrum of POPV with a first derivative lineshape.

Due to the limits of the electroabsorption spectrometer only one electroabsorption feature can be seen. The first electroabsorption feature from 2.20 eV to 2.60 eV can be attributed to the quadratic Stark effect of the lowest exciton ($1B_u$ are localised excitons). From the first derivative absorption fit it is possible to theoretically calculate the $_mAg$, which undergoes strong coupling to the $1B_u$ state. Using the first derivative lineshape, it can be seen that the $_mAg$ occurs at 3.50 eV. Using this calculated theoretical value of $_mAg$ and Equation 4.3 it is therefore possible to calculate the exciton binding energy, E_b (Liess, 1997). The exciton binding energy was calculated to be 0.79 eV for POPV. The calculated exciton binding energy for POPV is comparable to that of MEH-PPV which has a binding energy of 0.74 eV.

Figure 7.2 shows the electroabsorption spectra of POPV-ONV and POPV-OAV along with the appropriate derivatives of the solid-state absorption spectra. The electroabsorption spectra of both polymers closely resemble the first derivative of the absorption spectra. The electroabsorption spectrum of POPV-ONV shows three features. The first electroabsorption feature at 2.35 eV is attributed to the to the $1B_u$ state (quadratic Stark effect of the lowest exciton). The second feature at 2.53 eV can be attributed to a phonon sideband. The highest energy feature at 3.4 eV is the $_mA_g$ feature. Using Equation 4.3 the exciton binding energy was calculated to be 0.78 eV.

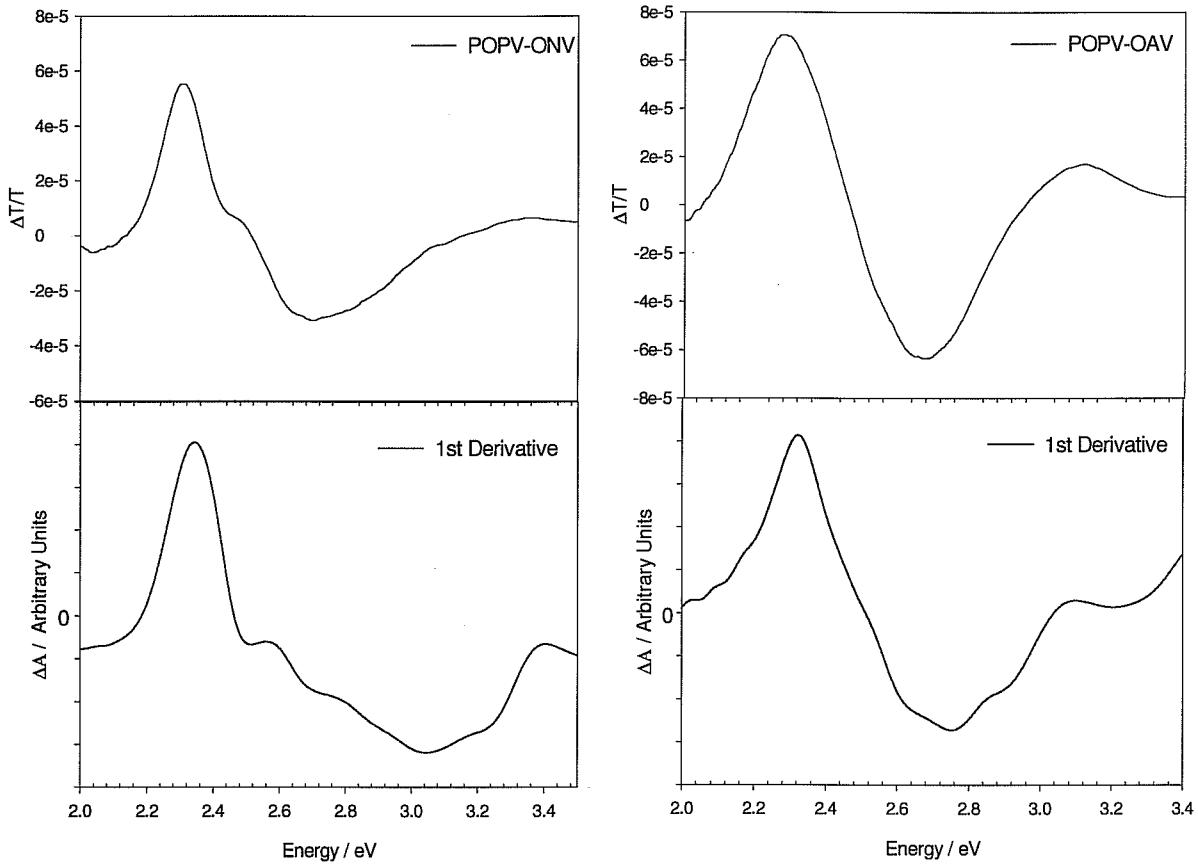

Figure 7.2: Electroabsorption spectrum of POPV-ONV and POPV-OAV along with first derivatives lineshapes of the solid-state absorption spectra of each polymer.

The electroabsorption spectrum of POPV-OAV shows two features. The first electroabsorption transition at 2.30 eV is the quadratic Stark effect of the lowest exciton followed by the $_{m}A_{g}$ state at 3.10 eV. There is a feature at 2.85 eV in the first derivative of the absorption spectrum which is not very clear in the electroabsorption spectrum. This is most likely a phonon sideband (Liess, 1997). Using Equation 4.3 the exciton binding energy was calculated to be 0.6 eV. In general the exciton transition energy of POPV-ONV and the POPV-OAV is lower than that of POPV. The lower exciton transition energy is a result of the addition of the naphthyl and anthryl groups. Similar

effects were also seen for the $\pi \rightarrow \pi^*$ transition of the polymers in the absorption spectra (Chapter 5).

Figure 7.3 shows the electroabsorption of PONV and PONV-OAV along with the first derivative absorption spectra of each polymer.

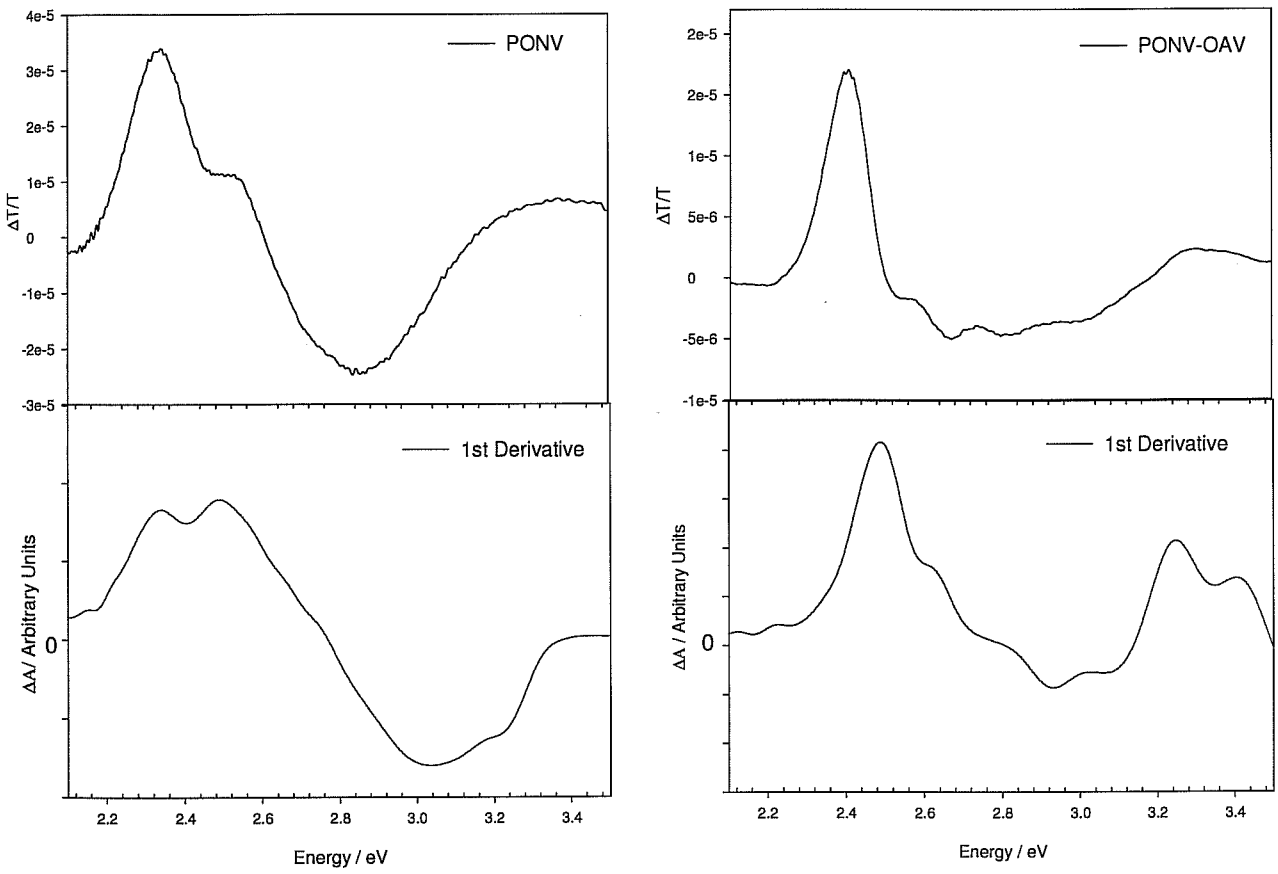

Figure 7.3: Electroabsorption spectrum of PONV and PONV-OAV with a first derivative lineshapes.

As before the electroabsorption spectra for PONV and PONV-OAV closely match the first derivative line shape. The electroabsorption spectrum of PONV contains three noticeable features. The first is the lowest energy exciton transition at 2.33 eV. The

feature at 2.52 eV is attributed to a phonon sideband, which also appears in the POPV-ONV electroabsorption spectrum and the highest energy feature at 3.23 eV is the $_mA_g$ state. The binding energy was calculated to be 0.6 eV. The PONV-OAV spectrum shows four electroabsorption features. The lowest energy feature of the ($1B_u$) exciton transitions occurs at 2.48 eV. This is followed by two phonon sidebands at 2.68 eV and 2.83 eV. The second phonon sideband is also in the POPV-OAV spectrum (although it is not very clear) and can be assigned to the anthryl units. The two phonon sidebands are followed by the $_mA_g$ state at 3.40 eV, which results in a binding energy of 0.8 eV.

Using Equation 3.9 (Sebastian, 1981, Weiser, 1993, Petelenz, 1993) it is possible to calculate the change in polarisability (Δp) for each of the polymers. The change in polarisability, Δp, supplies quantifiable information on an optical transition sensitivity of to an externally applied electric field and thus is particularly important in understanding the electronic properties of a material. Δp can be calculated theoretically but often not very accurately (Sebastian, 1981, Weiser, 1993, Petelenz, 1993). The function Δp reaches it maximum value, Δp at the lowest energy exciton transition in the electroabsorption spectrum which can be related with the longest respective conjugation in the conjugation length distribution (Liess, 1997). It has also been shown that the luminescent polymers have a larger Δp than non luminescent polymers (Liess, 1997). In other words a higher Δp value indicates a greater π-electron delocalisation within a molecule (Liess, 1997). A Δp value of MEH-PPV was first calculated (using data from the electroabsorption spectrum of MEH-PPV in Chapter 4, Figure 4.8), firstly for comparison to the other polymers and secondly to observe if the calculated value for MEH-PPV coincided with those reported in literature. The electric field value (F) was found to be 1.5×10^4 V/cm. A Δp value of 12700 $Å^3$ was calculated for MEH-PPV. This value is in close proximity to the value obtained by Liess *et al* of 12000 $Å^3$ (Liess,

1997) and Moses *et al* of 10000 $Å^3$ (Moses, 1997). Figure 7.4 shows the calculated electronic polarisability (Δp) for the polymer series and MEH-PPV as a function of the $1B_u$ exciton. Δp maximum of MEH-PPV is at least one order of magnitude larger than of the new polymers.

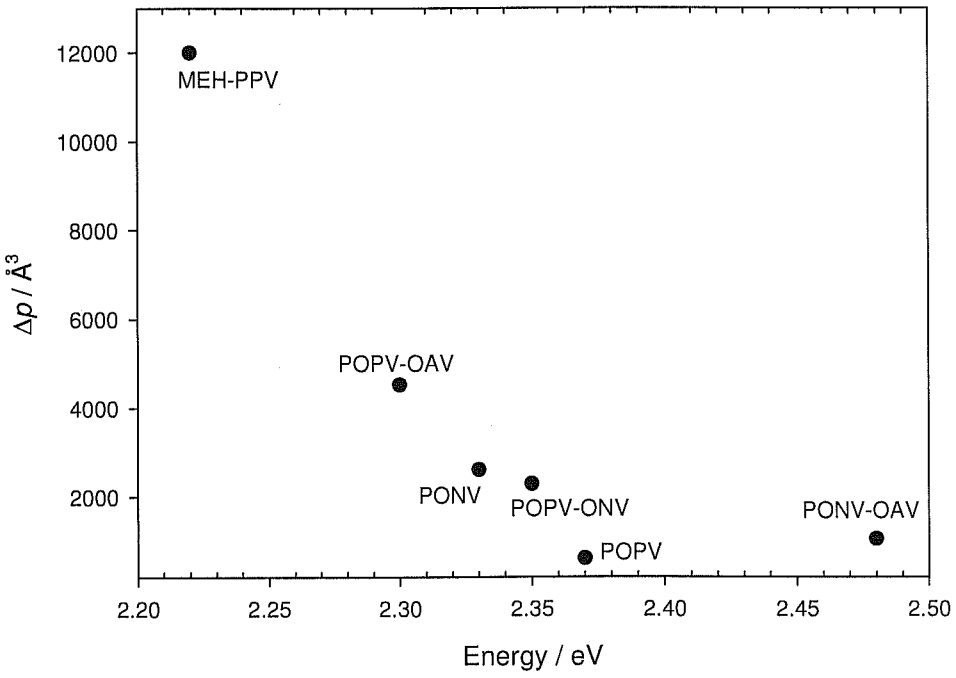

Figure 7.4: Calculated electronic polarisability (Δp) for the polymer series and MEH-PPV as a function of the $1B_u$ exciton.

It could also be said that as the Δp value increases the π-electron delocalisation increases (Liess, 1997). Under the influence of an electric field a highly polarisable molecular state will interact to a greater extent with other states. From Figure 7.4 it can be seen that the two polymers with the largest Δp values are POPV-OAV and PONV. There is no obvious trend observed from the above graph. Neglecting the PONV-OAV it could be said that the increase in polarisation with the addition of naphthyl and

anthryl units is linear. However if we recall Figure 6.7 from the Chapter 6 it was shown that it was possible to correlate a linear relationship between the electrochemical bandgap and the reduction potential of the polymer series. From Figure 6.7 it was shown that as the reduction potential decreased the electrochemical also decreased. It would appear that it is also possible to correlate a linear relationship for the electrochemical bandgap and the change in polarisability (Δp) for each of the polymers. Figure 7.5 shows a plot of Δp against the reduction potential for each polymer. Although an exact linear dependence is not inferred, a correlation is clearly evident.

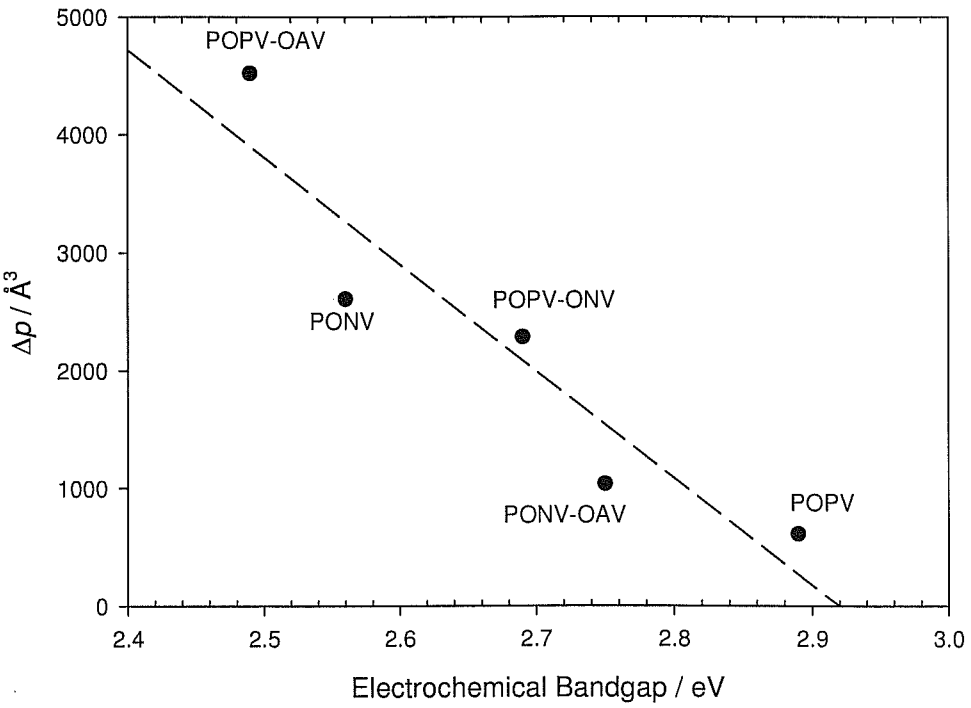

Figure 7.5: Correlation between change in polarisability (Δp) and electrochemical bandgap of polymer series.

The reduction in electrochemical bandgap is a result of the substituents naphthyl and anthryl units extracting electrons form the vinyl bond. In other words the molecules are communicating with each other. Δp is dependant on their ability to interact to a greater extent with other states in the polymer. Therefore it would be expected that as the bandgap is decreasing the polymer is becoming more conductive and interaction is occurring between the different states and hence a larger Δp is obtained. This correlation again highlights the benefits of the systematic approach of the analysis of the systems.

In summary it can be said that the electroabsorption spectra of the polymers is dominated by the quadratic Stark effect. The electroabsorption spectrum of each polymer closely resembles a first derivative fit of the absorption spectra, indicating a dominance of intramolecular transitions within each of the polymers. The exciton binding energy of each polymer was calculated, with values between 0.6 eV – 0.8 eV observed. These values seem reasonable at it has been shown that the exciton binding energy of most conjugated polymers are between 0.5 eV and 0.8 eV (Liess, 1997, Martin, 1998, Shimoi, 2000). A linear relationship between the electrochemical reduction potential and the change in polarisability (Δp) was found to exist.

7.3 Electroabsorption spectroscopy of composites

Figure 7.6 (A) shows the electroabsorption of the POPV-OAV/C_{60} composite along with the electroabsorption spectrum of POPV-OAV and Figure 7.6 (B) shows the electroabsorption spectrum of POPV-OAV/C_{60} with appropriate first derivative line shape.

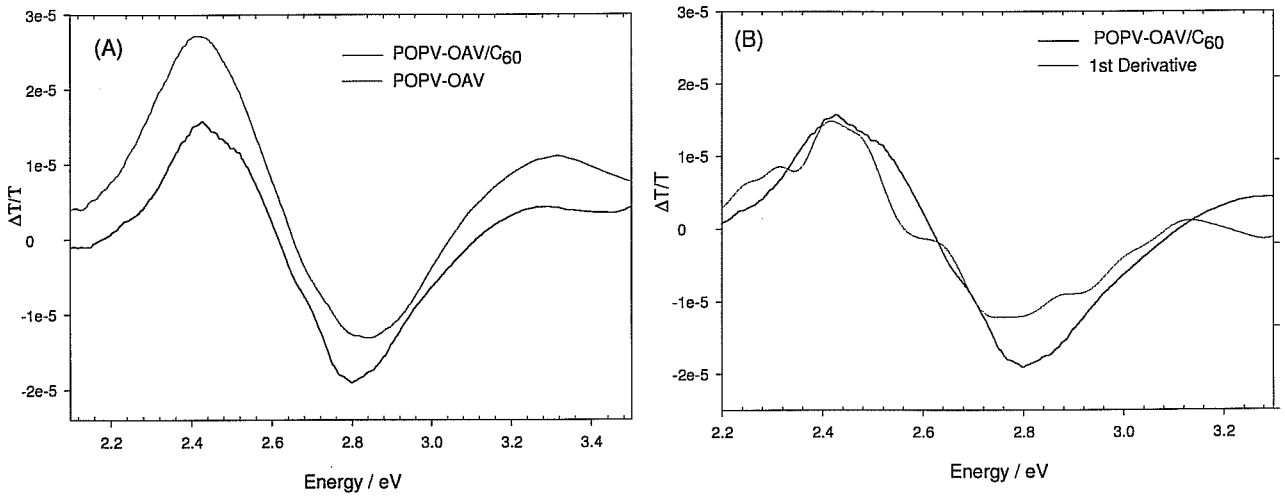

Figure 7.6: Electroabsorption spectra of (A) POPV-OAV/C_{60} and Pristine POPV-OAV and (B) POPV-OAV/C_{60} and first derivative lineshape.

The first electroabsorption feature of the composite occurs at 2.41 eV, which is slightly blue shifted compared to that of the pristine polymer. This is followed by a shoulder peak at 2.52 eV, which is absent in the pristine spectrum. This peak can be assigned to molecular C_{60} (Hess, 1996). In the solid-state electroabsorption spectrum of C_{60} this feature becomes a strong red-shifting derivative structure at 2.40 eV as shown in Chapter 4, Section 4.4; the change to derivative occurring as the transition becomes allowed in the solid, and then is Stark-shifted by the applied field (Hess, 1996). The evidence of this molecular feature maybe a further indication the C_{60} is well dispersed. The next feature of the composite at 3.12 eV is the $_mA_g$ state which also appears in the pristine material. In general it would appear that the electroabsorption spectrum of POPV-OAV/C_{60} is a summation of the two materials with no conclusive evidence of a charge transfer interaction. Figure 7.6 (B) shows the composite spectrum along with first derivative of the absorption spectrum. The spectrum closely resembles the first derivative lineshape. The one noticeable discrepancy is the absence of the phonon

sideband that appears in the first derivative spectrum. The absence of this band in the electroabsorption spectrum could indicate a broadening of the energy states, but again this may be due to structural effects and not a charge transfer.

Figure 7.7 (A) shows the electroabsorption of the PONV/C_{60} composite along with the electroabsorption spectrum of PONV and Figure 7.7 (B) shows the electroabsorption spectrum of POPV-OAV/C_{60} with first and second derivatives of the absorption spectrum. From Figure 7.7 (A) it can be seen that the PONV/C_{60} spectrum deviates from the pristine polymer spectrum. The electroabsorption spectrum of the PONV/C_{60} consists of four features. At 2.44 eV there is a very weak feature which can attributed to the PONV. This feature is blue shifted compared to the pristine PONV and also a point to mention is the loss of the phonon sideband in the PONV/C_{60} composite. The next three features at 2.76 eV, 2.96 eV and 3.17 eV are composites features. The features do not match up with previously reported molecular C_{60} features by Hess *et al* (Hess, 1996). From the pristine PONV spectrum in Figure 7.7 it can seen that the features are not attributable to the PONV. Therefore it could be assumed that these are charge transfer states of the composite. Further evidence to support the notion that the features are charge transfer states can be seen in Figure 7.7 (B). The electroabsorption spectrum of the PONV/C_{60} is a combination of both first and second derivative features. The second derivative features in the spectrum indicate that there is a change in dipole moment ($\Delta\mu$) in the composite (Weiser, 1998). This indicates that a charge separation (Wahadoszamen, 2006) is occurring and charge transfer is occurring or that charge transfer states exist.

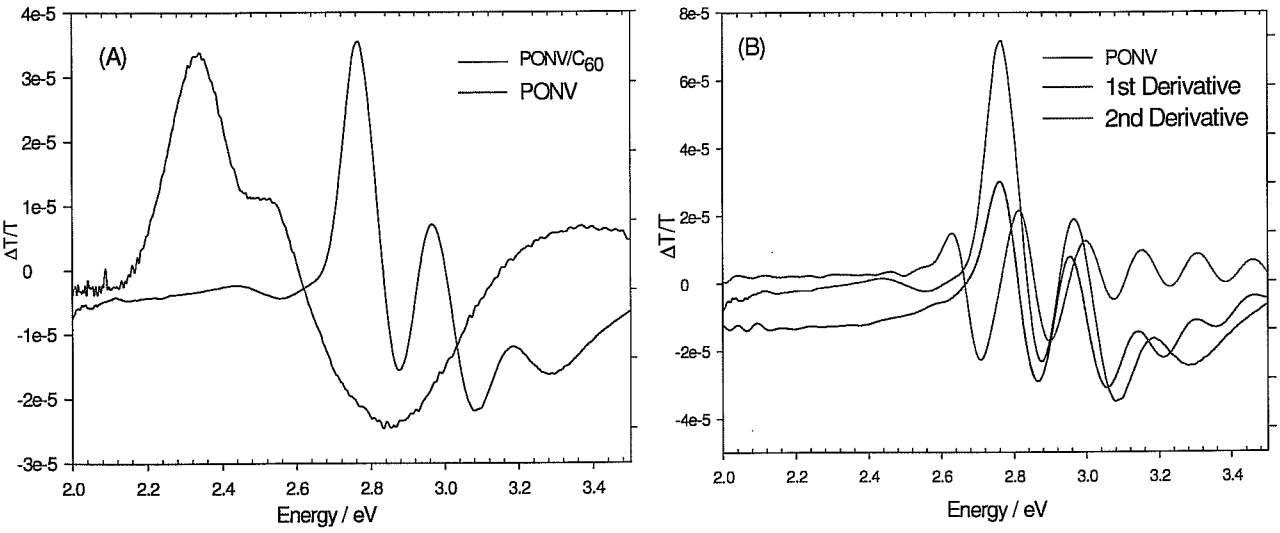

Figure 7.7: Electroabsorption spectra of (A) PONV/C_{60} and Pristine PONV and (B) PONV/C_{60} and first and second derivative linshapes.

7.4 Summary

The POPV-OAV/C_{60} showed no concrete evidence of a charge transfer in the electroabsorption spectrum. The molecular C_{60} peak at 2.52 eV confirms that the C_{60} is well dispersed. There was also a broadening of the energy states in the composite spectrum but as mentioned previously this effect could be due structural effects. The electroabsorption results for the POPV-OAV/C_{60} are inconclusive, it cannot be said for definite that this technique showed an interaction between the POPV-OAV and the C_{60}. At this point there is evidence of a charge transfer between the POPV-OAV/C_{60}. The fluorescence, cyclic voltammetry and conductivity results did show an interaction between the two but it was mentioned at the end of chapter six that the C_{60} interaction was not as strong with the POPV-OAV as it was with the PONV.

The PONV/C_{60} did show an interaction that could be deemed to be a charge transfer. The appearance of three new composite features and second derivative contributions leads to conclusive evidence that there is an interaction between the PONV and the C_{60}. The second derivative contributions indicate a change in dipole moment ($\Delta\mu$), which is associated with charge transfer states. This result reaffirms the fluorescence, cyclic voltammetry and conductivity results on PONV/C_{60} composite that there is an interaction occurring which can be said to be a charge transfer.

Chapter 8 provides an overall discussion of all of the results and provides an in depth summation of the study. The chapter also describes some of the future avenues this study may progress towards.

The PONV/C_{60} did show an interaction that could be deemed to be a charge transfer. The appearance of three new composite features and second derivative contributions leads to conclusive evidence that there is an interaction between the PONV and the C_{60}. The second derivative contributions indicate a change in dipole moment ($\Delta\mu$), which is associated with charge transfer states. This result reaffirms the fluorescence, cyclic voltammetry and conductivity results on PONV/C_{60} composite that there is an interaction occurring which can be said to be a charge transfer.

Chapter 8 provides an overall discussion of all of the results and provides an in depth summation of the study. The chapter also describes some of the future avenues this study may progress towards.

References:

Byrne H.J., in *"Physics and Chemistry of Fullerenes and Derivatives"*, Kuzmany H, Fink, J, Mehring M, Roth S eds., World Scientific Singapore, p183, (1995).

Cardona M, *"Solid State Physics Supplement 11: Modulation Spectroscopy"*, Academic Press, New York, (1969).

Hess B.C., Bowersox D.V, Mardirosian S.H., Unterberger L.D, *"Electroabsorption in C_{60} and C_{70}. Third-order nonlinearity in molecular and solid states"*, Chemical Physics Letters, 248, 14, (1996).

Kazaoui S, Minami N, Tanabe Y, Byrne H.J., Elimes A, Petelenz P, *"Comprehensive analysis of intermolecular charge-transfer excited states in C_{60} and C_{70} film"*, Phys Rev B. 58, 7689, (1998).

Liess M, Jeglinski S, Vardeny Z.V., *"Electroabsorption spectroscopy of luminescent and nonluminescent π-conjugated polymers"*, Phys. Rev. Lett B, Vol 56, 2415, (1997).

Martin S.J., Mellor H, Bradley D, Burn P.L., *"Electroabsorption studies of PPV and MEH-PPV"*, Optical Materials, Vol 9, 88, (1998).

Moses D, Comoretto D, Lee C.H., Heeger A.J., *"Fast Transient "Photoconductivity" in Semiconducting Polymers: Free Carrier Photocurrent or Displacement Current Generated by Electric-Field-Induced Polarisation of Bound Excitons"*, Synthetic Metals, 84, 559, (1997).

Petelenz P, *"Non-local polarisabilities in excited states of polyacene crystals"*, Chem. Phys. Lett. 215, 607, (1993).

Petelenz P, *"Electro-absorption spectra of degenerate charge transfer states"*, Chem. Phys. 171, 397, (1993).

Sebastian L and Weiser G, *"Charge transfer transitions in solid Tetracene and Pentacene studied by Electroabsorption"*, Chem Phys. 61, 125, (1981).

Shimoi Y, Murata K, Abe S, Noguchi T, Ohnishi T, *"Electroabsorption of electroluminescent polymer poly (p-phenylene vinylene) in a wide spectral region"*, Journal of Luminescence, 87, 753. (2000).

Takase T and Kotani M, *"Charge transfer states in phenothiazine crystal"*, J. Chem. Phys. 94, 2134, (1989).

Wahadoszamen W, Nakabayashi T, Ohta N, *"Electroabsorption spectra of a complex formed between tetraphenyl-porphyin and fullerene in a polymer film"*, Journal of Photochemistry and Photobiology A, Chemistry, 178, 177, (2006).

Weiser G, *"Stark effect of one-dimensional Wannier excitons in polydiacetylene single crystals"*, Phys. Rev. B 45, 14076, (1993).

Weiser G and Horvàth A, *"Variation with disorder of absorption and electroabsorption spectra of a π-conjugated polymer: 4BCMU"*, Chem. Phys, 227, 153. (1998).

Weiser G, *"Comparative electroabsorption studies of organic and inorganic solids"*, Journal of Luminescence, Vol 110,189, (2004).

Chapter 8: General Discussion and Conclusions

8.1 Introduction

British Petroleum recently stated that 'for every nine barrels of oil consumed, only one is discovered' (BP Statistical Review of World Energy, 2008). This frightening statistic highlights the global dependence on oil and the unavoidable crisis which is currently gabbing headlines around the world. The current oil crises has seen oil prices rise to record highs, with predictions of two hundred dollars a barrel before the end of 2008. Like previous oil crisis's economic downturns, disrupted supply chains and international conflict have played a significant part in pushing up the oil prices. However unlike previous crises this one is characterised by an international acknowledgement of the rapidly decreasing global oil reserves. The situation is in fact mirrored for all fossil fuels albeit with different timelines. The consumption of fossil fuels has increased dramatically over the past twenty years with strong evidence linking this consumption to potentially catastrophic environmental damage as well as developing a highly competitive energy market.

The combination of these social, economic and environmental issues has put considerable pressure on the development of clean, renewable and sustainable energy systems. However much of the technology underling renewable and sustainable energy systems is still at an early stage presenting the scientific community with a significant challenge and one upon which the clock is ticking. The knock on effect is that some of the fundamental underlying science and understanding may be discarded in favour of easy to market technologies resulting in lost opportunities to develop efficient technologies and systems. This is particularly the case for organic photovoltaic cells

where the material design and structure property relationships have often been neglected in favour of device architecture.

8.2 General discussion of thesis

This thesis has been designed to explore the fundamental properties of the base materials in a novel polymeric photovoltaic system, i.e. the relationship between the donor and acceptor materials. The understanding of molecular systems and how the properties of the molecule translate into bulk properties has been the focus of much research in recent years with the ever expanding nanotechnology area. Nanotechnology has demonstrated that the tailoring of a molecular structure to a specific property is not only possible but crucial in the design of molecular devices. The increasing pool of knowledge regarding the processes and mechanisms behind a number of molecular interactions including molecular conduction, photochemistry and photophysics has allowed the identification of key material design parameters for the promotion of specific properties. Using this knowledge and applying it to PV cells, it should be possible to design an electron donating material with direct consideration to the electron accepting material thereby optimising the relationship between the donor and acceptor materials and ensuring that an efficient charge separation is achievable.

This study proposed to test this hypothesis by taking a systematic approach to investigating the charge transfer between a homologous series of conjugated polymers and C_{60}. The polymers used were produced in house and were derivatives of PPV which has been systematically modified with naphthyl and anthryl units. Figure 8.1 shows a flow diagram of the idealised appropriates steps in the production of an organic photovoltaic cell.

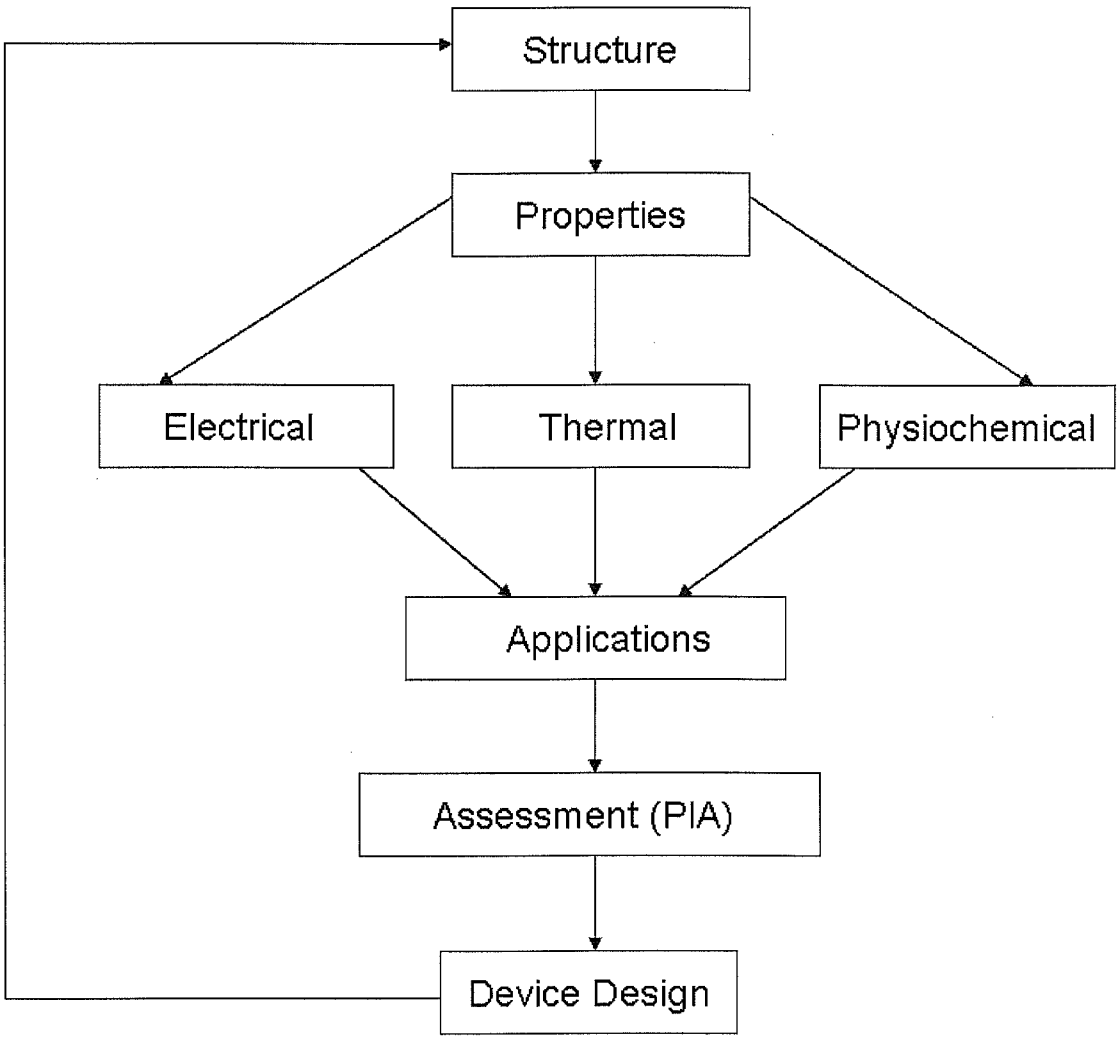

Figure 8.1: Flow diagram of the idealised appropriates steps in the production of a organic photovoltaic cell.

In general the first step regarding the structure of the fundamental materials is usually not considered by device engineers with much of the early stages focusing upon the fourth step (application), hence the fundamental science and in particular the exact charge transfer properties are still not fully understood. Using the new polymer series this study proposes to start at the first step and work through each step of the flow diagram to try and establish an understanding of the interactions in polymer/fullerene composites. The information gathered could potentially be related back to the polymer

structure allowing minor structural alterations of the polymer to give an improved interaction of the polymer with the C_{60} and ultimately device performance.

From the flow diagram it can be seen that the experimental techniques traditionally employed to observe the charge transfer between polymer/fullerene composites is photoinduced absorption spectroscopy (PIA). PIA spectroscopy is expensive and not readily available for use. Therefore there is a need to look for more simple techniques. This study also proposed to use steady state spectroscopic techniques coupled with electrochemical and conductivity measurements to characterise charge transfer signatures in polymer fullerene composites.

Initially these techniques were applied to a well know reference system. MEH-PPV has been shown to achieve efficient charge separation upon addition of C_{60}. Charge separation in MEH-PPV/C_{60} systems is achieved by ultrafast transfer of photoexcited electrons from the polymer to the C_{60}. This was first reported by Sariciftci *et al* (Sariciftci, 1992) as characterised by time resolved PIA spectroscopy. Since the first report by Sariciftci there have been a number of other studies on the charge transfer interactions between MEH-PPV and C_{60} (Kraabel, 1994, Halls, 1996, Vacar, 1997). It is suggested that MEH-PPV can be used as a reference material due to the sizeable body of work that exists in the literature.

The UV/VIS spectrum of the MEH-PPV/C_{60} composite was a summation of the two materials. The absence of any new spectral features leads to the conclusion that there is no charge transfer in the ground state between the MEH-PPV and C_{60}. However from the spectrum it was determined that the C_{60} was molecularly dispersed

Fluorescence quenching provided the first indication of the photoinduced charge transfer in MEH-PPV and C_{60}. The addition of the C_{60} prevents the electron hole pairs recombining and hence results in a fluorescence quenching. In addition from

fluorescence measurements it was possible to determine the optimum concentration of acceptor material that can be used without saturating the composite.

The first electroabsorption feature at 2.20 eV→2.50 eV of MEH-PPV was shown to broaden upon addition of C_{60}, which results in a broadening of the energy states distribution in MEH-PPV. The phonon sideband at 2.30 eV in pristine MEH-PPV was absent in the composite. These two occurrences have been shown to coincide with a charge transfer between the two materials (Liess, 1997).

The cyclic voltammetry measurements first showed a new composite feature in the p-doping scan. It is postulated that when the MEH-PPV loses an electron, the electron is transferred onto the C_{60}, i.e. charge transfer occurs and then the C_{60} is charged and can now be oxidised and hence the evolution of the second oxidisation feature. The n-doping scan was a summation of the two materials. The conductivity range of the reduction potential of MEH-PPV/C_{60} was shown to increase by two/three orders of magnitude compared with that of pristine MEH-PPV. The C_{60} is able to accept the electrons from the MEH-PPV, thus allowing a bigger current intake in the polymer. Conductivity measurements confirmed that the addition of the C_{60} increases the conductivity of the polymer.

Fluorescence measurements, electroabsorption spectroscopy, cyclic voltammetry and conductivity measurements were shown to be capable of detecting charge transfer signatures between MEH-PPV and C_{60}. Table 8.1 provides a brief summary of the useable techniques and the observed results.

Table 8.1: Experimental observations of interaction between MEH-PPV and C_{60} using various steady state techniques, cyclic voltammetry and conductivity measurements.

Techniques	Observations	Useable technique
UV/VIS	Spectrum a summation of two materials	-
Fluorescence	Fluorescence quenching upon addition of C_{60}	✓
Cyclic Voltammetry	Increase in current in n-doping scan, new peak in p-doping scan	✓
Conductivity Studies	Increase in current upon addition of C_{60}	✓
Electroabsorption Spectroscopy	Broadening of electroabsorption spectrum and loss of phonon sideband	✓

The elucidation of the potential of these techniques for the characterisation of the charge transfer process is a significant contribution to the field. To consider the above techniques for the new series it is important that a full characterisation of the polymers was performed in solution and in particular their solid-state form. Whereas the solution properties of the series have been reported, much the solid-state work in fact is reported here for the first time. Chapter 5 described the electronic properties of the polymer series. The solid-state optical absorption spectra of the polymers shows no discernable trends. The comparison of the isolated molecule to the solid-state form confirmed that there is significant aggregation occurring within the polymers. The electronic properties

of the molecular and solid-state forms are different and the structure property relationships previously determined for the molecular forms do not apply to the solid-state. The energy positioning of the solid-state fluorescence spectra shows no systematic trend with regard to the structural changes. Emissions of the polymers were all seen to be red shifted compared to those of their isolated molecular form. The fluorescence yield was also low, which also confirmed that there are aggregates within the polymers in their solid-state form. The degree of shifting from the solution spectrum varied from polymer to polymer, indicating a different degree of aggregation. The shift in both optical and emission spectrum leads to an increase in Stokes shift for each polymer. The optical bandgaps, emission energies and Stokes shifts for the molecular form and solid-state form of the polymers are shown in Table 8.2.

Table 8.2: Molecular and solid-state optical bandgaps, emission energy and Stokes shifts.

Polymer	Optical Bandgap Solid-State / eV	Optical Bandgap Solution / eV	Emission Energy Solid-State / eV	Emission Energy Molecular / eV	Stokes Shift Solid-state / eV	Stokes Shift Molecular / eV
POPV	2.71	2.41	2.13	2.27	0.58	0.14
POPV-ONV	2.62	2.58	2.18	2.43	0.44	0.15
POPV-OAV	2.51	2.48	1.9	2.38	0.61	0.10
PONV	2.78	2.81	2.19	2.69	0.59	0.12
PONV-OAV	2.76	2.63	2.05	2.53	0.71	0.10

The electrochemical properties of the polymer series were examined in Chapter 6. All the polymers were capable of being oxidised and reduced electrochemically.

Relationships were found to exist between the electrochemical properties, optical properties and to an extent the vibrational properties. The cyclic voltammetry measurements coupled with in-situ reflectance measurements provided a visualisation of the HOMO-LUMO levels, electrochemical bandgaps and excited state levels within the polymer series. The precise levels of the HOMO-LUMO levels are important when matching the energy levels of the polymer to the energy levels of the C_{60}. Electrochemical bandgaps were in close accordance to the optical bandgaps. Some of the structural changes made to the polymers could be quantified with the different changes to the reduction potential and HOMO-LUMO levels of the polymers.

Conductivity measurements were performed on POPV-OAV and PONV. PONV was shown to have a lower turn-on voltage compared to the POPV-OAV. This is due to the positioning of the HOMO-LUMO levels of the PONV relative to that of the ITO and aluminium electrodes. PONV also has a higher HOMO level and a lower LUMO than POPV-OAV, which provide a better hole blocking properties and a lower electron injection barrier

Chapter 7 examines the electroabsorption spectra of the polymer series. The electroabsorption spectrum of each polymer is dominated by the quadratic Stark effect. The electroabsorption spectrum of each polymer closely resembled a first derivative line shape of its absorption spectrum indicating a dominance of intramolecular transitions within each of the polymers. The exciton binding energy of each polymer was calculated, with values between 0.6 eV – 0.8 eV observed. The change in polarisability (Δp) for each of the polymers was calculated. Δp is a measure of the sensitivity of a transition to an applied electric field and is particularly important for understanding the electronic properties of the investigated molecular system. It was shown that the Δp

value could be related to the electrochemical bandgap of the polymers and a linear relationship was found to exist.

For the composite materials two of the polymers from the series were chosen. The first polymer chosen was POPV-OAV as it shows the smallest degree of aggregation and hence the solid-state absorption spectrum closely resembles the molecular spectrum. The second polymer chosen was PONV, which has an optical bandgap of 2.78 eV. PONV absorbs in the blue region of the solar spectrum whereas POPV-OAV absorbs more towards the red region. PONV is known to have greater stability towards photo-oxidation then any of the other polymers (Lynch, 2008). The development of Photovoltaics using organic materials has somewhat been limited by the degeneration of the active material (Atreya, 1999). Therefore the choice of a more photostable polymer is appropriate. UV/VIS absorption spectra of the POPV-OAV/C_{60} and PONV/C_{60} composites showed no evidence of charge transfer in the ground state, which was expected as similar results were observed with the MEH-PPV/C_{60} composite. The POPV-OAV/C_{60} spectrum was a direct summation of molecular POPV-OAV and molecular C_{60}. However the PONV/C_{60} composite was not a direct summation. The introduction of the C_{60} resolved the $\pi \rightarrow \pi^*$ transition into three individual features. The addition of the C_{60} led to a blue shift in the $\pi \rightarrow \pi^*$ transition of the conjugated backbone of each polymer. This is consistent with a reduction of the aggregation observed in the solid-state. In both composite it could be seen that the C_{60} was molecularly dispersed. Fluorescence quenching was observed within the two composites in solution. This is the first evidence of charge transfer between the two polymers and the C_{60}. The PONV showed a higher degree of fluorescence quenching.

Cyclic voltammetry measurements were next used to examine the composites. The POPV-OAV/C_{60} composite behaved similar to that of MEH-PPV/C_{60}. In the p-doping

scan, two peaks were observed. Firstly there is a very weak oxidation at 0.87 V, which can be attributed to the pristine polymer. The second peak at 1.15 V is an indication of a charge transfer between the polymer and C_{60}. When the POPV-OAV is oxidised, it then has an extra electron which C_{60} accepts and the under cyclic voltammetry conditions is forced to give the electron up. The n-doping scan was a summation of the POPV-OAV and molecular C_{60}. The composite current range is factor of five larger than that of the pristine POPV-OAV. This increase in current is consistent with C_{60} acting as an acceptor material allowing the polymer to accept or channel more charge and was also seen in the MEH-PPV/C_{60} results. The PONV/C_{60} p-doping scan was not similar to that of the POPV-OAV/C_{60} and MEH-PPV/C_{60} composites. The p-doping scan showed two oxidation peaks. The first peak occurs at a very low potential of 0.10 V and the second occurs at a potential of 0.69 V. The second peak can be attributed to the oxidation of the pristine PONV. The new peak occurs before the oxidation of the pristine PONV and therefore cannot be assumed to that of a charge transfer. This new peak is due to a new excited state produced in the composite. The n-doping cyclic voltammogram obtained for PONV/C_{60} composite was again a summation of the two materials (PONV and molecular C_{60}). The noticeable difference again is the increase in the current range of the polymer reduction. The composite current range was a factor of 2 larger than that of the pristine PONV. The current peaks were much broader in the PONV/C_{60} composite than those of POPV-OAV/C_{60} composite, which indicates that the amount of charge consumed is greater in the PONV/C_{60} composite (Li, 1999).

In-situ spectroscopic measurement reaffirmed that there is an interaction between the polymers and the C_{60} in the composites. The POPV-OAV/C_{60} UV/VIS reflectance spectrum showed a significant change with high doping levels, which is indicative of a potential charge transfer. The UV/VIS reflectance spectrum of PONV/C_{60} also showed

evidence of a charge transfer. However this charge transfer was shown to occur at a low doping level.

To clarify the cyclic voltammetry of the composites conductivity were then performed. The turn on voltage of POPV-OAV single layer device was found to occur at 2.30 volts. The addition of the C_{60} to the POPV-OAV results in a decrease in the turn on voltage to 1.40 volts. The short circuit current of the POPV-OAV/C_{60} device at 1.4 V is a factor of 1.5 larger than the POPV-OAV single layer device. The addition of the C_{60} enhances the transport of electrons and holes through the acceptor and donor material respectively in a preferred direction to the extracting electrodes. The turn on voltage for a PONV single layer device was 1.70 volts. The turn on voltage for a PONV/C_{60} single layer device was found to be 0.5 volts. The short circuit at 1.5 volts in the composite is a factor of 10,000 larger than that of the pristine PONV. The PONV/C_{60} composite showed a much larger increase than the POPV-OAV/C_{60} composite. Conductivity results did confirm the previous cyclic voltammetry results but both techniques show that the PONV behaves differently with the C_{60} than the POPV-OAV.

The last technique used to investigate the composite was electroabsorption spectroscopy. The electroabsorption spectrum of POPV-OAV/C_{60} closely resembled that of the first derivative of the absorption spectrum. The spectrum did show a molecular feature at 2.41 eV. The evidence of this molecular feature is a further indication that the C_{60} is well dispersed. In general the electroabsorption spectrum of POPV-OAV/C_{60} is a summation of the two materials with no conclusive evidence of a charge transfer interaction. The one discrepancy is the absence of the phonon sideband that appears in the first derivative spectrum. The absence of this band in the electroabsorption spectrum could indicate a broadening of the energy states, but could be due to structural effects and not a charge transfer. In order to know for definite the

electroabsorption scan would have be extended down to the low UV region which is beyond the limits of the spectrometer. The electroabsorption spectrum of POPV-OAV/C_{60} contained first and second derivatives contribution of the absorption spectrum. The electroabsorption spectrum of the PONV/C_{60} consisted of four features. At 2.44 eV there is a very weak feature which is attributed to the pristine PONV. This feature is blue shifted compared to the pristine PONV and there is the loss of the phonon sideband in the composite. The next three features at 2.76 eV, 2.96 eV and 3.17 eV are composites features. As the spectrum contains second derivative contributions it can be assumed that these are charge transfer states of the composite. The second derivative features in the spectrum indicate that there is a change in dipole moment ($\Delta\mu$) in the composite (Weiser, 1998) which indicates that a charge separation (Wahadoszamen, 2006) is occurring and charge transfer is occurring. The electroabsorption results are the third techniques which showed a difference interaction between the PONV/C_{60} composite and the POPV-OAV/C_{60} composite.

8.3 Future work

To further the research presented in this thesis a number of suggestions are made below. Additional research such the modification of the structure of PONV would further the knowledge of the charge transfer mechanism of the polymer with C_{60}. The PONV displayed clear indicators of charge transfer with C_{60}. Alterations of the PONV structure could result in an improved interaction with the C_{60}. The structural changes could result in a change in the HOMO-LUMO levels and excited state levels and hence it may be possible to tune the levels to achieve the optimum levels for charge transfer. From the previous results a decrease in the LUMO level to bring it closer to the LUMO level of

C_{60} would be desirable. Figure 8.2 shows the possible changes that could be made to the PONV. Cyano (CN) groups have already been shown to decrease the reduction potential and increase the LUMO level of MEH-PPV (Li, 1999).

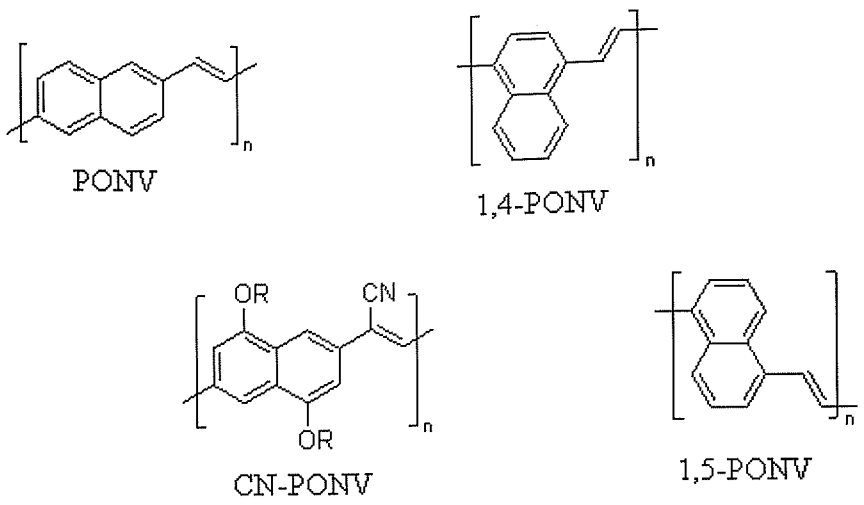

Figure 8.2: Pristine PONV and PONV alternative structures.

Reconstruction of the electroabsorption spectrometer:

The electroabsorption spectrometer is limited from 2.00 eV to 3.50 eV. A broader range would allow a more detailed investigation of the electronic structure of the polymer and of the composites. Three main changes would have to be made to the current electroabsorption set-up. Firstly all the glass lenses would need to be replaced with quartz lenses, as quartz optics are needed to investigate UV region as they have little or no absorption. Second ITO could not be used as the bottom electrode as it absorbs in UV region, therefore nickel would have to be used. Finally the Labview programme would need to be adjusted to accommodate the new energy range of the spectrometer.

Construction of photoconductivity set-up:

In order to construct a photoconductivity detector the electroabsorption spectrometer would be reconfigured to include the Keithley 237 electrometer. Photoconductivity is necessary for the polymer/C_{60} devices. The polymers themselves will produce a photocurrent. However when the C_{60} is added and the device is illuminated the I–V curve is shifted down by the short-circuit. Using this short circuit current and the open circuit voltage it is possible to calculate the fill factor for a device. The fill factor (FF) is defined as the ratio of the maximum power divided by the short-circuit current and open-circuit voltage in light. Fill factor can also be related to the overall device efficiency.

Temperature studies:

The Linkham stage is capable of achieving temperature of 77 K up to 873 K, with heating and cooling ramp rates of 130 K/min and boasts a temperature stability of greater than 0.1 K. Electroabsorption spectra of the PONV/C_{60} could be acquired from low temperatures up to high temperatures on the same sample to observe change in oscillator strength of charge transfer states or evolution of new states. Also annealing of pristine polymer has been shown to cause a decrease in florescence, which could result in a decrease in the concentration of C_{60} needed in the composites.

8.4 Conclusions

Over the past fifteen years a number of studies investigating the charge transfer between polymer/fullerene composites using time resolved photoinduced absorption spectroscopy have been reported. However it has been shown throughout the course of this study that is it possible to detect charge transfer signature in polymer fullerene composites using simpler and more cost effective techniques. Fluorescence, electroabsorption spectroscopy, cyclic voltammetry and conductivity measurements all provided evidence of charge transfer in polymer/fullerene composites.

Using these techniques, charge transfer signatures were identified in two new polymer composites. The polymers used had varying electronic properties, which was seen to effect their interaction with the C_{60}. From the results it was seen that the PONV interacts more efficiently with the C_{60}. In order to understand this, it is important to investigate the energy levels of both polymer and C_{60}. Figure 8.3 shows the energy levels obtained for POPV-OAV, PONV and C_{60} (energy levels were obtained from cyclic voltammetry measurements and in-situ reflectance measurements). From the energy level diagram it can be seen that the LUMO level of PONV is lower than that of POPV-OAV, it is closer to the C_{60} LUMO level. It would appear that the lower LUMO level of PONV results in a better interaction with the C_{60} and hence leads to a more efficient interaction.

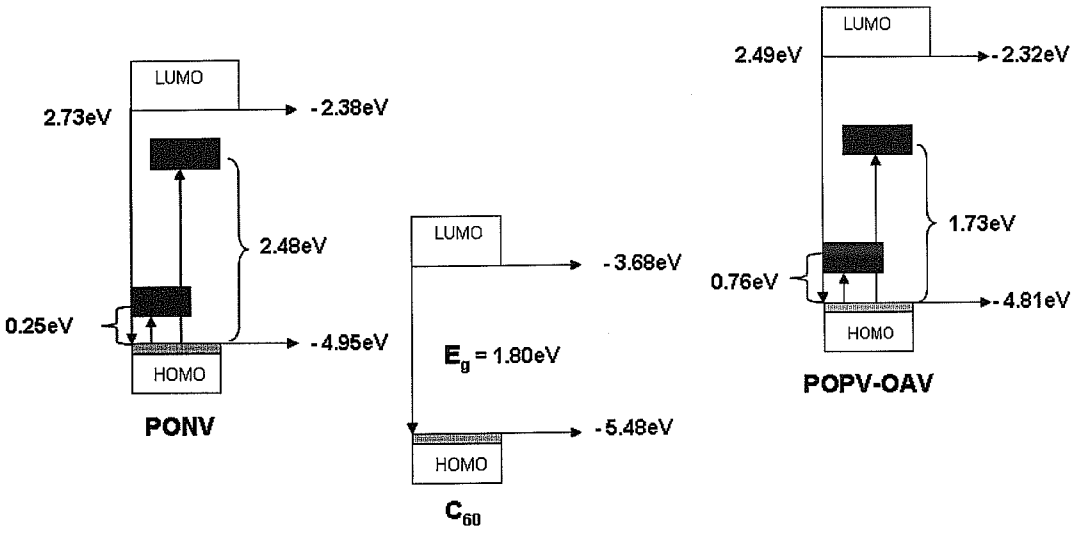

Figure 8.3: Energy level diagram of PONV, POPV-OAV and C_{60}.

Another factor to take into account is the bipolaron energy levels. The bipolaron level at 2.51 eV (4.95 eV-2.48 eV) in the PONV is close to the PONV LUMO level, whereas the bipolaron level at 3.08 eV (4.81 eV-1.73 eV) is not close to the POPV-OAV LUMO level. In fact it could be proposed that the bipolaron level in PONV is actually a polaron level. It has been suggested that polarons are dominant at low doping levels whereas bipolarons are more favourable at high doping levels (Patil, 1988). Hence the PONV/C_{60} composite was shown to change dramatically at low doping levels compared to the POPV-OAV/C_{60} composite. In general from the behaviour of the two composites, it can be said that in order to achieve charge transfer from a conjugated polymer to C_{60}, the LUMO level of the polymer should be as close as possible to the LUMO level of C_{60}. Also it is favourable that the bipolaron levels of the polymers be as close as possible to the HOMO-LUMO levels. Therefore it can be concluded that a systematic approach is more favourable when considering the matching of the appropriate energy levels of a polymer to that of C_{60}.

References:

Atreya M, Li S, Kang E.T, Neoh K.G, Ma Z.H, Tan K.L, Huang W, *"Stability studies of poly(2-methoxy-5-(2'-ethyl hexyloxy)-p- (phenylene vinylene) [MEH-PPV]"*, Poly. Degr. And Stability, 65, 287, (1999).

BP Statistical Review of World Energy, http://www.bp.com, 12/07/08, (2008).

Halls J.J.M, Pichler K, Friend R.H, Moratti S.C, Holmes A.B, *"Exciton diffusion and dissociation in a poly(p-phenylenevinylene)/C_{60} heterojunction photovoltaic cell"*, Appl. Phys. Lett. 68 (22), 3120, (1996).

Kraabel B, McBranch D, Sariciftci N.S, Moses D, Heeger A.J, *"Ultrafast spectroscopic studies of induced electron transfer from semiconducting polymers to C_{60}"*, Phys. Rev. B 50, 18543, (1994).

Li Y, Cao Y, Gao J, Wang D, Yu G, Heeger A.J, *"The synthesis, optical and charge transport properties of poly (aromatic oxadiazole)s"*, Synthetic Metals 99, 243, (1999).

Liess M, Lane P.A, Vardeny Z.V, Kafafi Z.H, *"Electro modulated induced absorption of C_{60} doped MEH-PPV"*, Synthetic Metals 84, 683, (1997).

Lynch P, *"Synthesis and characterisation of conjugated polymers with a view to developing an understanding of structure property relationships"*, PhD Dissertation, Dublin Institute of Technology, (2008).

Patil A.O, Heeger A.J, Wudl F, *"Optical Properties of Conducting Polymers"*, Chem. Rev. 88, 183, (1988).

Sariciftci N.S, Smilowitz L, Heeger A.J, Wudl F, *"Photoinduced electron transfer from a conducting polymer to buckminsterfullerene"*, Science 258, 1474-1476 (1992).

Vacar D, Maniloff E.S, McBranch D.W, Heeger A.J, *"Charge-transfer range for photoexcitations in conjugated polymer/fullerene bilayers and blends"*, Phys. Rev. B 56(8), 4573 (1997).

Wahadoszamen W, Nakabayashi T, Ohta N, *"Electroabsorption spectra of a complex formed between tetraphenyl-porphyin and fullerene in a polymer film"*, Journal of Photochemistry and Photobiology A, Chemistry, 178, 177, (2006).

Weiser G and Horvàth A, *"Variation with disorder of absorption and electroabsorption spectra of a π-conjugated polymer: 4BCMU"*, Chem. Phys, 227, 153. (1998).